# Elucidating the principal role of cholecystokinin neurons of the ventromedial hypothalamic nucleus in energy homeostasis


**Vasileios Eftychidis**

St Hilda's College

Department of Pharmacology

University of Oxford

This dissertation is submitted for the degree of

*Doctor of Philosophy*

Michaelmas 2017

# Declaration

I hereby declare that the contents of this dissertation are original and have not been submitted in whole or in part for consideration for any other degree or qualification in this, or any other University. This dissertation contains less than 37,000 words excluding appendices, bibliography and tables and has less than 250 figures. All the results presented are the results of my own work.

# Acknowledgments

You wouldn't be reading this thesis if it weren't for the support, teaching and inspiration I received from many wonderful people, both during and prior to my DPhil.

First of all, my gratitude goes to my supervisor, Dr Liliana Minichiello, who chose me as a DPhil candidate for her lab. Thanks to her kind, careful and encouraging supervision, I never lost motivation or passion for research.

Sincere thanks to Dr Louise Upton for the training I received from her in stereotactic injections, a technique that was so important for my research. I also thank Dr Tommas Ellender for the collaboration and assistance in electrophysiology.

I am very grateful for having an excellent and supportive college advisor, Dr Maike Glitsch, while I am also thankful to St Hilda's College and the immense support the have provided me.

I would also like to thank past and current members of the Minichiello lab for their help throughout all this time, for the great support and enjoyable moments during these years. I am also thankful for the great technical and administrative support of the Animal Unit, for always supporting us and providing great assistance.

During these years, I had the privilege to meet awesome people that helped me cope through the tough times without losing enthusiasm. I thank them for helpful scientific discussions, but especially for being great friends I could always count on. This thesis is dedicated to my parents, Vasilis and Elina, my sister Anastasia, and to Lora for all the love and support they have given me. I would not be here if it wasn't for you.

I would also like to thank the Medical Research council for the 3 Year studentship and the Onassis Foundation for their scholarship for my 4$^{th}$ year.

# Abstract

The central nervous system (CNS) has a crucial role in the maintenance of energy homeostasis by orchestrating a plethora of signals from peripheral organs about the state of energy stores and the current energy intake needed to match energy expenditure. These signals converge into the hypothalamic regions and its complex local circuitry. CNS-derived cholecystokinin (CCK) is acting at central level to modulate energy balance by regulating the neuronal activity of hypothalamic neuronal populations that regulate food intake, energy storage and consumption. Moreover, our recent published work identifies CCK neurons as key integrators of the neuroendocrine negative feedback of glucocorticoids to the PVN. Glucose sensing neurons of the Ventromedial Hypothalamus (VMH) are integrating energy signals and are essential for mounting a counter-regulatory response and glucose homeostasis. VMH is also important in energy expenditure by regulating body weight and thermogenesis. CCK neurons are present in high density in the VMH.The source of endogenous CCK that acts on distinct neuronal components has not been elucidated. The research so far does not address the purpose of CCK neurons in the hypothalamus and their potential role in the network dynamics regarding energy homeostasis.

In this study, we untangle the role of CCK neurons in the VMH nucleus by employing stereotactic intracranial delivery of adeno-associated viruses that result in cell-type specific chemogenetic inhibition or ablation of these neurons. Acute silencing of their neurotransmission with the cre-dependent AAV expression of the chemogenetic tool of Designer Receptors Exclusively Activated by Designer Drugs (DREADDs) increases their daily food intake due to increased meal numbers and eating frequency without meal size or meal duration being affected. CCK ablation by a newly generated double-recombinase-mediated Diphtheria Toxin Receptor (DTR) mouse line or AAV-DTA-mediated ablation resulted in hyperphagia, obesity and hyperglycaemia. We conclude that $CCK^{VMH}$ neurons are implicated in the regulation of food intake, body weight and glucose homeostasis in the adult brain.

# Table of Contents

# Chapter 1: Introduction

## 1.1 Central nervous system orchestrates the maintenance of energy homeostasis

Energy homeostasis is the balance of energy intake and energy expenditure of an organism and can be separated in mechanisms controlling food intake, energy storage and energy consumption. Many components of the central nervous system, ranging from the peripheral nerves around the gastrointestinal tract to specific brain regions such as the brainstem and the hypothalamus, are integrating a multitude of signals and relating information between them in order to coordinate actions leading to energy balance.

The signals that are conveyed to the central nervous system that control ingestive behaviour and the initiation/termination of food intake can be categorised in 4 classes (Berthoud *et al.*, 2006). Each signal class carries information regarding the availability of potentially ingestible food in the environment (class 1), digestible food and absorbed nutrients in the alimentary canal (class 2), circulating fuels (class 3) and stored fuels (class 4). The interaction and integration of these signals in various neural circuits lead to the adjustment of food intake consumption. Class 1 signals are detected by all senses especially smell and taste and are processed by the cortico-limbic system while learning/memory and reward are often involved. Class 2 signals, such as the release of peripheral CCK, are generated during the interaction of nutrients with the mechano- and chemo-sensors before and during absorption as well as signals generated from organs such as the liver and pancreas based on interactions of absorbed nutrients with respective sensors of these organs. These signals are processed by afferent vagal and dorsal root neurons or directly

by the brain from the nucleus of the solitary tract (NTS) and the area postrema of the caudal brainstem. Class 3 signals, such as glucose, are detected at various peripheral and central locations. The arcuate nucleus of the hypothalamus is a centre of integration that receives such signals and transmits information regarding the metabolic status. Lastly, class 4 signals regarding the storage of energy, such as fat in adipose tissue and glycogen in liver, are detected at periphery and central areas such as the arcuate nucleus. A characteristic example of such signals is the hormone leptin.

Upon meal ingestion, the gastrointestinal tract senses the chemical, nutritive, osmotic, and volumetric properties of the ingested food via interaction of endocrine cells, vagal and spinal afferents. An early monitoring of the status of meal ingestion is performed from signals related to volumetric-mechanical distension of the gastric laminar walls of the stomach by the vagal sensory endings which results in glutamatergic neuronal transmission from the vagal axon projections to the nucleus of tractus solitarius (NTS) (Ritter, 2004). The nutritive and chemical properties of the food stimulate the release of a number of gut peptides and neurotransmitters from the small intestine that act as satiation signals, such as cholecystokinin (CCK), serotonin (5-HT), peptide YY (PYY), glutamate, enterostatin and glucagon-like protein 1 (GLP-1) (Chaudhri, Small and Bloom, 2006). The GI-derived satiety signals are acting on specific receptors of dendritic terminals of vagal afferent neurons whose cell bodies are found in the nodose ganglion (Smith, 1996; Ritter, 2004; Hayes *et al.*, 2010). Satiety signals are being processed and integrated based on selectivity of vagal afferent branches with varying receptor expression patterns different afferent types (i.e, myelinated or non-myelinated), different vagal neurotransmitter types (i.e, 5-HT or glutamate) and differences in intensity duration

and frequency of neuronal excitation by each gut peptide. These differences constitute to varying transmission patterns to the NTS (Ritter, 2004). One of the characteristic examples of vagal integration of satiety signals is that of CCK and gastric distension. Single vagal afferents respond to CCK release and gastric distension in response to food intake, resulting in synergistic effect in the excitation of the vagal terminals (Schwartz and Moran, 1996). Activation of CCK receptors inhibits gastric emptying therefore increasing distension (Moran and McHugh, 1982). Gastric distension leads to release of gastric 5-HT which in turn participates in the interaction of CCK with the vagal nerves in conjunction with mechanical input due to distension (Mazda *et al.*, 2004; Hayes and Covasa, 2005). Vagal integrations extend to circulating signals such as leptin. Leptin is also secreted from gastric chief cells and mucosal cells during nutrient digestion while leptin receptors are expressed both in terminals and cell bodies of vagal afferent neurons and integrate gastric and circulating leptin signalling with other GI-satiety signals such as CCK in order to enhance and increase the vagal signal to the NTS (Peters, Ritter and Simasko, 2006).

Blood circulating signals that transmit energy status are reaching the hindbrain and are directly modulating the neuronal circuits involved in energy balance. Leptin receptors (LepRb) are expressed in the parabrachial nucleus (PBN), the area postrema (AP) and the NTS (Patterson *et al.*, 2011). Parenchymal NTS leptin injection reduces food intake and body weight (Kanoski *et al.*, 2012). Viral knock down of LepRb expression in the medial NTS causes hyperphagia due to increased meal size and not frequency and CCK suppression of food intake is abolished (Hayes *et al.*, 2010; Kanoski *et al.*, 2012). Leptin has been shown to depolarise mNTS neurons while amplifying the GI satiation signals through vagal

afferents (Hisadome *et al.*, 2010). The GLP-1R is also expressed in NTS neurons and they are involved in the regulation of food intake and body weight (Hayes *et al.*, 2011). GLP-1 and Leptin signalling interact in an additive manner in the NTS while leptin's intake inhibitory effects are attenuated in the absence of GLP-1R signalling (Zhao *et al.*, 2012). The intracellular signalling involved in intake suppression is shared between GLP-1R and LepR activation in the NTS, this includes the mitogen-activated protein kinase (MAPK) and AMP-activated protein kinase (AMPK) (Bjørbæk *et al.*, 2001; Gao *et al.*, 2007; Hayes *et al.*, 2011). A small subset of NTS neurons also express CCK (Garfield *et al.*, 2012). Chemogenetic activation of the $CCK^{NTS}$ neurons reduces appetite and body weight likely mediated by their projections to MC4R-expressing neurons of the PVN in the hypothalamus (D'Agostino *et al.*, 2016). It is possible that simultaneous activation of shared signalling cascades from multiple effectors within the same NTS neuronal populations contribute to the additive and enhanced intake inhibitory signal in satiation (Berthoud *et al.*, 2006).

The hindbrain is also capable of sensing blood glucose level changes, an idea first described by Mayer, where glucose levels have an effect in the neuronal excitability of set of neurons that take part in the neuronal control of energy balance (Mayer, 1953). Glucose sensitive neurons are also found in the hypothalamus apart from the hindbrain. These neurons together with their downstream targets, are responsible for the regulation of glucose and energy homeostasis by controlling pancreas secretions, hepatic glucose production, feeding behaviour and energy expenditure (Thorens, 2010). Knock-out mice of glucose transporter 2 (GLUT2) show hyperphagia and are not capable of responding appropriately in intracerebroventricular injections of glucose or 2-deoxyglucose (Bady *et al.*, 2006).

GLUT2 expressing neurons are found in the NTS, dorsal motor nucleus of the vagus nerve (DMV) and ventrolateral medulla (VLM) (Arluison *et al.*, 2004). Their location in the hindbrain nuclei overlaps with those implicated in counter-regulatory responses for controlling glucose homeostasis (Ritter, Dinh and Zhang, 2000). Ghrelin is another gastric peptide which is inhibited by food intake and it stimulates feeding when the endogenous levels rise by binding on the growth hormone secretogue receptor (GHSR) (Overduin *et al.*, 2005). GHSR is expressed in neurons throughout the CNS and particularly in NTS and other hindbrain regions (Zigman *et al.*, 2006a). Injections of low doses of ghrelin directly in NTS increases food intake (Faulconbridge *et al.*, 2003). One reported mechanism of action, is the attenuation of neuronal activity driven by GI satiety signalling through vagal afferents. Bath application of ghrelin inhibits tyrosine hydroxylase expressing A2/C2 neurons of the mNTS which are activated by visceral afferent stimulation (Cui, Li and Appleyard, 2011).

Hindbrain nuclei control the feeding behaviour and integrate signals from various peripheral and central locations. There are primary motor neurons that control movement of the tongue, jaw, pharynx, and facial muscles and the premotor neurons that constitute the central pattern generators for patterned rhythmic oral motor behaviours such as licking, chewing, swallowing, and food rejection (Benarroch, 1998). These premotor neurons are the target of afferent projections from the hypothalamus and other forebrain nuclei in response to satiety signals (Gutierrez *et al.*, 2006).

DMV neurons that are located in the dorsomedial medulla provide vagal efferent output that controls gastric emptying rates, pancreatic and intestinal enzymatic secretions, and intestinal motility rates for the purpose of nutrient

partitioning, storage, and mobilization (Ahrén, 2000). Upon food ingestion, NTS receives vagal afferents signals, processes the information and relays it to DMV where efferent vagal output results in modulation of peripheral organs for nutrient storage control and modulation of counterregulatory hormone secretions (Travagli *et al.*, 2003; Hayes, Skibicka and Grill, 2008).

Hindbrain neurons regulate sympathetic and behavioural responses for hepatic glucose production and counterregulation (Bernard, 1855; Jordan, Könner and Brüning, 2010). Catecholaminergic (CA) neurons in the medulla are critical regulators for sympathoadrenal hyperglycemia, glucagon, and corticosterone secretion, and for food intake responses driven by glucopenia or hypoglycaemia (Ritter, Dinh and Zhang, 2000). Localised administration of an antiglycolytic agent, 5-d-thioglucose (5TG), in caudal hindbrain sites resulted in increased circulating corticosterone and glucagon plasma concentrations (Andrew, Dinh and Ritter, 2007). Neurons in the dorsal motor nucleus of the vagus (DMV) project to the pancreatic ganglions while sympathetic and parasympathetic nerve terminals are found in pancreatic islets and both can stimulate glucagon release (Ionescu *et al.*, 1983; Ahrén, 2000; Thorens, 2010). Hypothalamic descending pathways to the NTS and DMV from nuclei such as the ARC,VMH and DMH are shown to induce glucagon adrenaline and noradrenaline release (Verberne, Sabetghadam and Korim, 2014). Adrenergic neurons located in C2 (NTS) and C3 cell groups of the dorsal medulla, as well as the A1/C1 neurons of the (VLM), are targets of activation by systemic glucopenia (Ritter, Llewellyn-Smith and Dinh, 1998). The local circuits within the brainstem seem to be sufficient for an intact glucose homeostasis (Banihashemi and Rinaman, 2006; Darling and Ritter, 2009). The premotor neurons located in hindbrain's DMV nucleus are innervated by CNS locations with nutrient

sensors such as the hypothalamus. Signals of energy repletion such as long chain coenzyme A, glucose, insulin, and leptin, mediate vagal efferent output from the DMV to the liver and stimulate glucose production (Obici *et al.*, 2002; Lam *et al.*, 2005; Pocai *et al.*, 2005).

In addition to the integration of energy related signals from the local circuits of the hindbrain, these hindbrain neurons also receive input from other brain regions receiving energy signals such as forebrain and hypothalamic nuclei which also participate in the control of feeding behaviour. Orexin/hypocretin neurons of the lateral hypothalamus are involved in the control of autonomic control, sleep/wake cycle and energy balance. Some of these neurons project directly to hindbrain nuclei such as the NTS, caudal raphe, and VLM (Ciriello *et al.*, 2003; Zheng, Patterson and Berthoud, 2005). Orexin positive fibres form synaptic contacts with CA-expressing neurons of the NTS and with cfos positive neurons that are activated by gastric nutrient infusion while orexin A infusion in the hindbrain increases food intake (Zheng, Patterson and Berthoud, 2005; Puskás *et al.*, 2010). Electrical or chemical stimulation of LH neurons elicits feeding behaviour in satiated rats while inhibiting mNTS neurons. Taken together, orexin neurons from the LH stimulate feeding by suppressing NTS processing of the satiety signals from the vagal afferents (Jiang, Fogel and Zhang, 2003; Berthoud and Münzberg, 2011). The central melanocortinergic system is important in energy homeostasis as MC4-R mutations result in hyperphagia and obesity in humans and mice (Huszar *et al.*, 1997; Hinney *et al.*, 1999). The NTS and DMV nuclei have one of the highest expression of MC4-R and they receive input of MC agonist ligands such as aMSH, from local POMC neurons or MC antagonists from the ARC nucleus of the hypothalamus (Broberger *et al.*, 1998; Kishi *et al.*, 2003; Zheng *et al.*, 2010). Delivery of MC4-R agonists in

NTS reduces food intake and increases body temperature and heart rate, whereas antagonist delivery has the opposite effects. Meal size is reduced by hindbrain delivery of a MC3/4-R agonist whereas hindbrain delivery of a MC3/4-R antagonist increases meal size (Sutton *et al.*, 2005; Skibicka and Grill, 2009). These effects mimic the CCK mediated vagal afferent signals to the NTS, suggesting that MC4R signalling acts downstream of CCK intake suppression (Fan *et al.*, 2004). The melanocortin circuit from the ARC to the NTS contributes to ARC and hindbrain's intake suppressive effect of leptin signalling (Skibicka and Grill, 2009; Zheng *et al.*, 2010). There is also indirect input from ARC to NTS through the Paraventricular nucleus (PVN) of hypothalamus. POMC neurons of the ARC, that respond to leptin signalling, project to PVN neurons expressing MC4-R and a variety of hormones including oxytocin (OT). These PVN neurons, including OT-expressing neurons, send projections to the hindbrain (Rinaman, 1998; Liu, Kishi, Aaron G. Roseberry, *et al.*, 2003). NTS neurons activated upon CCK injection are in contact with OT positive fibers while OT antagonist injection in NTS attenuates the intake suppression observed by systemic CCK administration. Application of OT on NTS slices, stimulated by vagal afferent axons, increases the frequency of miniature EPSCs in NTS neurons through increased glutamate release from vagal afferent terminals leading to enhanced visceral afferent transmission (Blevins *et al.*, 2003; Peters *et al.*, 2008). OT communication to the NTS from the hypothalamus is necessary for the emanation of various other hypothalamic satiety signals. Hypothalamic leptin induced anorexia is attenuated by OT antagonist icv injection. Leucine infusion in the hypothalamus suppresses food intake but the effect is abolished upon hindbrain icv of Ot antagonist. Nesfatin-1, an intake suppressing peptide located in PVN neurons, co-expressing also OT, is ineffective in reducing

intake while OT antagonist is infused in the hindbrain (Blevins, Schwartz and Baskin, 2004; Blouet *et al.*, 2009a; Maejima *et al.*, 2009).

The reward aspect of food intake is modulated by mesolimbic structures that are associated with reward processing which receive input from the oral cavity. The hindbrain receives cranial afferent input which innervate neurons in the rostral NTS expressing taste receptors. In turn, these neurons then project to the PBN. PBN axons then convey gustatory afferent activity to the medial extension of the thalamic trigeminal relay, or along a separate pathway to the LH, central nucleus of the amygdala (CeA), and the bed nucleus of the stria terminalis (BNST). PBN neurons then project to limbic structures such as CeA and BNST which engage with the NAc in order to modulate dopamine signalling (Norgren, Hajnal and Mungarndee, 2006). This feed-forward neural circuitry leads to the initiation and appetitive mechanisms of food intake. The inhibitory feedback circuitry that is activated during the meal progression is relayed via vagal afferents to the caudal NTS and direct projections from the NTS to VTA and NAc (Dossat *et al.*, 2011; Alhadeff, Rupprecht and Hayes, 2012). Such a connection is the one from the GLP-1 neurons that monosynaptically project to VTA and NAc and are required for normal food intake and body weight regulation. During a meal, vagally mediated satiation signals (such as CCK) activate the GLP-1 neurons (Hisadome *et al.*, 2011). Hence, this acts as an integration mechanism for satiation signals to communicate with higher-order regions of the forebrain, and modulate food intake by decreasing the rewarding value of the ongoing meal.

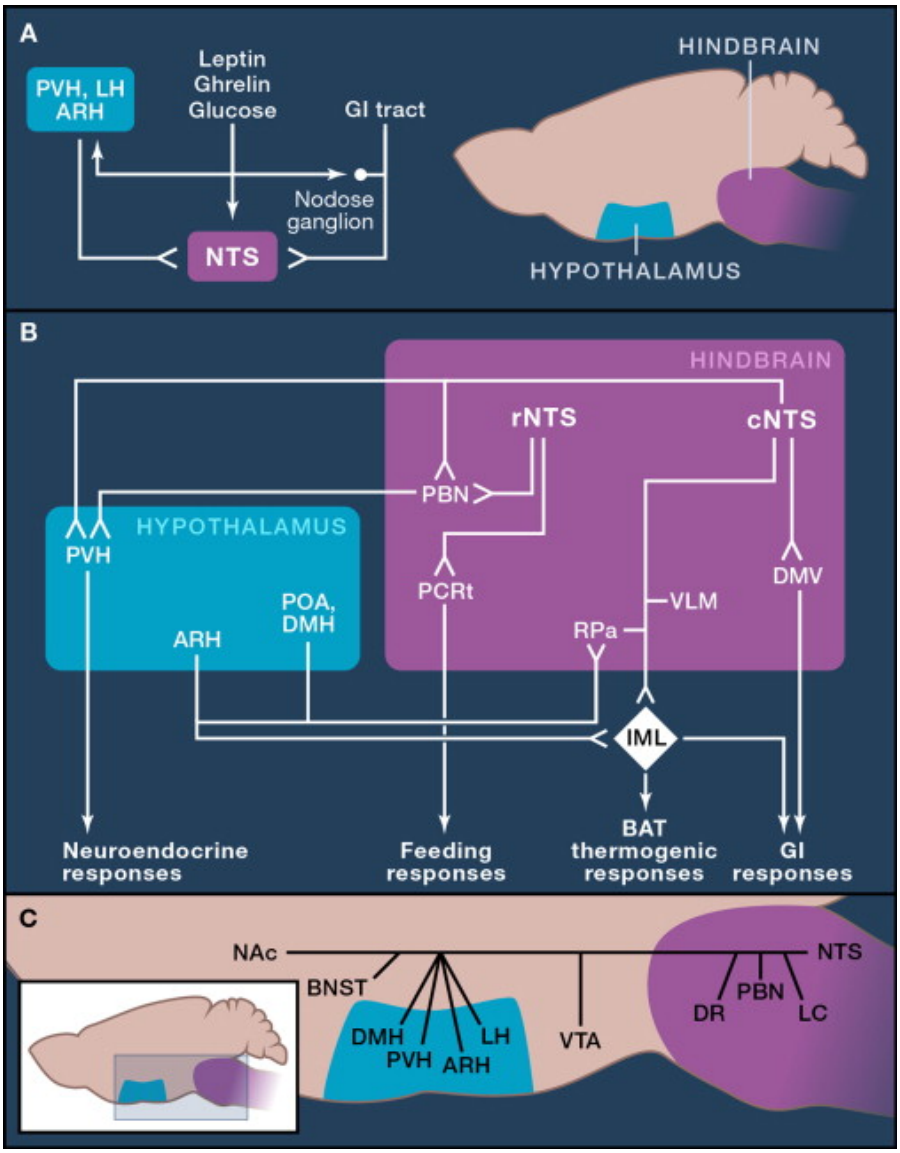


**Figure 1: Schematic of hindbrain neuronal networks and their afferents to hypothalamic regions participating in the regulation of energy balance.** A) Input to NTS from signals such as leptin, ghrelin and glucose, GI via vagus nerve and hypothalamic neurons. B) summary of NTS output. Neurons project to DMV to control parasympathetic gastrointestinal responses or to other hindbrain and hypothalamic regions to control sympathetic efferent responses of relevance to energy expenditure and gastrointestinal responses, and to PVH neurons to influence neuroendocrine responses. Neurons from rostral regions of NTS (rNTS) and PBN neurons project to the parvocellular reticular formation (PCRt) to control ingestive consummatory response. C) Rostral monosynaptic projections of NTS neurons to the mentioned regions. Adapted from: (Grill and Hayes, 2012).

## 1.2 Hypothalamus as a central integrator of the neuronal circuits in response to energy and metabolic needs

The hypothalamus is a brain region which has been studied extensively as it is one of the most important regulators of food intake and energy homeostasis. One of the most significant and well researched nuclei, is the arcuate nucleus (ARC) which has a central role in feeding and metabolism (Myers and Olson, 2012). The ARC is located near to the median eminence (ME), a circumventricular organ that has dense fenestrated capillaries that create a 'leaky' blood-brain barrier (BBB) environment for the adjacent region of the hypothalamus. The ME facilitates transport of peripheral hormonal and nutrient signals and their sensing by the ARC neurons (Rodríguez, Blázquez and Guerra, 2010). The ARC is well situated to receive hormonal and nutritional metabolic signals from the peripheral circulation as well as peripheral and central neuronal inputs to integrate information and respond appropriately for food intake and energy homeostasis regulation.

There are two distinct, functionally antagonistic types of neurons in the ARC: the orexigenic (appetite-stimulating) neuropeptide Y (NPY) and agouti-related peptide (AgRP)-expressing AgRP/NPY neurons and the anorexigenic (appetite-suppressing) pro-opiomelanocortin (POMC)-expressing POMC neurons (Balthasar *et al.*, 2005; Gropp *et al.*, 2005). POMC neurons project mainly to nearby local regions in neurons in the paraventricular hypothalamic nucleus (PVN), but also to the dorsomedial hypothalamus (DMH), the lateral hypothalamus (LH) and the ventromedial hypothalamus (VMH). These neurons that receive ARC input are called second-order neurons in the circuit and further process the received information and project to multiple neuronal circuits outside of the hypothalamus, leading to an integrated response on energy intake and expenditure (Kleinridders,

Könner and Brüning, 2009; Waterson and Horvath, 2015; Roh, Song and Kim, 2016). PVN neurons control the outflow of sympathetic signals to peripheral organs and early studies of destruction of the PVN leads to obesity due to increased food intake (hyperphagia) (Leibowitz, Hammer and Chang, 1981; Kannan, Hayashida and Yamashita, 1989). Likewise, destruction of the VMH also leads to hyperphagia and obese phenotype. However, studies that destroy the DMH and the LH produce an opposite effect with animals decreasing dramatically their food intake, leading to a lean phenotype (Milam *et al.*, 1980; Shimizu *et al.*, 1987; Bellinger and Bernardis, 2002).

Upon nutrient ingestion, POMC is cleaved to α-melanocyte-stimulating hormone (α-MSH) which is released from POMC-axons to activate melanocortin 3 and 4 receptors (MC3/4R) on downstream neurons, including neurons in the PVN, resulting in a decrease in food intake and an increase in energy expenditure (Könner, Klöckener and Brüning, 2009). Disruption of the MC4R of the PVN results in obesity as a result of hyperphagia and reduced energy expenditure, along with dysregulation in glucose homeostasis (Balthasar *et al.*, 2005). Downstream of MC4 signalling are brain-derived neurotrophic factor (BDNF), corticotropin-releasing hormone (CRH) and thyrotropin-releasing hormone (TRH) (Kim *et al.*, 2000; Lu *et al.*, 2003; Nicholson *et al.*, 2007). Despite the food intake inhibiting role of hypothalamic melanocortinergic neurons, MC4R activation increases energy expenditure via brown adipose tissue (BAT) activation via activation of the sympathetic nervous system (Voss-Andreae *et al.*, 2007).

Upon a decrease in available energy, for example during fasting, AgRP/NPY neurons are activated which also send projections to the PVN and LH and co-release NPY and AgRP (Betley *et al.*, 2013). NPY directly stimulates food intake via

activation of NPY Y1 and Y5 receptors (Stanley and Leibowitz, 1984; Yokosuka, Kalra and Kalra, 1999; Cabrele *et al.*, 2000). NPY reduces energy expenditure via a Y1-receptor-mediated reduction in tyrosine hydroxylase expression in the PVN and the brainstem, which leads to a decreased sympathetic output to the BAT and concomitantly reduced BAT activity (Shi *et al.*, 2013). AgRP acts as an inverse agonist of MC3/4R, thereby preventing the anorexigenic effect of α-MSH on second-order neurons (Ollmann *et al.*, 1997).

AgRP/NPY neurons directly inhibit POMC neurons of the ARC via inhibitory γ-aminobutyric acid (GABA) action (Cowley *et al.*, 2001). Recent optogenetic modulations (activation or inhibition) of the ARC AgRP neurons have elucidated further the role of their synaptic connections. Interestingly, suppression of POMC neuron activity by AgRP neurons was shown not to be required for acute feeding induction. The exclusive activation of the ARC to PVN connection strongly induces feeding while exclusive activation of the AgRP/NPY→PBN interconnection is not sufficient to induce feeding. Distinct AgRP neuron subpopulations project to different brain regions and that activation of some projections – including those to the PVN and LH, but not to the PBN – are able to independently induce feeding similar to somatic activation of AgRP neurons (Atasoy *et al.*, 2012; Betley *et al.*, 2013).

POMC and AgRP/NPY neurons also receive activating glutamatergic feedback input from the VMH and the PVN, whereas PVN neurons receive inhibitory innervation from LH neurons that promote feeding, leading to a precise and controlled integration of signals for food intake regulation (Waterson and Horvath, 2015). Their projections to the PVN also regulate energy expenditure, with POMC neurons increasing and AgRP/NPY neurons decreasing the metabolic activity of brown adipose tissue (BAT). Thus, in the fasting state, energy expenditure is

decreased, and following food intake, energy expenditure is increased (Enriori *et al.*, 2011; Shi *et al.*, 2013). AgRP/NPY neuron activation regulates BAT glucose uptake through specific projections to the bed nucleus of the stria terminalis (BNST) (Steculorum *et al.*, 2016). BNST is involved in the control of neuroendocrine and autonomic responses, as well as feeding and reward behaviour (Dong and Swanson, 2006).

Both POMC and AgRP/NPY neurons express receptors for peripheral metabolic hormones such as insulin and leptin. Insulin is secreted from pancreatic β-cells upon nutrient ingestion and plays an important role in the peripheral regulation of energy and glucose homeostasis (Prentki, Matschinsky and Madiraju, 2013). It controls peripheral glucose metabolism by suppressing hepatic glucose production (HGP) via direct action on hepatic insulin receptors. It also regulates glucose and energy homeostasis at the level of the hypothalamus (Belgardt and Brüning, 2010). POMC neurons are excited by application of purified insulin while activation of insulin receptors increases POMC mRNA expression (Benoit *et al.*, 2002; Qiu *et al.*, 2014). Deletion of both insulin and leptin receptors from POMC neurons impairs glucose homeostasis and specifically leads to systemic insulin resistance (Hill *et al.*, 2010). Insulin and leptin action on POMC neurons also increases the browning of white fat which leads to enhanced metabolic activity(Dodd *et al.*, 2015). The insulin action on POMC neurons also controls adipose-tissue lipolysis and prevents high-fat-diet-induced liver steatosis (Shin *et al.*, 2017). On AgRP/NPY neurons, insulin action is required for the suppressive effect of insulin on HGP. Insulin induces a hyperpolarization and a decreased firing rate of AgRP neurons, thus reducing the release of AgRP and other neurotransmitters, affecting peripheral hepatic innervation, and finally leading to increased interleukin (IL)-6

expression in the liver. IL-6 leads to decreased expression of glucose-6-phosphatase and subsequently to reduced gluconeogenesis (Könner *et al.*, 2007). Leptin is released from adipose tissue in response to insulin levels and enters the blood circulation, with levels being directly proportional to the amount of fat stores of the whole body (Russell *et al.*, 2001; Myers and Olson, 2012). Leptin directly excites POMC neurons and induces *POMC* expression, while exerting an inhibitory effect on AgRP/NPY neurons and the expression of *AGRP* (Russell *et al.*, 2001). Leptin and insulin are both required in coordination to act at the level of the hypothalamus for their anorexic and glucoregulatory effect. However, they are acting on different subpopulations of POMC neurons, the characterisation of which is still pending (Belgardt and Brüning, 2010; Williams *et al.*, 2010; Vogt and Brüning, 2013). In the DMH, leptin increases energy expenditure via enhanced sympathetic activation of the BAT, regulating body weight but with no change in food intake (Rezai-Zadeh *et al.*, 2014).

The VMH has been implicated in a wide array of physiological and behavioural processes (Hetherington and Ranson, 1940; King, 2006). Based on rodent lesion analyses, this hypothalamic region appears critical for female reproductive behaviour, initiating an innate fear response, maintaining daily rhythms of glucocorticoid secretion, lordosis response, thermogenesis, and salt and water balance and for normal feeding responses (Fujimoto, 1980; Perkins *et al.*, 1981; Egawa *et al.*, 1991; Cohen and Pfaff, 1992). In the rodent brain, the VMH is easily recognized by the prominent bilateral Nissl-stained clusters located dorsal to the ARC and posteroventral to the PVN. These clusters are visible as early as embryonic day 15 (E15) (McClellan, Parker and Tobet, 2006). In the adult, the VMH can be subdivided crudely into three anatomical regions: the dorsomedial ($VMH_{DM}$),

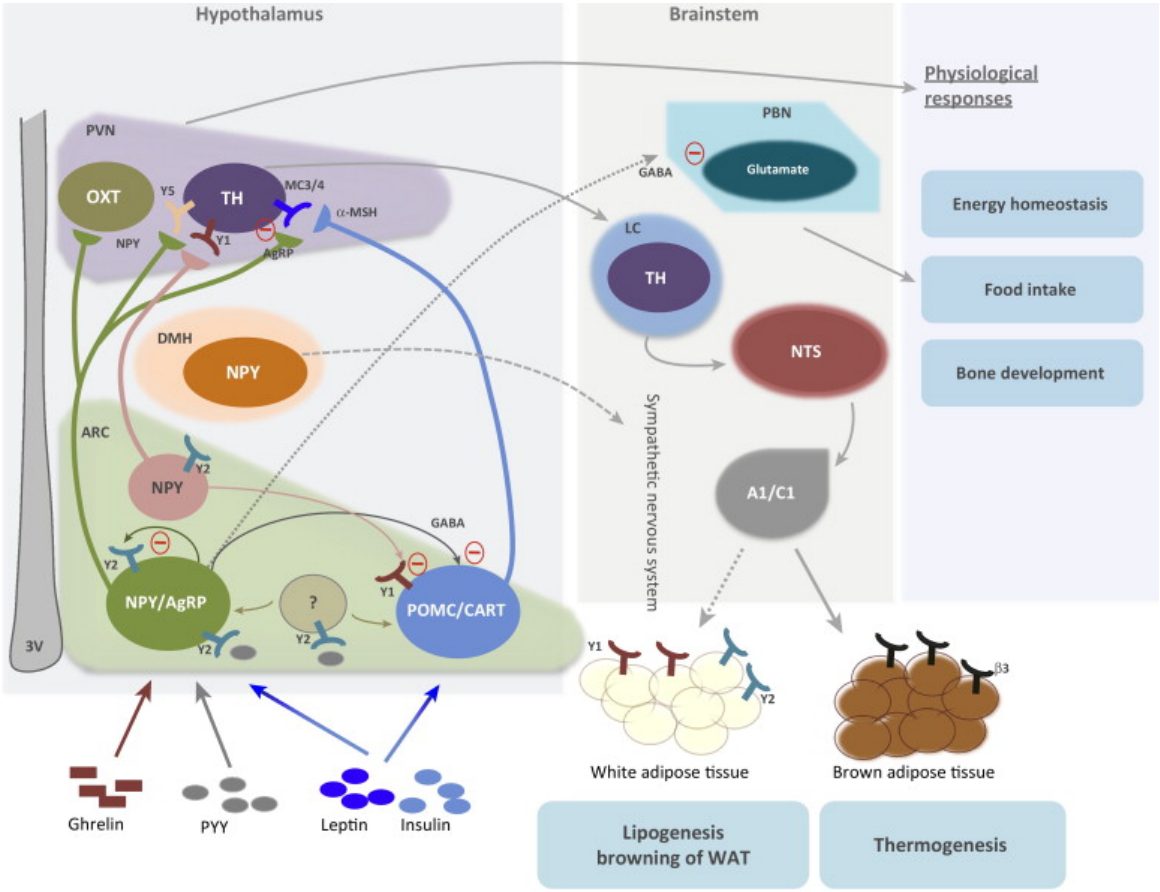


**Figure 2: Schematic of the main neuronal networks of the hypothalamus and their afferent projections that regulate various physiological responses.** ARC-derived NPY can activate Y5 receptors located on neurons in the PVN to regulate feeding. PYY exerts its satiety effects through the activation of Y2 receptors expressed on NPY/AgRP neurons in the ARC. Y2 receptors can also serve as an autoreceptor for NPY to inhibit its neuronal activity. Y1 and Y2 receptors are expressed in several peripheral tissues such as white adipose tissue. Abbreviations: 3 V, third ventricle; ARC, arcuate nucleus; TH, tyrosine hydroxylase; PVN, paraventricular nucleus; NTS, nucleus tractus solitarius; DMH, dorsomedial hypothalamus; LC, locus coeruleus; AgRP, agouti-related peptide; POMC, proopiomelanocortin; CART, cocaine- and amphetamine-regulated transcript; GABA, γ-aminobutyric acid; α-MSH, α-melanocyte-stimulating hormone; OXT, oxytocin. Adapted from: (Loh, Herzog and Shi, 2015).

central ($VMH_C$), and ventrolateral ($VMH_{VL}$). Functional studies suggest that the $VMH_{DM}$ regulates energy homeostasis, whereas the $VMH_{VL}$ controls female reproduction. To date, the $VMH_C$ is not associated with any specific function, and there are no known molecular markers specific to this subregion.

Earlier studies of VMH lesions (potentially affecting nearby hypothalamic regions) affect both body weight and food intake (Choi *et al.*, 2013b). Neurons from the VMH have also been shown to project to the brainstem nuclei involved in the control of thermogenesis (Morrison, 1999). VMH neurons also connect locally to the ARC to POMC expressing neurons. POMC neurons received strong excitatory input from the medial VMH (mVMH). The strength of the excitatory input from the mVMH neurons to POMC neurons was diminished by fasting (Sternson, Shepherd and Friedman, 2005; Krashes *et al.*, 2014). The cytoarchitecture of the VMH is regulated by a transcription factor, stereoidogenic factor 1 (SF1), which is selectively expressed only in VMH region in the brain although it is also found in the gonads, pituitary and adrenal glands. Loss of SF-1 leads to changes not only in VMH cellular topography, but also in neuronal connections of the VMH (Ikeda *et al.*, 1995). Mice lacking SF1 in the VMH develop obesity in the absence of increased food intake (Majdic *et al.*, 2002).

Leptin and insulin also act on the VMH to control energy homeostasis. Mice with insulin receptor deletion in VMH-specific steroidogenic-factor-1 (SF-1) neurons are protected from diet-induced obesity and deterioration of glucose metabolism and POMC neuron activity is increased under high-fat diet conditions (Klöckener *et al.*, 2011). Enhanced leptin receptor signalling in SF-1 neurons within the VMH results in improved glucose homeostasis while body weight is not significantly affected (Zhang *et al.*, 2008). Targeted disruption of leptin signalling in SF1 neurons affects

body weight and susceptibility to diet-induced obesity, primarily by affecting thermogenesis (Dhillon *et al.*, 2006; Xu *et al.*, 2010a). LepR deleted in both Pomc and SF-1 neurons resulted in an additive effect in body weight increase, showing that LepRs in SF-1 neurons are essential for normal body weight homeostasis (Balthasar *et al.*, 2004). Leptin mediates some of its effects via activation of phosphatidyl inositol 3-kinase (PI3K) signalling in the SF-1 neurons and it is required for diet-induced obesity (Xu *et al.*, 2010b). Leptin and insulin are both acting via PI3K signalling but on different subpopulations of SF-1 neurons while utilising specific PI3K catalytic subunits (p110α or p110β). Leptin activates or inhibits distinct subpopulations while insulin uniformly inhibits the SF-1 neurons (Sohn *et al.*, 2016). Postnatal deletion of *SF1* also impairs BAT thermogenesis (Kim *et al.*, 2011). Genetic lesion of the glutamate synaptic vesicular transporter VGLUT2 from the VMH neurons also result in a moderate disruption of normal energy homeostasis (Kim *et al.*, 2011).

Glucose is the primary fuel of the brain. Hypothalamic glucose sensing neurons were discovered in the 1960s, and there is evidence that they play a role in maintaining cerebral glucose levels (Anand *et al.*, 1964). The hypothalamus also receives and integrates input from other central and peripheral glucose sensors (Routh, Donovan and Ritter, 2012). The saturable glucose transporter isoform-1 is the primary glucose transporter at the blood brain barrier (Cardoso, Brites and Brito, 2010). However, blood glucose entry does not only rely on this transporter, and suggests the evidence of distinct diffusion barriers. As a result, glucose concentrations in the brain are lower than that of the periphery. Differential organization and expression of the tight junction proteins within the ependymal cells which line the third ventricle and the median eminence leads to distinct patterns of

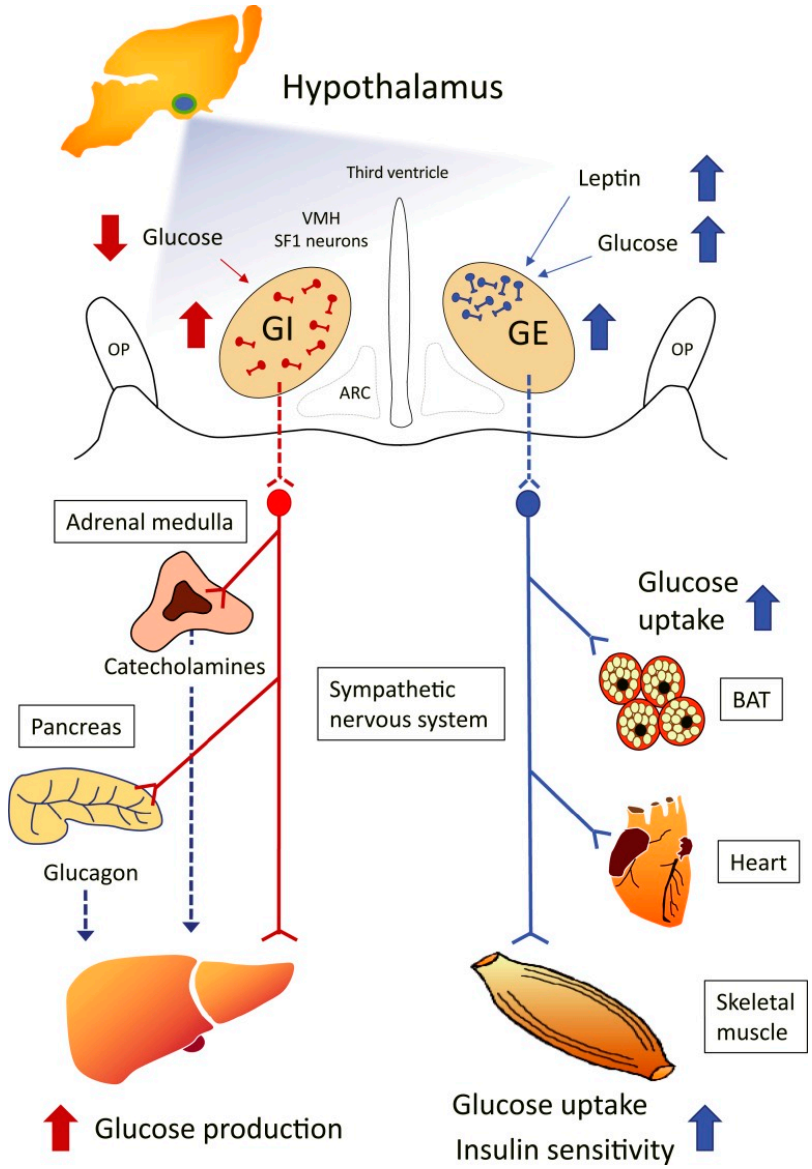


**Figure 3: Schematic of the GE and GI neurons of the VMH and their role in systemic glucoregulation.** Subsets of VMH neurons also express SF1 and leptin receptors, with some of these neurons overlapping with GE and GI neurons. An increase in blood glucose level activates the GE neurons in the VMH, which in turn activate the sympathetic nervous system and increase insulin sensitivity and glucose uptake in BAT, the heart, and skeletal muscle, but not in white adipose tissue. A decrease in blood glucose level activates the GI neurons in the VMH, which results in activation of the sympathetic nerves innervating the liver, adrenal medulla (stimulating the release of catecholamines), and pancreas (stimulating the release of glucagon) and an increase in hepatic glucose production. ARC, arcuate nucleus of the hypothalamus; OP, optic tract. Adapted from: (Shimazu and Minokoshi, 2017).

diffusion from blood and cerebrospinal fluid. These barriers are not constant under all physiological conditions. During fasting and glucoprivation the structural components of these hypothalamic diffusion barriers were altered such that ARC glucose levels significantly exceeded those in the VMH (Mullier *et al.*, 2010; Langlet *et al.*, 2013).

There are glucose sensing neurons dispersed throughout the hypothalamus, but especially in the ARC, VMH, PVN and LH nuclei. They are further characterised as glucose-excited (GE) or glucose-inhibited (GI) neurons based on their response to physiological changes in extracellular glucose. (Kang *et al.*, 2004; Burdakov, Gerasimenko and Verkhratsky, 2005; Melnick, Price and Colmers, 2011). The mechanism underlying glucose sensing by VMH GE neurons has been the most extensively characterized. GE neurons utilize a glucose sensing mechanism similar to that of the pancreatic β-cell. Increased glucose metabolism raises the ATP/ADP ratio and closes the ATP sensitive potassium channel (KATP) leading to depolarization while the initial phosphorylation of glucose to glucose-6-phosphate is catalyzed by the pancreatic form of hexokinase IV, glucokinase. In addition to the ubiquitous glucose transporter 3 (GLUT3), subpopulations of VMH GE neurons also express GLUT2 and the insulin-sensitive GLUT4. Interestingly, a fairly large percentage of GE neurons express both GLUT4 and the insulin receptor. About 25% of VMH GE neurons possess the sodium glucose co-transporter (SGLT) which could couple glucose uptake with membrane depolarization. GnRH neurons and PVN GE neurons use a non-selective cation channel, while the melanin-concentrating hormone neurons use an unidentified K channel. Taken together, GE neurons demonstrate a high degree of heterogeneity in the cellular mechanisms for sensing glucose (Song *et al.*, 2001; Kang *et al.*, 2004, 2006; Burdakov, Gerasimenko and

Verkhratsky, 2005; Melnick, Price and Colmers, 2011; Roland and Moenter, 2011). GI neurons are also widely dispersed throughout the hypothalamus, including the VMH, ARC, paraventricular nucleus, dorsomedial nucleus, and the lateral hypothalamus (Song and Routh, 2006; Williams *et al.*, 2008). GI neurons either respond to glucose itself or regulated by glucose metabolism (e.g changes in ATP) Similar to GE neurons, some of the metabolism-dependent GI neurons also express GLUT2, GLUT4, SGLT2, and/or the insulin receptor (Kang *et al.*, 2004).The VMH GI neurons are the most extensively researched. Low glucose levels enable AMPK to interact with nitric oxide, enabling the chloride channel closure, membrane depolarization, and increased action potential frequency. NO synthase and NO signalling through its receptor, soluble guanylyl cyclase (sGC), are critical for both glucose sensing by GI neurons and the *in vivo* counter-regulatory response (CRR) to hypoglycaemia (Murphy, Fakira, *et al.*, 2009; Fioramonti *et al.*, 2010, 2013). VMH neurons have distinct glucose sensing mechanisms from the ARC NPY/AgRP neurons since they don't express nNOS and their activity is not affected by changes in intracellular AMPK. They do however respond to presynaptic changes in AMPK activity (Sternson, Shepherd and Friedman, 2005; Fioramonti *et al.*, 2007; Yang *et al.*, 2011).

Orexin-expressing GI neurons, which are only found in the lateral, perifornical and dorsomedial hypothalamus are inhibited by glucose and the glucose analog, 2-deoxyglucose but not downstream metabolites (Gonzalez *et al.*, 2008; Sheng *et al.*, 2014). Glucose activates a leak tandem-pore potassium (K2P) channel and Twik-related acid-sensitive potassium-like (TASK) 1/3 channels which increase their firing rate (González *et al.*, 2009). The GABA-GI neurons of the LH are also metabolism independent but distinct from the orexin neurons whereas the NPY-GI neurons are

not studied adequately yet. The PVN GI neurons may also be metabolism independent because they do not appear to express GK (Marston *et al.*, 2011; Karnani *et al.*, 2013; Stanley *et al.*, 2013).

The regulation of glucose sensing in the hypothalamus is dependent on receiving hormonal signals and the detection of other nutrients apart from glucose. VMH GE neurons are inhibited by insulin and peripheral leptin in the presence of extracellular levels of glucose. Insulin effect persists in physiological glucose concentrations while at low concentrations prevents inhibition of GE neurons. Hypothalamic insulin infusion suppresses hepatic glucose production *in vivo* (Cotero, Zhang and Routh, 2010; Rojas and Schwartz, 2014). Leptin inhibits the GI population of ARC NPY/AgRP neurons while it also attenuates the activation of VMH- and lateral hypothalamic orexin-GI neurons by decreased glucose (Baver *et al.*, 2014; Sheng *et al.*, 2014). Insulin stimulates NO production by VMH GI neurons under decreased glucose conditions while the insulin signalling is important for their activation as shown in a neuronal insulin-receptor knockout (NIRKO) mouse (Canabal, Song, *et al.*, 2007; Diggs-Andrews *et al.*, 2010). Insulin-induced hypoglycaemia also activates the orexin GI neurons of the LH (Kohno *et al.*, 2003). Ghrelin activates both NPY-GI and orexin-GI neurons (Kohno *et al.*, 2003). Both GE and GI neurons of the VMH, apart from glucose, respond to free fatty acids and ketones (Le Foll *et al.*, 2014). Central fatty acid infusion modulates glucose-induced insulin secretion and peripheral insulin sensitivity (Cruciani-Guglielmacci *et al.*, 2004; Marsollier *et al.*, 2009). L-leucine injection to the 3$^{rd}$ ventricle reduces food intake which is mediated by mTOR signalling in GI neurons of the VMH (Cota *et al.*, 2006; Canabal, Song, *et al.*, 2007). Direct application of leucine in the ARC increases the action potential frequency of POMC neurons (Blouet *et al.*, 2009b).

The physiological role of glucose sensing neurons can be summarised in integration and reinforcement of neuronal circuits that compensate energy deficits when glucose levels decrease. This integration is achieved at various levels through the variable sensitivity and integrated inputs of multiple glucose sensing neurons. Their roles can be further analysed at the level of hypoglycaemic detection, during fasting/starvation or energy surplus. Inducing hypoglycaemia with insulin, increases *cfos* activation in a number of hypothalamic nuclei, including the ARC, the PVN, the DMH and the LH (Diggs-Andrews *et al.*, 2010). Hypoglycaemia or central glucoprivation induces *cfos* expression in several known hypothalamic glucose sensing populations including the LH orexin neurons as well as NPY neurons in the ARC, DMH and LH (Cai *et al.*, 2001; Marston *et al.*, 2011). Interestingly, insulin-induced hypoglycemia or glucoprivation does not induce cfos expression in VMH GI neurons which could be explained by the requirement of the NO-sGC pathway under low glucose levels as cfos may not be upregulated downstream (Szepietowska *et al.*, 2011; Stanley *et al.*, 2013). The VMH GI neurons have a key role in CRR. VMH NO signaling is critical for glucose sensing by VMH nNOS-GI neurons as well as for the full CRR. That is, nNOS inhibition prevents activation of VMH nNOS-GI neurons by decreased glucose while the CRR is significantly impaired (Fioramonti *et al.*, 2010).

Glucose sensing neurons have a primary role in sensing the state of energy fuels during starvation and orchestrate energy mobilisation. The brain utilises exclusively glucose as its fuel. Thus, adequate levels of glucose in the blood is a primary aim of the neuroendocrine system. During starvation, there is first mobilisation of glycogen stores from the liver for gluconeogenesis while fatty acids are used to cover the energy needs of the rest of the body. Upon glycogen stores

depletion, muscle catabolism provides the amino acids for gluconeogenesis while at final stages fatty acids are converted to ketones in the liver to fuel the brain (Straub *et al.*, 2010). Hormonal changes which occur during fasting (e.g., reduced leptin and increased ghrelin) activate GI neurons and enhance their activation by decreased glucose (Kohno *et al.*, 2003; Murphy, Fioramonti, *et al.*, 2009; Sheng *et al.*, 2014). Fasting increases NPY gene expression and its release as well as *cfos* expression and action potential frequency in ARC NPY/AgRP-GI neurons (Murphy, Fioramonti, *et al.*, 2009). AgRP deficiency impairs ketone body release from the liver during starvation (Warne *et al.*, 2013). Increased activation of VMH nNOS-GI neurons at low glucose is consistent with enhanced gluconeogenesis (Fioramonti *et al.*, 2010). Glucose sensing during hyperglycemia is less well studied so far. Acute hyperglycemia prevents VMH GI neurons from producing NO and depolarizing in response to decreased glucose as a result of mTOR inhibition of AMPK (Canabal, Potian, *et al.*, 2007). Assessing the inhibition of VMH GE neurons from *db/db* (LepR deficient) diabetic mice, there are changes in the range of glucose decrease that is required to effectively inhibit them. A maximal glucose decrease of 0.1 mM led to same inhibition with the non-diabetic controls while a mid-range decrease of 0.5 mM significantly enhanced their inhibition (Cotero, Zhang and Routh, 2010). Also, there are two additional populations of ARC glucose sensing neurons which respond to changes in extracellular glucose above 5 mM: the high-GE (HGE) and high-GI (HGI) neurons (Fioramonti *et al.*, 2004). Such high glucose concentrations in the brain have not been reported but it could be possible that the hypothalamic BBB permeability transiently changes under certain nutrient status and metabolic signals from the environment to allow for higher transient glucose concentrations to accommodate those ARC glucose sensing neurons (Langlet *et al.*, 2013).

## 1.3 CCK-expressing neurons in the brain

CCK is expressed as a 115-amino acid long pre-mature form which is then subjected to a series of post-translational modifications such as signal peptide cleavage, sulfation and carboxylation and then cleaved into several active peptides (CCK-83, CCK-58, CCK-33, CCK-22, CCK-8) of which the CCK-8 is the predominant form found in neurons in the central nervous system (CNS) (Rehfeld *et al.*, 2003). CNS CCK is expressed in the NTS and several hypothalamic nuclei, both regions that are implicated in the control of food intake (Vanderhaeghen *et al.*, 1980; Beinfeld, 2001).

CCK is expressed in various brain regions in the neonatal and adult brain. At E8.5 in the mouse, CCK expression is found in neural crest and in the neural tube cells. At E12.5, there is expression in the spinal cord, trigeminal ganglion, the primordium of the anterior pituitary and encephalic regions. At E14.5 *Cck* mRNA is apparent in the median eminence, the anterior amygdala, anterior hypothalamus and the thalamus. By E17.5, CCK is being expressed by most brain areas including the cortex, the hippocampus and in many hypothalamic nuclei (Giacobini and Wray, 2008). In adult rats, *Cck* mRNA expression was found in the olfactory bulb, the cerebral cortex in layers II/III and V/VI, the piriform cortex, the amygdala, the subiculum, the hippocampus, most hypothalamic nuclei (para- and periventricular nucleus, supraoptic, dorsomedial and supramammillary nuclei and few cells in the posterior area and the medial mammillary nucleus), the thalamus, midbrain (ventral tegmental area, interfascicularis nucleus, substantia nigra, linearis rostralis, central gray, edinger-westphal nucleus, superior and inferior colliculus), in the cerebellum (reticular formation, parabrachial nucleus) and rostral striatum and nucleus accumbens (Hökfelt *et al.*, 1985; Schiffmann and Vanderhaeghen, 1991).

CCK can be released from neurons as it has been directly in brain slices and its presence in synaptosomes. Potassium-induced depolarization caused a calcium-dependent release of CCK-8 (Dodd, Edwardson and Dockray, 1980; Emson, Lee and Rehfeld, 1980).

CCK was originally thought to be expressed in interneurons (Hendry *et al.*, 1984; Nunzi *et al.*, 1985; Sloviter and Nilaver, 1987) but it was later shown by *in-situ* hybridisation that pyramidal neurons in cortex and hippocampus express C*ck* mRNA (Schiffmann and Vanderhaeghen, 1991) while tracing studies from cortex to striatum and the thalamus have also found cortical pyramidal neurons that contain C*ck* mRNA (Burgunder and Young, 1990; Senatorov, Trudeau and Hu, 1995). CCK immunoreactivity in the amygdala has also been shown in the axon hillocks and initial segments of pyramidal neurons after colchicine injections. The detection of CCK only under colchicine treatment, which inhibits axonal transport by disrupting microtubules, suggests that CCK-8 or a larger precursor is synthesised in the somata of pyramidal neurons and immediately transported to the axons (Mascagni and McDonald, 2003). This is in alignment with the CCK in situ hybridisation publications which show high number of CCK positive neurons that have pyramidal morphology and size.

Despite the presence of CCK neurons throughout the brain, they haven't been extensively characterised in most of the brain regions with the exception of the hippocampus. Hippocampal CCK interneurons have been extensively studied to reveal the distribution of somatic, axonal and synaptic receptors and electrophysiological properties as well as their afferent and efferent connections that give rise to behaviour dependent electrical activity patterns (Freund and Katona, 2007). Hippocampal and cortical CCK interneurons are born in the Caudal

ganglionic eminence (CGE) and specifically the hippocampal CCK neurons are being born between E11.5 to E16.5 (Morozov, Torii and Rakic, 2009; Tricoire *et al.*, 2011). Most CCK neurons in the CA1 region are basket cells that innervate pyramidal neurons and other interneurons. Sub-populations of them also express VIP or vGlut3. There are also Schaffer collateral associated cells that are positive for CCK with some of them co-expressing calbindin. They project to apical and basal dendrites of pyramidal cells and to other interneurons including other Schaffer collateral associated cells and they exert perisomatic inhibition (Somogyi and Klausberger, 2005). CCK interneurons are regular spiking cells with a maximum firing rate of 40-50 Hz (Pawelzik, Hughes and Thomson, 2002). CCK basket cells receive strong GABAergic and serotonergic input and are innervated by distal subcortical regions. They express serotonin (5HT-3), acetylcholine, endocanabinoid and estrogen receptors. They have been implicated in mood disorders and anxiety-related phenotypes mediated by nicotinic, 5-$HT_3$ and cannabinoid receptors due to their ability to fine tune the activity of pyramidal neurons they innervate (Freund, 2003; Freund and Katona, 2007).

In relation to the hippocampal CCK neurons and their importance to anxiety and other mood-related disorders, CCK neurons have also been studied in nuclei of the amygdala and especially in basolateral amygdala (BLA) and they have been shown to modulate responses to anxiety and similar behaviours (Bowers, Choi and Ressler, 2012; Zwanzger, Domschke and Bradwejn, 2012). The CCK system of amygdala has been shown to be anxiogenic and critical for the amygdala to drive fear exression. There are many functional and behavioural studies that show CCK2R knock out mice having a decrease in anxious behaviour (Horinouchi *et al.*, 2004) while CCK2R antagonists are anxiolytic (Cohen *et al.*, 2004). Most

importantly, CCK expression within the BLA nucleus has an anxiogenic effect as demonstrated by CCK knock down using a CCK-targeted AAV-shRNA (Del Boca *et al.*, 2012). The morphological and anatomical properties of CCK interneurons of the amygdala have been well studied. They are widely found in BLA nucleus of the amygdala as large multipolar neurons and sub populations of them express calbindin or VIP and/or calretinin (Mascagni and McDonald, 2003). A small population also co-expresses 5-$HT_3$ serotonin receptor subtype (5-HT3R) and it has been suggested that the anxiolytic effects of 5-HT are through the modulation of GABA and CCK neurotransmission (Mascagni and McDonald, 2007). BLA CCK neurons are a highly heterogeneous population of interneurons. They can be grouped according to their electrophysiological properties in three distinct subtypes (subtypes I-III) according to their passive and active membrane properties. Jasnow and colleagues identified the BLA CCK neurons using a CCK promoter specific lentivirus and revealed differences between them in input resistance which had a range from 230 up to 521 MΩ, spike frequency adaptation and instantaneous firing frequency with some of them having regular 20Hz spiking while others displayed an initial 90Hz fast spiking before reverting to regular spiking similar to the other subtypes. They also found differences in their response to depolarizing and hyperpolarizing current injection with their single action potential amplitudes being significantly different between the subgroups (Jasnow *et al.*, 2009).

## 1.4 Cholecystokinin's role in energy homeostasis from periphery to CNS

CCK was initially identified as a gut peptide hormone involved in intestinal motility and in gall bladder and pancreatic enzyme secretion (Mutt and Jorpes, 1968) but is also expressed in the brain where it acts as a neuropeptide (Vanderhaeghen *et al.*, 1980; Beinfeld, 2001; Giacobini and Wray, 2008). Peripheral CCK is released from the duodenum in response to gastric filling and stimulates vagal afferents that target the NTS (nucleus tractus solitarius) in the brainstem (Fan *et al.*, 2004; Berthoud *et al.*, 2006).

CCK was the first gut hormone reported to affect appetite and reduce food intake in a dose-dependent manner in rats (Gibbs, Young and Smith, 1973). The reduction of food intake by intravenous injections of CCK was also shown in humans (Lieverse *et al.*, 1995). CCK was also shown to be increased in plasma of humans 15mins after meal initiation (Liddle *et al.*, 1985). In the GI tract, the duodenum and jejunum synthesizes and releases CCK in response to food intake (Buffa, Solcia and Go, 1976; Himeno *et al.*, 1983). The released CCK first acts locally to stimulate gallbladder contraction and inhibit gastric emptying (Dufresne, Seva and Fourmy, 2006). It stimulates the release of bile via CCK mediated muscle contraction and it regulates and stimulates the secretion of pancreatic and several small intestinal enzymes (Dyck *et al.*, 1974; Anagnostides *et al.*, 1985; Bragado, Tashiro and Williams, 2000). CCK also participates in intestinal motility. CCK neurons can be found abundantly in the colon with CCK fibers in the circular muscle layer, they release CCK which then excites the colonic smooth muscle while also releases acetylcholine from the postganglionic parasympathetic nerves in the submucosa (Vizi *et al.*, 1973; Larsson and Rehfeld, 1979). CCK also regulates gastric acid

release by stimulating somatostatin release from the fundic D cells which subsequently inhibit acid secretion from the parietal cells (Chen *et al.*, 2004).

Peripheral CCK acts on the CCKAR of the afferent vagal nerves that synapse at the NTS nuclei of the brainstem (Wang *et al.*, 1998). It supresses feeding via activation of the brainstem melanocortin system. The POMC neurons which are present in the NTS (Joseph, Pilcher and Bennett-Clarke, 1983) are being activated via MC4-R signalling (Fan *et al.*, 2004). The ERK1/2 signalling pathway is also activated by the vagal afferents to the NTS neurons in response to CCK (Berthoud *et al.*, 2006). Peripheral CCK also causes activation of the A2/C2 catecholaminergic neurons of the NTS which supress food intake (Rinaman *et al.*, 1998; Rinaman, 2003). Recently, a subset of NTS neurons that express CCK were shown to be activated by nutrient intake after fasting as shown by cfos upregulation. Pharmacogenetic activation of the $CCK^{NTS}$ neurons reduced food intake and resulted in a decrease in body weight but with no effect in glucose homeostasis. The effect was attenuated in the presence of CCKAR antagonists. Optogenetic activation of CCK axons in the PVN of the hypothalamus suppressed re-feeding in fasted animals likely via MC4R-expressing PVH neurons which were shown to express CCKAR and are excited by CCK-8 application in patch clamp electrophysiological recordings (D'Agostino *et al.*, 2016).

It is well known that the CNS-derived CCK is acting on a central level to modulate energy balance by modulating the neuronal activity of hypothalamic neuronal populations. Injections of CCK in the hypothalamus were shown to suppress feeding in rats (Blevins, Stanley and Reidelberger, 2000) while rats with CCK1 receptor deficiency become hyperphagic due to disrupted function of NPY/AgRP-expressing neurons in the ARC and DMH (Bi *et al.*, 2001, 2004).

Injection of CCK to the DMH has been shown to increase the c-Fos immunoreactivity in the medial part of the ARC where the feeding-related and well characterised NPY/AgRP expressing neurons have been identified. However, it does not activate neurons in the NTS of the brainstem (Chen *et al.*, 2008). The effect of CCK in local hypothalamic networks is further demonstrated by restoring CCK1 receptors by viral transduction in receptor deficient animals which partially attenuated the disrupted feeding activity and enhanced glucose tolerance (Zhu *et al.*, 2012). While the AgRP/NPY neurons of ARC have drawn most of the scientific enquiries, it is not till recently that a molecularly distinct NPY population in the DMH (Draper *et al.*, 2010) has been implicated in specific metabolic dysregulations (Bi, 2013).

Moreover, our recent published work identifies CCK neurons as key integrators of the negative neuroendocrine feedback of glucorticoids to the PVN. Selective removal of BDNF/TrkB signalling from CCK-positive neurons in Trkb-CCK-KO mice leads to central glucocorticoid resistance, increased secretion of corticotropin releasing hormone (CRH), adrenocorticotropic hormone (ACTH), corticosterone (CORT), adrenal hyperplasia, and mature-onset obesity without hyperphagia (Geibel *et al.*, 2014). Glucocorticoids (GCs) have a central role in this regulation and exert negative feedback loop on the HPA axis activity both at the peripheral (pituitary) and central level. The latter occurs on different brain regions including the paraventricular nucleus (PVN) of the hypothalamus. However, recent evidence suggests that PVN innervation and integration of inputs is mainly mediated through local circuits (peri-PVN). These areas are being innervated by mostly GABAergic afferents while there are also dense populations of CCK positive neurons in this hypothalamic region. These neurons form a ring around the PVN

and are in the medial-dorsal region of the anterior hypothalamic nucleus (AHN) and the dorsomedial nucleus of the hypothalamus (DMH), and they have been described to integrate glutamatergic and GABAergic input from limbic areas, and to modulate HPA axis activity (Herman *et al.*, 2002).

The CCK neuronal populations are throughout the distinct hypothalamic nuclei, as revealed by mRNA analysis (Schiffmann and Vanderhaeghen, 1991) of the region as well as by our lab's recent work. There is also an increasing amount of evidence implicating the role of local CCK in the hypothalamic circuits for homeostatic regulation and recently for HPA axis dysfunction (Geibel *et al.*, 2014). However, the source of endogenous CCK that acts on distinct neuronal components has not been elucidated. The research so far does not address the purpose of CCK neurons in the hypothalamus and the roles they are most likely to possess in the network dynamics regarding energy homeostasis and neuroendocrine outputs.

## 1.5 Aims of the thesis

My PhD project seeks to untangle the role of CCK neurons in the hypothalamic circuits responsible for energy homeostasis and specifically to identify the importance of these neurons in feeding circuits and the regulation of body weight. The source of endogenous CCK that acts on the hypothalamic networks and its role in feeding circuits, is not fully elucidated. The CCK-expressing neurons of the VMH region of the hypothalamus are well situated neurons that can have an effect in the regulation of food intake with long-term effects in body weight balance and implications in glucose sensing and homeostasis. However, they are inadequately researched in their capacity to directly affect energy homeostasis on a short-term time period while also researching their long-term contribution. We have addressed these questions by modulating the activity of CCK neurons by silencing them and assessing their role in food intake. Moreover, we are investigating their long-term role in food intake, body weight regulation and in glucose homeostasis in the absence of CCK neurons from the VMH region by selective spatiotemporal ablation techniques. We therefore deployed two experimental approaches towards our goal:

a. Acute modulation of feeding circuits by pharmacogenetic silencing of CCK neurons in the VMH nucleus of the hypothalamus. Cre-dependent viral particles expressing Gi coupled DREADDs (Designer Receptors Exclusively Activated by Designer Drugs) (Roth, Hill and Carolina, 2013) were injected in the VMH region of BAC-CCK-Cre animals. Upon CNO delivery, we induced an increase in food intake and changes in meal pattern characteristics.

b. The ablation of CCK neurons from the VMH region of the hypothalamus was performed with two similar techniques that rely on apoptotic mechanisms

induced by diphtheria toxin. We generated a double recombinase inducible diphtheria toxin receptor (DTR) mouse line for spatiotemporally restricting DTR expression only to CCK neurons of the VMH region. We crossed the line to the BAC-CCK-Cre line so that the Cre recombinase removes the first stop cassette in all CCK cells while a second stop cassette is removed only in the $CCK^{VMH}$ neurons by stereotactically injecting an AAV that expresses FLPo recombinase. Consequently, the expression of DTR is only limited to CCK neurons of the brain area (VMH in this case) that was injected with AAV. The diphtheria toxin (DT) was then administered systemically to ablate the $CCK^{VMH}$ neurons that express DTR. The ablation efficiency achieved was not adequate for observing any significant effect so we employed an alternative ablation strategy. We stereotactically injected a cre-dependent AAV that expresses Diphtheria Toxin A subunit (DTA) in the BAC-CCK-Cre mouse line to selectively express DTA in $CCK^{VMH}$ neurons and efficiently ablate them from the region. We assessed the long-term effect of their ablation in weight regulation over a period of months as well as changes in their food intake and glucose homeostasis.

# Chapter 2: Materials and Methods

## 2.1 Chemicals and consumables

All chemicals were purchased from Sigma Aldrich (Sigma-Aldrich Ltd, Gillingham, UK) or VWR (VWR International, Lutterworth, UK) in molecular biology grade unless otherwise stated.

Consumables were purchased from Roth (Carl Roth GmbH, Karlsruhe, Germany), Eppendorf (Eppendorf UK Limited, Cambridge, UK), BD (BD, Oxford, UK), Greiner (Greiner Bio-One Ltd., Stonehouse, UK), Thermo Fisher Scientific (Fisher Scientific UK Ltd., Loughborough, UK), Gilson (Gilson UK, Luton, UK) and Rainin (Anachem Ltd, Luton, UK).

## 2.2 Buffers

All buffers were prepared with ultrafiltered water unless stated otherwise. Water was purified using the "Milli-Q-water purification system" from Millipore (Millipore Ltd, Watford, UK).

10x DNA loading buffer

50% glycerol, 0.2% OrangeG (Sigma, cat. no. O-1625), in 1xTAE or 1xTBE

SDS-PAGE 10x running buffer 1L stock

30 g Tris Base, 144 g glycine, 10 g SDS and 1000 ml distilled water

SDS protein loading buffer

150mM TrisHCL pH 6.8, 6% SDS, 0.3% bromophenol blue, 30% glycerol and 100mM DTT to denature proteins.

20x SSC southern blot transfer buffer

3M NaOH and 0.3M Sodium Citrate. 47% HCl was added to the solution to adjust the pH to 7

Transfer buffer 1x western blot

Prepared fresh before use. 6 g Tris base, 28.8 g glycine, Bring volume to 1600 ml with distilled water and add 400 ml methanol.

50x TAE

2 M Tris, 1 M glacial acetic acid, 50 mM EDTA, pH 8.0

Tail lysis buffer

100 mM Tris, 1 mM EDTA, 250 mM NaCl, 0.2% SDS, pH 7.5

TB

50 mM Tris, pH 8.3

10x TBE

890 mM Tris, 890 mM boric acid, 20 mM EDTA, pH 8.3

Ponceau solution

0.1% Ponceau S, 5% acetic acid

PB

100 mM PB, pH 7.4 (77.4 ml of 1 M Na2HPO4, 22.6 ml of 1 M NaH2PO4 for 1 litre)

PBS

0.01 M phosphate buffer, 0.0027 M potassium chloride and 0.137 M sodium chloride, pH 7.4 (was prepared from Thermo Fisher Scientific PBS tablets, cat. no. 18912014)

RiPA (Radioimmunoprecipitation assay) protein lysis buffer

MilliQ purified water at 18Ωμ was used. 7.5ml of 1M NaCl (2.922g), 500μl Triton X, 1.25ml of 2M Tris at pH 7.4, 100μl of 0.5M EDTA pH8, 500μl 10% SDS and 0.25g sodium deoxycholate. Before use, 1 PIERCE mini tablet proteinase inhibitor (Thermo Fisher Scientific, cat.no. 88665) was added to 10ml of buffer and left on ice with occasional short duration vortexing until it dissolves. Then 100μl of PMSF (Phenylmethylsulfonyl fluoride, Sigma) were added and mixed well. (Short life of 30mins)

4% Paraformadehyde (PFA) solution

For 1 litre of final solution 40 g of paraformaldehyde (Sigma, stored at 4 °C) were dissolved by continuous stirring in 800 ml PB buffer (pH 7.4) by heating to just below 60 °C. The solution was cooled down to room temperature, adjusted to pH 7.4 with sodium hydroxide if necessary, and filtered through a 50 μm syringe filter. Aliquots were stored at -20 °C, for experiments the required amount was thawed in a waterbath at 56 °C and then cooled to 4 °C.

## 2.3 Animals

All animal procedures performed, conform to UK legislation (Scientific procedures ACT 1986) and the University of Oxford ethical review committee policy. Mice were maintained under standard laboratory conditions with water and food freely available unless otherwise stated. Mice were housed on a 12 h light/12 h dark cycle with lights on at 07:00 and off at 19:00. All experimental groups within one experiment contained mice of same strain and sex, being similar in age and body weight.

### 2.3.1 Mouse lines

| Mouse line | Description | Reference |
|---|---|---|
| BAC-CCK-Cre | BAC transgenic line expressing Cre recombinase under the CCK promoter | (Geibel *et al.*, 2014) |
| *Gt(ROSA)26Sor*$^{tm9(CAG-tdTomato)Hze}$ | Reporter line knock-in in Rosa26 locus, expressing tdtomato fluorescent protein in Cre recombinase positive cells | (Madisen *et al.*, 2010) |
| *Gt(ROSA)26Sor*$^{tm1(FLP1)Dym}$ | Rosa26 locus knock-in of FLP recombinase | (Farley *et al.*, 2000) |
| R26R$^{LxP-FRT-iDTR}$ | Rosa26 knock-in of double recombinase mediated diphtheria toxin receptor fused to GFP | Unpublished/ generated for this study |

### 2.3.2 Animal handling and colony organisation

The *Gt(ROSA)26Sor*$^{tm9(CAG-tdTomato)Hze}$ and *Gt(ROSA)26Sor*$^{tm1(FLP1)Dym}$ were maintained on a C57B6 background. The BAC-CCK-Cre transgenic founder was a CBA/C57B6 hybrid that was crossed back to C57B6 mice for at least five generations. The R26R$^{LxP-FRT-iDTR}$ mousse line are 129/SvJ / C57B6 hybrid crossed back to C57B6 for at least 5 generations. Male heterozygous mice (CCK-Cre$^{tg/+}$) were crossed to homozygous R26R$^{LxP-FRT-iDTR}$ females.

Female and male mice were housed separately with a maximum of six animals per cage. In the case of males only littermates were housed together whereas females were combined from several litters if possible. Mice were only kept alone if males had no littermates, were removed from a breeding, for food intake measurements or overnight after surgery to assist recovery and avoid suture opening by littermates. In the case of food intake, mice were kept separately for at

least two weeks in metabolic cages before the experiment. For all other behavioural experiments mice were always kept with company. The males cannot be housed together after singly housing them to avoid aggressive behaviour among themselves. Therefore, the experimental protocol ended after singly housing them and they were not housed separately for prolonged periods.

The breeding of the lines was done by keeping one male with two females, the first female to litter was generally separated in order to reduce stress. The minimal breeding age for males was 8 weeks and for females 6 weeks. Pups were separated from their mother at about P20. Animals were identified by ear clipping (punching of both ears) which were taken by the technicians of the Biomedical sciences of Oxford University animal facility according to the Universal mouse numbering system (Roscoe B. Jackson Memorial Laboratory. and Green, 1966) and were used for identification as well as biopsies for genotyping. The genotyping from the ear punches was performed by our former lab technician, Dr Jacqui Horn.

Mice were sacrificed either by cervical dislocation for the acquisition of fresh tissue or in the case of stock surplus. Alternatively, they were terminally anaesthetised and perfused with PBS or PFA as described below.

### 2.3.3 Generation of R26R$^{LxP\text{-}FRT\text{-}iDTR}$ line

This line has not been published but the generation of the construct, the homologous recombination into embryonic stem cells (ESC) and their subsequent injection into blastocysts was done by a service on our behalf. The details of each element within the construct and the site of homologous recombination into the Rosa26 locus are presented below. The ESC screening strategy with southern blots was performed by me as detailed in the respective section (Southern blotting). The

positive ESC clones that the constructed was inserted successfully, were ordered for the generation of the mouse line.

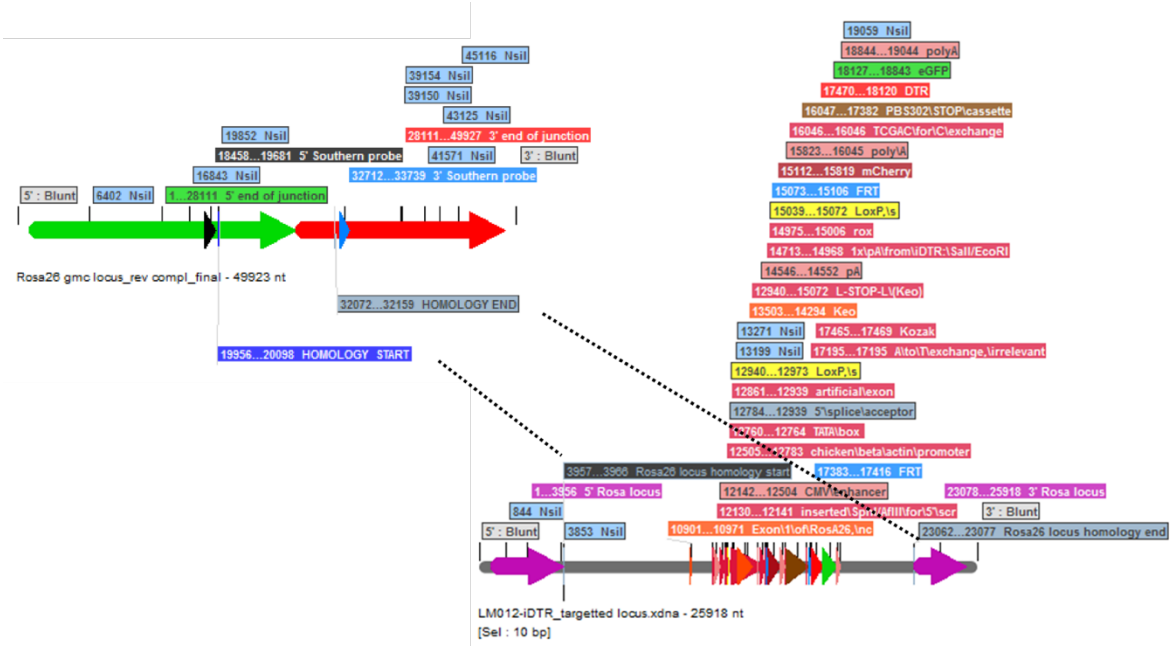


**Figure 4: LxP-FRT-iDTR construct inserted with homologous recombination in the R26 locus (sites depicted above) for the generation of the R26R$^{LxP\text{-}FRT\text{-}iDTR}$ mouse line.** The expression is driven by a CAG promoter (hybrid promoter consisting of CMV enhancer and chicken beta actin promoter). LoxP sites are anchoring a STOP cassette upstream of an mcherry fluorescent protein ORF (open reading frame). Downstream of mcherry there is another stop cassette. Both elements are anchored by FRT sites. Further downstream there is the diphtheria toxin receptor fused to GFP on the C terminus (ORF).

## 2.4 Genotyping

### 2.4.1 DNA purification

Genotyping samples from weaned mice were obtained by ear punching and kept at -20 °C until processed. The biopsies were then lysed with 200 µl of tail lysis buffer (see Buffers) supplemented with 4 µl of Proteinase K (20 mg/ml stock, Sigma) at 56°C in a waterbath (Grant Instruments, Shepreth, UK) overnight. The samples

were then incubated for 10 minutes at 95 °C in a heatblock apparatus (Grant Instruments, Shepreth, UK) to deactivate the Proteinase K.

The biopsies were then centrifuged for 5 minutes at 8000 g (Eppendorf 5417R centrifuge) in order to precipitate any debris or not lysed tissue. Samples were stored at 4 °C until genotyped and then transferred to -20 °C.

### 2.4.2 Primers and Polymerase Chain Reaction (PCR)

Primers were ordered in lyophilized form from Metabion or Sigma, reconstituted with ddH2O to 100 µM and stored at -20 °C. Unless otherwise stated, PCR reactions were set up in 50 µl (49 µl mastermix and 1 µl DNA) with 5 µl 10x buffer (see chapter 2.2), 3 µl MgCl2 (25m M stock), 8 µl dNTPs (1.25 mM stock, 1.25 mM per nucleotide type), 0.5 µl of each primer, 31.5 µl ddH2O and 0.5 µl Taq polymerase (Proteomics Core Facility at EMBL-Heidelberg). All PCRs were performed on a PTC-200 Peltier Thermal Cycler (MJ Research) or on a BioRad DNA Engine Peltier Thermal Cycler.

<u>Cre PCR</u>

Primers: Cre1 5'- GCC TGC ATT ACC GGT CGA TGC AAC GA -3'

Cre2 5'- GTG GCA GAT GGC GCG GCA ACA CCA TT -3'

Product size: 726 bp

Cycling conditions: 94 °C 3 min, 94 °C 30 sec, 67 °C 1min, 72 °C 1min, go to step 2: 35 times, 72 °C 5 min, 4 °C 10 min

### 2.4.3 Agarose gel electrophoresis

PCR reactions were run on 1 or 2% agarose gels. Gels were prepared with agarose from Sigma in 1x TAE or 1X TBE buffer (see Buffers). Agarose was melted in a commercial microwave oven until completely dissolved, cooled down and 2.5 µl

of a 10 mg/ml ethidium bromide stock solution (Sigma) per 100 ml was added before casting the gel. 5 µl of 10x DNA loading buffer (see Buffers) was added to the samples and 20 µl of each sample loaded. A 1kb DNA ladder (Invitrogen) was used as marker. Gels were run at 140 – 200 V for 20-40 mins until the desirable separation of the bands was achieved. Bands were visualized with a Gel Document Illuminator (Uvitech Cambridge).

## 2.5 Biochemistry

### 2.5.1 Tissue collection and lysate preparation

The animals were perfused as described previously(Gage, Kipke and Shain, 2012).For biochemistry the perfusion was done only with PB to clear most of the blood from the brain. Mice were terminally anaesthetised with 50µl of sodium pentobarbital 200mg/ml concentration (Euthatal, Merial). Their depth of anaesthesia was monitored by the toe and tail pinch reflex. Upon losing both reflex to pinches, a small piece from their tail tip was removed by scissors for re-genotyping purposes. Mice were securely pinned onto a perfusion table at an angle to allow the flow of liquids. The chest cavity was exposed by making an incision to the skin on top of the sternum. Incisions around the diaphragm were made and the chest was cut on the sides to allow the chest rib cage to lift and expose the heart. A small incision at the right atrium was made to allow the flow of the blood while a 30G needle (BD Microlance 3 30G x 1 1⁄2 inch) fixed to the perfusion tube was inserted at the bottom of the left ventricle. We used a perfusion pump (Masterflex Economy, easy-load II, with tube L/S 13, Cole Parmer) to pass around 7-10ml of ice cold 0.1M PB,pH 7.4 until the liquid escaping from the right atrium was clear from blood and the liver was pale. The head was removed and the brain retrieved from the skull. The brain was harvested as quickly as possible on top of an ice-cold metal plate by making

incisions on the sides of the cerebellum and lifting pieces of the skull from each hemisphere while also cutting the skull around the olfactory bulbs to allow the lifting of the brain from the skull. The brain was immediately frozen on dry ice and stored at -80°C until used.

Before lysis samples were weighed frozen. Then tissues were quickly transferred into 10 volumes (vol/wt) of RiPA protein lysis buffer in a tissue grinder (VWR) on ice. Tissue was homogenised by 10 slow strokes with the loose dounce of the grinder or until no big particles were visible and then with 10 slow strokes with the tight to the walls dounce for a finer result. The samples remained on ice throughout the homogenisation and then let to rest for 20mins on ice. To get rid of remaining particles samples were centrifuged for 30mins at 14.000 rpm at 4°C. The supernatant was split into 50 µl aliquots which were frozen on dry ice and stored at -80 °C. Before a western blot, a 50 µl aliquot was thawed and mixed with 10 µl protein loading buffer and if required stored at -20°C before used for blotting.

### 2.5.2 Protein concentration measurements

Protein concentration was determined with a BCA (bicinchoninic acid) assay (BCA Protein Assay Kit, Thermo Scientific, cat.no 23227) which is tolerant of detergents such as Triton X-100 without a decrease in sensitivity of readings. The BCA assay relies on a two-step reaction that leads to colour development which is highly selective to the protein concentration. The first step is a biuret reaction where amino acids form a coloured chelate complex with Cu ions. While in the second step, BCA reacts to the reduced $Cu^{1+}$ resulting in a purple coloured product with linear absorbance in 562nm wavelength with increasing protein concentration. The assay was performed according to manufacturer's instructions. We prepared a working solution by mixing 50 volumes of reagent A (1% BCA-Na2, 2%

Na2CO3·H2O, 0.16% $Na_2$ tartrate, 0.4% NaOH, 0.95% NaHCO3) with 1 volume of reagent B (4% CuSO4·5H2O in ddH2O). Standards were prepared from bovine serum albumin (BSA) provided with the kit with the respective lysis buffer in the following concentrations: 2,000 µg/ml, 1,000 µg/ml, 500 µg/ml, 250 µg/ml, 125 µg/ml and 0 µg/ml (blank). Brain lysates were thawed and 5 µl of them further diluted 1:50 and 1:100. The diluent used for both standards and samples was 50mM Tris at pH8.3. 10 µl of each standard or sample were applied to a 96-well plate in duplicate and 200 µl of working solution was added. The plate was incubated for half an hour at 37°C, then absorption was measured at 562 nm in a plate reader (Tecan)

### 2.5.3 Southern blotting

DNA purification

The construct containing the diphtheria toxin receptor under the Rosa26 promoter was inserted by homologous recombination in embryonic stem cells (ESC). This was performed by a service. The genomic DNA was purified from the received ESC lysates by phenol/chloroform/isoamylalcohol (ratio 25:24:1) DNA extraction protocol. Each ESC lysate was around 500-700 µl in volume in 24well plates. The lysates were transferred on Eppendorf tubes and an equal volume of phenol/chloroform/isoamylalcohol was added to each lysate and mixed continuously by inversion of the tubes for a total of 5 mins. The tubes were spun at 14,000 rpm on a table top centrifuge for 5 mins. The resulting upper layer containing the DNA was transferred to fresh tubes and an equal volume of isopropanol was added and mixed by inverting the tubes until a visible DNA precipitate is seen. A flame-sealed Pasteur pipette was used as a hook to retrieve the visible DNA precipitant which was immediately dipped to 70% ethanol for washing. The pipette with the DNA on top was left to air-dry for 10 mins and then dissolved in solution by incubating in 50

µl of 10 mM Tris-HCl pH 8.0 for 30 mins. The DNA yield was measured in a nanodrop equipment for a couple of samples from each plate to get an indication of the concentration achieved. DNA samples were stored at 4°C until required.

DNA digestion and gel electrophoresis

The DNA from each clone was then digested with the appropriate restriction endonuclease enzymes according to the southern blot strategy designed to allow the detection of a 5' and a 3' end radioactive probes hybridised to DNA fragments with band sizes indicative of successful recombination. DNA was digested with either NsiI (New England Biolabs (NEB), cat.no. R0127S) for the 3' probe or AflII (NEB, cat.no. R0520L) for the 5' probe. The expected bands for the 3' probe are 19.298 kb for wildtype allele and 11.010 kb for targeted allele whereas for the 5' probe are 13.293 kb and 10.404 kb respectively. DNA digestion was performed per manufacturer's instructions at 37°C for 6 hours. The digested clones were run on a 0.7% agarose gel in 1x Tris-Glacial Acetic acid-EDTA (TAE) overnight at 50V.

Preparation of gel and blotting

The gel was prepared for blotting onto a membrane. Because the resulting bands are greater than 10kb in size, acid depurination of the DNA was performed. The gel was treated with 0.2M HCl on a shaker for 20mins and then rinsed briefly with distilled water. The DNA was denatured by treating the gel with denaturation buffer (0.5M NaOH,1.5M NaCl) for 30 mins with gentle shaking. Denaturation allows hybridisation of double stranded DNA to the radioactive probes. The gel was rinsed briefly with distilled water and then incubated for 30mins with neutralisation buffer (0.5M Tris pH7.4, 1.5M NaCl) with gentle shaking. The agarose gel was then blotted by capillary transfer onto a positively charged nylon membrane (Amersham Hybond

N+, no: RPN203B, GE Healthcare). The nylon membrane was cut at the size of the gel and soaked in 2x SSC buffer until required. The assembly of the southern blot apparatus was done as follows: Two long pieces of whatman 3MM paper were placed on top of a gel tray with its edges extending into the transfer solution (20xSSC buffer) followed by two more papers in the size of the gel. The gel was flipped onto the 3MM papers. The edges of the gel were surrounded with cling film to ensure capillary transfer of the SSC through the gel without bypassing it from the sides. The nylon membrane was placed on top of the gel, followed by two more 3MM papers. A pile of highly absorbent paper towels cut in gel dimensions was stacked on top of the sandwich to drive the capillary transfer of the SSC buffer. Gentle pressure was applied by placing a heavy object like a glassware on a tray on top of the piled paper towels. The blotting was done overnight for 18 hours at room temperature. Paper towels were replaced with dry ones after 6h to achieve optimal DNA transfer onto the nylon membrane. The transfer efficiency was assessed by staining the gel with ethidium bromide. The membrane was rinsed in 2x SSC buffer and let to air dry. The DNA was fixed onto the membrane by UV-crosslinking for 2 mins at 1200 energy of UV light in a stratalinker stratagene UV crosslinker (Biorad). The membrane was then stored at room temperature between 3MM papers until required for the hybridisation step.

Probe labelling and hybridisation

The blot was briefly incubated in 6xSSC buffer and then inserted to a hybridisation tube containing Perfecthyb Plus hybridisation buffer (Sigma, cat.no. H7033) pre-warmed to 65°C in a hybridisation oven. The blot was then blocked with 1.5mg of denatured (5mins at 95°C) sheared salmon sperm (10mg/ml stock). It was then hybridised with the respective $^{32}$P-dCTP labelled probe (3' or 5' probe

mentioned above). Each labelled probe was prepared using the RadPrime DNA labelling system (Invitrogen, no: 18428-011) and the reaction purified using illustra probe quanta G-50 micro columns (GE healthcare, no: 28-9034-08). Briefly, 25ng of probe DNA in 2 µl sterile distilled water were incubated at 100°C for 5 mins on a heatblock and immediately cooled on ice. 1 µl of 500 µM dATP, dGTP, dTTP and 5 µl of $^{32}$P-dCTP (3000 Ci/mmol) in 20 µl of 2.5X Random primers solution were added to the probe DNA and filled with distilled water to a total volume of 49 µl and mixed briefly on ice. 1 µl of Klenow fragment was added to the reaction, centrifuged for 15s and incubated at 37°C for 10 mins. The reaction was then stopped by adding 5 µl of the Stop buffer. The solution was then applied directly to the resin of a G-50 micro column attached to a collection tube and centrifuged for 2 mins at 3000 rpm. The purified labelled probe was then transferred to a screw-capped tube and denatured at 95°C for 5 mins before immediately added to the hybridisation tube containing the blotted membrane for overnight incubation at 65°C. All steps of radioactive labelling were performed in accordance to the department's health and safety regulations set in place for $^{32}$P experimental work. The membrane was washed with decreasing dilutions of SSC/SDS wash solutions. The blot was washed for 5 mins with 2% SSC/ 0.1% SDS at room temperature, the temperature was adjusted to 40°C and washed with fresh solution for 15mins, then with 1% SSC/ 0.1% SDS for 20mins and finally with 0.5% SSC/0.1 SDS for 15 mins. The blot was then removed from the tube, wrapped in cling film and placed onto a phosphorimager cassette for 3 days. The cassette was then imaged by a phosphorimager.

### 2.5.4 Western blotting

SDS-PAGE gel and electrophoresis

Polyacrylamide gels were prepared and run in a Mini Vertical Electrophoresis Unit (Hoefer, Holliston, US). Taking into consideration the size of the proteins that we desired to detect (20-300 kDa), we prepared a 10% separating gel by mixing 4.66 ml dd$H_2O$, 3.25 ml 40% polyacrylamid, 4.88 ml 1 M Tris pH 8.8 (375mM in final solution), 130 µl 20% SDS, 130 µl of freshly prepared 10% APS (ammonium persulfate) (0.1% final) and 13 µl TEMED. After casting, 95% ethanol was poured gently on top of the casted gel to ensure an even surface and the removal of any bubbles formed. Once the gel had polymerized the ethanol was removed and washed with distilled water with any excess liquid removed using a piece 3mm whatman paper. We immediately poured over the stacking gel (4%: 2.2 ml ddH2O, 0.3 ml 40% polyacrylamid, 0.375 ml 1 M Tris pH 6.8 (125mM final), 40 µl 20% SDS (final 0.1%), 80 µl 10% APS and 3 µl TEMED) and a 1mm comb was inserted to form the wells for sample loading. The finished gels were transferred into the gel chamber with 1x SDS page running buffer. Samples had been mixed with protein loading buffer before freezing and were now just thawed and boiled for 5 minutes at 95 °C. 20 µl of sample was loaded per well and 5 µl of Novex Sharp pre-stained molecular weight protein marker (Thermo Fisher Scientific, cat. No. LC5800). Gels were run at 120 V until the dye had passed the stacking gel and then at 140 V until the dye ran out of the bottom of the gel.

Protein transfer to PVDF membrane

Blotting was performed by wet transfer using a Mini Trans-Blot Cell (Biorad). In order to transfer the proteins from the gel to the PVDF membrane, a sandwich for blotting was prepared in a box filled with 1x transfer buffer as described below. One layer of blotting paper was placed on a foam pad, then a PVDF membrane (Thermo fisher scientific, cat.no. 88518) in the size of the gel (previously activated in

methanol), the gel, another layer of blotting paper and a second foam pad were placed on top. Air bubbles were removed by carefully rolling a plastic pipette over the sandwich. The holder was closed (white site towards the membrane) and placed into the transfer chamber with the buffer and an ice pack to keep the temperature close to 4°C. The transfer was performed for 1 hour at 100 V.

Membrane probing with antibodies

After blotting the membrane was rinsed in ddH2O, then Ponceau solution was added for two minutes and washed with distilled water in order to see if the transfer to the PVDF membrane had worked and all samples were equally loaded and run properly on the SDS gel. The staining was washed out by applying several times PBS. All washing and incubation steps were performed on a rocking platform at RT unless otherwise stated. We blocked the membrane in 5% milk, 0.2% Tween 20 for 1 hr at room temperature. The primary antibody chicken a-GFP 1:2000 dilution was suspended in blocking buffer and was applied to the membrane and incubated overnight at 4°C. The membrane was washed three times in PBS-T (0.1% Tween) and then the secondary antibody a-chicken IgY HRP 1:1000 dilution in blocking buffer was applied for 1h at room temperature. The membrane was then washed with PBS three times.

Development of blots in film

Protein bands were detected by incubating membranes in 2 ml of a 1:1 mixture of the reagents of a peroxidase substrate for enhanced chemoluminescence (ECL) (Western blotting luminol reagent, Santa Crux sc-2048). Membranes were placed in a film cassette, covered with Saran wrap and films (BioMax Light Films, Kodak) were exposed in the dark room for 30 seconds. Films were developed for

2.5 minutes in developing solution (4153, developer for Curix 60, Agfa), washed thoroughly 5 times in water, fixed 3 minutes in fixative solution (4354 rapid fixer, Agfa), washed again and were then dried.

### 2.5.5 Glucose tolerance test

We used female Ai9-CCK mice that had been injected stereotactically with AAV9-FLEX-CAG-DTA-IRES-mcherry in the VMH nucleus 3 months after surgery. Whole blood glucose levels were measured with a hand-held glucose meter (One Touch Verio). The meter and its test strips were calibrated the day before the experiment according to the manufacturer's instructions. Briefly, we measured the glucose control solution provided which is automatically being recognised by the meter as a control solution of known glucose concentration. Food was removed from the animals' cages at 18:00 on the day before the experiment (16h overnight fasting). Around 5µl (a drop) of blood was removed from the animals' tails. Each animal was very briefly restrained using a mouse restrain cylinder and their tail was cleaned with 70% ethanol. A small puncture was made on top of their tail vain closer to the tail tip using the lancet provided with the glucometer. The blood drop was immediately absorbed using a fresh test strip attached to the glucometer and a baseline reading was recorded for each mouse. Immediately after, a D-glucose solution with a concentration of 200g/L (Thermo Fisher Scientific, cat.no. A2494001) was ip injected at a dose of 2g/Kg body weight. Blood glucose readings were obtained 30 mins and 180 mins after the glucose injection. Blood was removed as described above from the existing puncture by removing the freshly formed scab. At the final time point the animals were sacrificed by transcardial perfusion and their brains harvested.

## 2.6 Histology and immunohistochemistry

### 2.6.1 Collection and sectioning of brains

All brains used were prefixed by cardiac perfusion with 20ml ice-cold 4% (paraformaldehyde) PFA preceded by clearing of blood by circulating 0.1M PB as detailed in the tissue collection section above. Briefly, mice were deeply anaesthetised with Euthatal (pentobarbital) by intraperitoneal injection and depth of anaesthesia was checked by pinching the paw and base of tail of the mouse until it was completely unresponsive. 20ml of ice cold 0.1M PB were passed through the animal followed by ice cold 4% PFA/0.1M PB. The brain was extracted and post-fixed on 4% PFA/0.1M PB for 3 hours. The brains were cryoprotected with a series of increasing concentrations (10, 20 and 30%) of sucrose/0.1M PB overnight. They were then briefly dried onto a 3M whatman paper and snap frozen in optimal cutting temperature compound (OCT) (CellPath, cat. no. KMA-0100-00A) within plastic molds (Sigma, cat. no. E6032) by using isopentane cooled by dry ice. The OCT-embedded brains were stored at -80°C until required for sectioning.

The brains were sectioned on a Leica cryostat with the sectioning chamber set at -23°C and the specimen holder at -18°C. The brains were incubated to -20°C for a couple of hours prior to sectioning. They were sectioned at 20 µm thickness either at coronal or sagittal orientation and collected directly into ice-cold 1x PBS floating in 24-well plates. The sections were washed from OCT by transferring them with a small brush to 48-well plates with fresh PBS. They were then stored for a short-term period (2-3 months) at 4°C in PBS supplemented with 0.01% Sodium Azide.

### 2.6.2 Preparation of gelatine-coated slides

Gelatine-coated slides were used for mounting floating sections used for immunohistochemistry. 0.5% (w/v) gelatine was dissolved in water at 70 °C in an Erlenmeyer flask, the solution was cooled to RT and 0.05% (w/v) chromium potassium sulphate was added. The solution was cooled to 4°C and immediately used to coat the slides. Non-coated glass slides (VWR) were placed into plastic slide holders and washed two times for a period of ten minutes for each wash in distilled water. Slides were placed into the gelatine solution for 5 minutes and any bubbles forming between the slides were carefully removed. Afterwards, the holders were placed on paper towels and tilted in order to remove any excess solution around the slides. The slides were then left to dry in the tilted position under a hood overnight and then stored in a sealed box for not more than two months.

### 2.6.3 Antibodies for immunohistochemistry

### 2.6.4 Immunofluorescence, imaging and quantification

Free-floating sections in 1x PBS of 20 µm thickness were transferred to 24-well plates (1-2 sections per well). All washing steps were done with 500 µl and antibody incubations and blocking with 200 µl, on a shaking platform at 20-30 rpm at room temperature unless otherwise stated. The sections were washed three times for 10 mins with PBS and then incubated with blocking solution (5% fish gelatine and 0.5% Triton in PBS) for 1h. The blocking solution was aspirated with a Pasteur pipette and they were then incubated with 1:1000 dilution of rabbit anti-dsred antibody (Clontech, 632496) in blocking solution overnight for 16h. They were then washed three times for 10mins with PBST (PBS with 0.1% Triton) and incubated in the dark for 2-3 hours with the secondary antibody, Alexa-555 goat anti-rabbit (Invitrogen, 21428) diluted 1:1000 in blocking solution. Afterwards, they

were washed three times for 10 mins with PBS in the dark. For DAPI counterstaining, sections were incubated with 1:10000 dilution of DAPI (5 mg/ml stock) in PBS for 5 mins and then washed three times for 10 mins with PBS. They were then mounted on gelatine-coated slides and air-dried overnight under the hood in the dark. Slides were then coverslipped with a drop of Vectashield (Vector Labs) and stored at 4°C in the dark.

The sections were fluorescently imaged with an upright widefield epifluorescent microscope from Leica (DM6000B) and images acquired using a digital Color Camera (Leica, DFC310 FX). The following objectives were used for image acquisition: HCX PL APO 10x/0.40 CS, HC PL 20x/0.75 CS2 and HCX PL APO 40x/0.85 CORR CS.

The quantification of mcherry/GFP/dsred expression, CCK cell counts and cell density of the VMH nucleus were performed in three non-consecutive and equally spaced (100 µm) sections per mouse brain from three mice in total. An equal between images area of the VMH nucleus per hemisphere was drawn as ROI (Region of interest) in NIH ImageJ based on the mouse brain atlas. Cell counts were performed manually on images with the order scrambled with the purpose of blinding the experimenter to the condition/phenotype.

### 2.6.5 DAB (3'3-diaminobenzidine) staining

DAB staining was performed on 20 µm thick floating sections which were placed on 24-well plates with 1 or 2 sections in each well. All steps were performed at RT on a rocking platform unless otherwise stated. Sections were washed three times with PB for 15 minutes and then the endogenous peroxidase activity was quenched by incubating for 20 minutes in 3% $H_2O_2$ (Fluka, cat. no. 95321) (diluted in water). Three 10 minute washes in PBS were performed and then sections were

blocked with 5% fish gelatine with 0.5% Triton-X 100 in PBS for one hour. Sections were incubated with primary antibody diluted in blocking buffer overnight at room temperature. Afterwards, sections were washed three times with PBST (0,1% Triton) for 15 minutes. The secondary antibody biotinylated donkey a-rabbit (Jackson, cat. no. 703-065-155) was applied at a dilution of 1:200 in blocking buffer and sections incubated for 2 hours at room temperature. Sections were then washed three times for 15 minutes with PBST. The peroxidase Vectastain ABC system from (Vector Biolabs, cat. no. PK-6100) was used for the addition of peroxidase onto the biotinalyted secondary antibody. This system contains avidin and peroxidase that were pre-incubated for half an hour in PBS (1:100 dilution of reagent A and B) to form biotin-avidin-peroxidase complexes. These were then incubated with the sections for one hour to allow the free biotin-binding sites of avidin to bind to the biotinylated secondary antibody on the sections. Sections were washed three times for 15 minutes with TBS and two times for 15 minutes with TB. DAB (3'3-diaminobenzidine) was then used which gets converted to a brown precipitate by the peroxidase in the presence of hydrogen peroxide. DAB tablets suspended in water (Sigma, cat. no. D4168) were used which give a ready-to-use solution. Sections were incubated usually for 1-3 minutes until adequate neuronal staining was visible without any background staining in control sections that were not incubated with primary antibody. The reaction was immediately stopped by washing three times for 1 minute with ice-cold TB with mild shaking on ice. The sections were then mounted on gelatine-coated slides and dried overnight. Sections were dehydrated for one minute in 90% and then 100% EtOH, incubated 10 minutes in xylene and then coverslipped with Vectamount and the slides air-dried for at least a

day before imaging them. Brightfield images were taken with a Leica Microscope with 10x and 20x Leica objectives as described above.

## 2.7 Intracranial injections

### 2.7.1 Adeno-Associated Viral (AAV) particles

AAV2/5-eSyn-FLPo-WPRE (Vector Biolabs, VB4858)

AAV viral particles packaged in serotype 5 capsid expressing FLPo recombinase driven by the eSyn promoter and its expression enhanced by the WPRE (woodchuck hepatitis B post-transcriptional regulatory element). The eSYN is a hybrid promoter consisting of a 0.4Kb CMV enhancer (E) and the 0.45Kb human Synapsin I promoter fragment (hSYN1). eSYN hybrid promoter gives about 2-4 fold higher expression than that of the parental hSYN1 promoter. CCK-iDTR animals were injected bilaterally with 1µl of a titre of $1.4 \times 10^{13}$ GC/ml. Upon expression of FLPo in the injected area, the mcherry fluorescent protein and the second stop cassette upstream of the diphtheria toxin receptor will be removed.

AAV1-CAG-FLEX-eGFP-WPRE-bGH (Pennsylvania Vector core, AV-1-ALL854)

AAV particles in serotype 1 capsid expressing the GFP fluorescent protein in a cre-dependent manner under the CAG promoter (hybrid of cytomegalovirus (CMV) enhancer fused to the chicken beta-actin promoter). This AAV utilised the FLEX system. Upon cre recombination the coding sequence with respect to the promoter is switched from the anti-sense to the sense orientation. GFP is flanked by loxP and lox2272 variant for irreversible cre recombination. We injected 200nl of this AAV at a titre of $9.16 \times 10^{12}$ GC/ml. A mixture with 800nl of AAV2/5-eSyn-FLPo-WPRE was used for the DT systemic ablation neuronal counts.

AAV9-FLEX-CAG-DTA-IRES-mcherry (Virovek, Lot 15-335)

AAV particles in serotype 9 capsid expressing Diphtheria Toxin A subunit (DTA) and mcherry fluorescent protein on a cre-dependent manner under the CAG promoter. Cre-dependent expression is achieved by the FLEx system described above. The mcherry fluorescent protein is expressed independently from the DTA as there is an IRES (Internal Ribosome Entry Site) element in-between. We injected 300nl of this AAV at a titre of $2.32 \times 10^{13}$ GC/ml and $2.32 \times 10^{11}$ GC/ml.

AAV9-CAG-mCherry (Virovek, Lot 11-148)

AAV particles in serotype 9 capsid expressing mcherry fluorescent protein under the CAG promoter. We injected 500nl of this virus at a titre of $2.1 \times 10^{13}$ GC/ml.

AAV2/5-hSyn-DIO-hm4D-mcherry (University of North Carolina vector core)

AAV particles in serotype 5 capsid expressing on a cre-dependent manner the inhibitory G protein-coupled receptor hm4Di DREADD (Designer Receptors Exclusively Activated by Designer Drugs). The expression is driven by the hsyn promoter and the DREADD is fused to mcherry protein at the C terminus for easier visualisation of expression by immunofluorescence. DREADDs are members of the muscarinic receptors family and have point mutations introduced to them through directed molecular evolution, in order to be activated by the otherwise inert drug clozapine-N-oxide (CNO) but do not respond to the native ligand ACh or in the absence of ligand. In neurons, activation of hM4Di induces neuronal silencing by coupling to Gi protein and stimulating calcium release and ERK1/2 activation, inhibits forskolin-induced cAMP formation, and, in cultured neurons, it was shown to activate GIRK, thereby causing hyperpolarization and inhibition of basal action potential firing. We injected 200nl of this AAV at a titre of $5.1 \times 10^{12}$ GC/ml.

### 2.7.2 Stereotactic surgery

Experimental animals were first weighed prior to the procedure and then anaesthetised with vaporised 2-3% Isoflurane in 2L O2/min (Abbott, No: B506). Each animal was placed on a standard stereotactic frame (Stoelting) by placing its teeth on the clamp and the head position fixed with ear bars and a nose clamp. Ocular lubricant (Allergan, Marlow, UK) was applied. The temperature was monitored constantly with a probe underneath the animal and an insulator on top of it to help in keeping the temperature steady at around 36.5$^{o}$C. The % of the anaesthetic was usually set to 2-2.5% to sustain sufficient depth of anaesthesia at 60 breaths per min and with no pinch toe reflex and adjusted as needed during procedure. An analgesic cocktail consisting of Metacam (active substance: Meloxicam, non-steroidal anti-inflammatory and analgesic) (5mg/Kg) and Vetergesic (active substance: Buprenorphine, potent partial mu agonist analgesic) (0.1mg/Kg), was administered by intraperitoneal injection and a local injection of Marcain solution (2mg/Kg) underneath the skin of the head. The scalp was shaved with electric clippers, and the operative field was disinfected with iodine solution. The iodine application was done from the centre of the shaved part and working in circular mode outwards. A surgical stereoscope (Wild Heerbrugg M655, Gais, Switzerland) was used for better precision in the stereotactic surgery. A 1cm long sagittal incision was made to expose the bregma and lamda points and the skull was cleaned with sterile saline from any soft tissue. Cotton buds with or without saline were used for cleaning the skull and adsorb any blood from small vessels at the site of the burr holes throughout the procedure. The skull was adjusted flat in the horizontal plane, by tweaking the height of the nose clamp and the ear bars, as measured by the coordinates of bregma and lamda and two juxtaposed lateral

coordinates. The distance between bregma and lambda was measured and subsequently divided by 4.15 mm, which is the average distance between lambda and bregma for C57BL/6J mice (Allen Mouse Brain Atlas). This value was then multiplied by the predetermined stereotaxic coordinates, resulting in stereotaxic coordinates adjusted for the size of the mouse brain. The coordinates for the optimisation experiments were as follows: for the AHNc the predetermined coordinates (Allen Mouse Brain Atlas) were: Anterior-posterior -0.5mm, mediolateral ±0.5mm, dorsoventral -5.8mm. The VMHvl predetermined coordinates were: AP -1.28mm, ML: ±0.5mm, DV -6.25mm. For targeting the whole VMH nucleus, the coordinates were adjusted to AP 1.5mm, ML ±0.6mm and DV -6.5mm. Burr holes of 0.8mm diameter were drilled until the dura was exposed. Drilling was done in a circular mode and not with direct force down the skull and forceps were used to assist by holding down the skull. Drilling was intermittent with small 2 second intervals so that heat from friction is not damaging and cracking the skull. A precision 5µl syringe (Hamilton 75 RN 5uL SYR W/O NEEDLE, ESSLAB, cat.no.:7634-01) with a 34G bevelled needle (45º) with length 30mm (Hamilton RN Needle, ESSLAB, cat.no.: 207434) was used to inject any of the aforementioned AAV particles or 200nl of 0.1% (w/v) yellow-green fluorescent microspheres (Life technologies, No: F-8795) for the optimisation surgeries. The injectate was administered at a rate of 125nl/min using an automatic motorised micropump (Ultramicropump3 microsyringe injector with micro4 controller, World Precision Instruments). After injection, the needle was left in place for 10 minutes to prevent reflux and enable diffusion of the viral suspension, and then slowly withdrawn. The needle was retracted with a moderately fast pace from the site around 200-500µm and after 2mins of wait it was completely retracted at a steady pace. Sutures were made to close the incision with

3-4 surgical knots by using Ethicon Coated vicryl 5-0 FS3 conv 16mm 3/8c cutting ( Johnson Johnson, cat.no: W9442). Each animal was observed until complete recovery from anaesthesia. The recovery was done on a pre-warmed to 30$^{o}$C incubator chamber. When the animal regained its consciousness, and demonstrated it could independently move around the chamber, it was then transferred to its home cage. Each animal was closely observed for a week following the surgery and post-operative care was given by administering Metacam by intraperitoneal injection if the mouse expressed signs of pain and distress from the surgery. The animals were allowed to recover for 3-4 weeks prior of any experiments, this allowed enough time for any AAVs to be adequately expressed in the brain.

## 2.8 Food intake measurements and analysis

### 2.8.1 Metabolic cages and measurements

The animals that had undergone surgery were allowed to recover for at least 3-4 weeks. Food intake was measured in LabMaster metabolic cages from TSE Systems (Bad Homburg, Germany) that are equipped with sensors that measure food and water intake by averaging weight changes of the food hopper in ten second intervals with a sensitivity of 0.01 g through a calibrated sensor. Food and water was provided ad libitum. The mice were fed the normal chow diet '2018 Teklad Rodent Diet' (60% calories from carbohydrates, 23% from protein and 17% from fat, 3.3 Kcal/g digestible energy). Two days prior the experiment, we habituated the mice to the new water bottle nozzle which releases water upon touch. We changed their water bottles of their home cage so that they get trained to drink water freely. The animals were also handled daily as part of the habituation. The height of the drinking bottle and food hopper were adjusted accordingly (above half of each animal's body

height) so that the animal can comfortably reach them while minimising the possibility of accidental hits of the food hopper by their body which could interfere with the sensor readings. We singly housed the animals in the metabolic cages and allowed them at least a week to habituate to the new environment before recording any food sensor measurements. The cages were inspected daily for any dropped pellets and the small pellets removed from the food hopper to avoid any future drops. We defined each meal event (meal bout) as the sum of all the sensor measurements that were spaced less than 15mins from each other (minimum intermeal interval) which is commonly used in defining meals in mice and rats (Farley *et al.*, 2003; Atalayer and Rowland, 2011; Bake *et al.*, 2014). The minimum food intake recorded per meal bout was 0.02g in order to exclude any false positive events of the sensor. Analysing the data after varying the minimum meal size and intermeal interval did not alter the results. The following measurements were taken in any given day or for a specific time window according to the experiment. Each meal as defined above was recorded with date and time stamps, its duration in minutes, the total amount of food consumed for each meal (meal size) and the time between the end of each meal and the start of the next (intermeal time). Also, the rate of consumption was calculated per meal (g/min). The meal numbers were calculated as the sum of each of these meal events that were recorded for the respective time window in question and recordings from a given amount of consecutive days were averaged. Meal size, duration, rate and intermeal time were all averaged for the time window examined either that would be daily (average of days) or in specific hours (i.e. 6h post DREADD activation).

### 2.8.2 Pharmacogenetic DREADD inhibition

The animals were subjected to stereotactic surgery as described above and injected bilaterally in the VMH region with AAV2/5-hSyn-DIO-hm4D-mcherry and were allowed to recover for 3-4 weeks. While the animals remained housed in groups, we habituated them in handling for 3 days twice a day to imitate the protocol of intraperitoneal (ip) injections. The animals were trained in the metabolic cage water bottle a day before singly housing them, as described above. They were habituated to the metabolic cages for 2 days while being handled twice a day. Intraperitoneal injections of sterile saline (with 10% DMSO, see below) were administered every 10am and 6pm for a total of 10 days in order to habituate the animals to the ip injections. Food intake data was collected throughout these habituation days. Following habituation, we subjected the animals to increasing doses of CNO (clozapine-N-oxide, Tocris biosciences, cat.no. 4936) by ip injections twice daily as mentioned earlier. The doses used were 0.75/1.5/2 and 3 mg/Kg of body weight. A CNO stock solution of 1mg/ml in sterile PBS with 10% DMSO (dimethylsulfoxide) was prepared. CNO is soluble in organic solvents so we had to dilute it first in 100% DMSO and then add PBS. The CNO stock was aliquoted and kept at -20$^{o}$C until day of use and dilutions for ip injections prepared fresh in PBS each day. Each CNO dose was prepared by diluting the stock solution with PBS to a final injectate volume of 10µl/g body weight. Each dose was administered for a total of 3 days twice daily at the times mentioned and daily or 6h post-CNO data was averaged across the days. Food intake measurements and meal pattern analysis was performed as described above. Prior to every ip injection each animal's cage sensors were paused for 1min and the animal was handled for performing the

ip injection. Disturbance was kept at a minimum and attention was given in ensuring similar handling between all mice of the experiment.

### 2.9 Diphtheria toxin administration

BAC-CCK-Cre;R26R$^{LxP\text{-}FRT\text{-}iDTR}$ (CCK-iDTR) mice were injected stereotactically with AAV-FLPo (AAV2/5-eSyn-FLPo-WPRE) as described above and were allowed to recover from surgery for 3-4 weeks. They were then intraperitoneally injected twice with DT 30-40ng/g of body weight with the injections 72h apart from each other. A stock of 500µg/ml Diphtheria toxin (DT) (Sigma Aldrich, ca.no. D0654) was made by re-suspending the pre-weighted 1mg of lyophilised DT in 2ml of sterile PBS. Starting three days before the first ip injection, we recorded the animal weights and assessed their health every day. On the day of the first ip injection, the animals were weighted and the first DT injection was administered at 9am. The animals' health was assessed on the same day at 6pm before their active period to ensure they are not affected by the DT dose. We continued to monitor the animals and record their weight every day. On the 3$^{rd}$ day at 9am, the second DT dose was administered. As mentioned in the respective results section, the 40ng/g BW dose resulted in malaise and even death in our first experimental cohort. Hence, in consultation with the veterinary unit of the establishment, we established intervention points and close monitoring for health assessment which included distress scoring and weight loss records with decision points according to any weight loss or signs of distress observed. In the event of observing 5-10% weight loss the NACWO/Vet was informed. In the case of 10% weight loss with distress signs, the second DT dose would be postponed and NACWO/Vet would be consulted. If more than 15% weight loss was observed with signs of distress, immediate advice would be sought and experiment terminated.

## 2.10 Statistical analysis

All experiments and analysis were carried out blind to the genotype and with at least three animals per genotype unless stated otherwise. All results are indicated as mean ± standard error of the mean (s.e.m.) unless stated otherwise. Significance between samples was assessed by paired or unpaired two-tailed Student's t-test and one or two-way analysis of variance followed by post-hoc multiple comparisons tests either Dunnett's or Sidak's post hoc test or Fisher's LSD test as it was deemed appropriate for each data set. The statistical analysis is indicated in each figure's legend. Differences were considered significant when $p<0.05$. No statistical methods were used in this study in order to predetermine sample sizes. Nevertheless, the reported sample sizes conformed to those commonly used in analogous studies. Analyses were performed with GraphPad Software (La Jolla, CA, USA)

# Chapter 3: The development of techniques and tools for cell-type and region-specific investigation of the CCK neurons of the VMH nucleus

## 3.1 CCK neurons around the hypothalamic nuclei and the VMH

We utilised the already generated and characterised BAC-CCK-Cre mouse line to harvest the power of Cre-lox technology to affect exclusively the CCK neurons. Primarily we crossed the Cre line to the R26R-Ai9 reporter line which has a floxed variant of tdtomato fluorescent protein named Ai9. Upon cre recombination, Ai9 is expressed only on the cre+ cells which then allows the visualisation of these neurons by microscopy. Ai9 strain is known to give strong and robust fluorescence, so we relied only on endogenous fluorescence of td-tomato for imaging the tissue. We mapped the Ai9-CCK brain with emphasis to the hypothalamus and the nuclei surrounding the VMH nucleus. I used immunofluorescence imaging and immunohistochemical staining with 3,3'-diaminobenzidine (DAB) and visualised in both coronal and sagittal sections the CCK positive neurons and their fibres (Figure 5). As it has been previously shown by Dr Mirjam Geibel, a PhD student at the time in the lab, I found CCK neuronal bodies in the AHN, DMH and VMH nuclei, some in ARH and SCH and very few in the PVN.

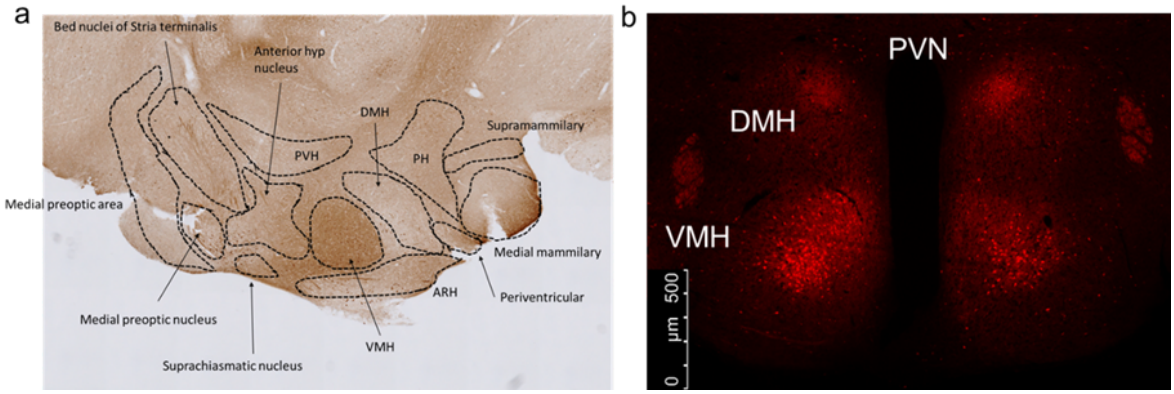


**Figure 5: Immunohistochemical and fluorescence imaging of td tomato-positive CCK neurons in the hypothalamic regions around PVN**. A) Tile image of DAB stained 20µm thick sagittal sections of Ai9-CCK brain, B) fluorescent image of 20µm thick coronal section from Ai9-CCK brain showing endogenous td-tomato expressing CCK neurons around the Paraventricular Nucleus (PVN) in the dorsomedial nucleus (DMH) and the ventromedial hypothalamus (VMH).

## 3.2 Stereotactic injection to the hypothalamus for delivering AAV injections to the VMH nucleus

I successfully injected latex beads to the hypothalamic VMH nucleus and co-localised green fluorescence with Ai9-CCK neurons within a radius of 100µm. This was a technically challenging surgery for which I had to develop my own stereotactic protocol relying on custom calculations considering the precision limitations regarding skull alignment of manual/digital stereotactic equipment for each individual surgery. There are no other groups in Oxford that do injections in the hypothalamus and it is a relatively rare region to be targeted by stereotactic surgeries compared to other accessible regions in the adult rodent brain (i.e. hippocampus, cortex). The main difficulty arises from the depth required (5.8-6.25mm ventral from surface) in combination with the variable estimation of the exact bregma location and the limitation in placing the skull horizontal flat with almost no tilt in all axes (horizontal, lateral and rostrocaudal axes). Initially, we

targeted two coordinates, anterior and posterior to the PVN nucleus, aiming at maximising the affected location around the VMH region. At first few attempts, the rostro-caudal angle of the brain (most critical variable) resulted in 400μm more caudal injection from the planned coordinates. After nine surgeries, I managed to overcome the problem of tilted brain by using coordinate reference points laterally from midline in combination with the bregma and lamda coordinates. I used these to calculate by trigonometry the angles in degrees for each axis and to adjust accordingly the coordinates for each individual mouse during surgery in real time. The rotation of the stereotactic arm was also utilised, when possible, to correct the lateral axis tilt of the brain. Representative images from two stereotactic injections in the same brain, show the co-localisation of green microspheres with CCK neurons in three serial sections spaced 100μm from each other both anterior and posterior to the PVN (Figure 6, 7). At the anterior set of coordinates, you can see the final part of the trajectory and the spread of the microspheres in the AHN nucleus (Figure 6). Similarly, the posterior (to PVN) injection delivers the beads around the posterior part of AHN, the anterior part of DMH and the VMH nucleus (Figure 7). The tile images of both injections show no backflow of beads to the needle trajectory, restricting the injection to the hypothalamus and not to any dorsal regions that the injection passes through. Following this optimisation, we restricted further the coordinate selection by adjusting the anterior-posterior and mediolateral coordinates for targeting exclusively the VMH nucleus and not any anterior hypothalamic nuclei. Collectively, these results form the basis of my project for stereotactic delivery of AAV particles expressing either DREADDs for synaptic inhibition or FLPo and DTA for the ablation of hypothalamic CCK neurons specifically at the region of the VMH nucleus.

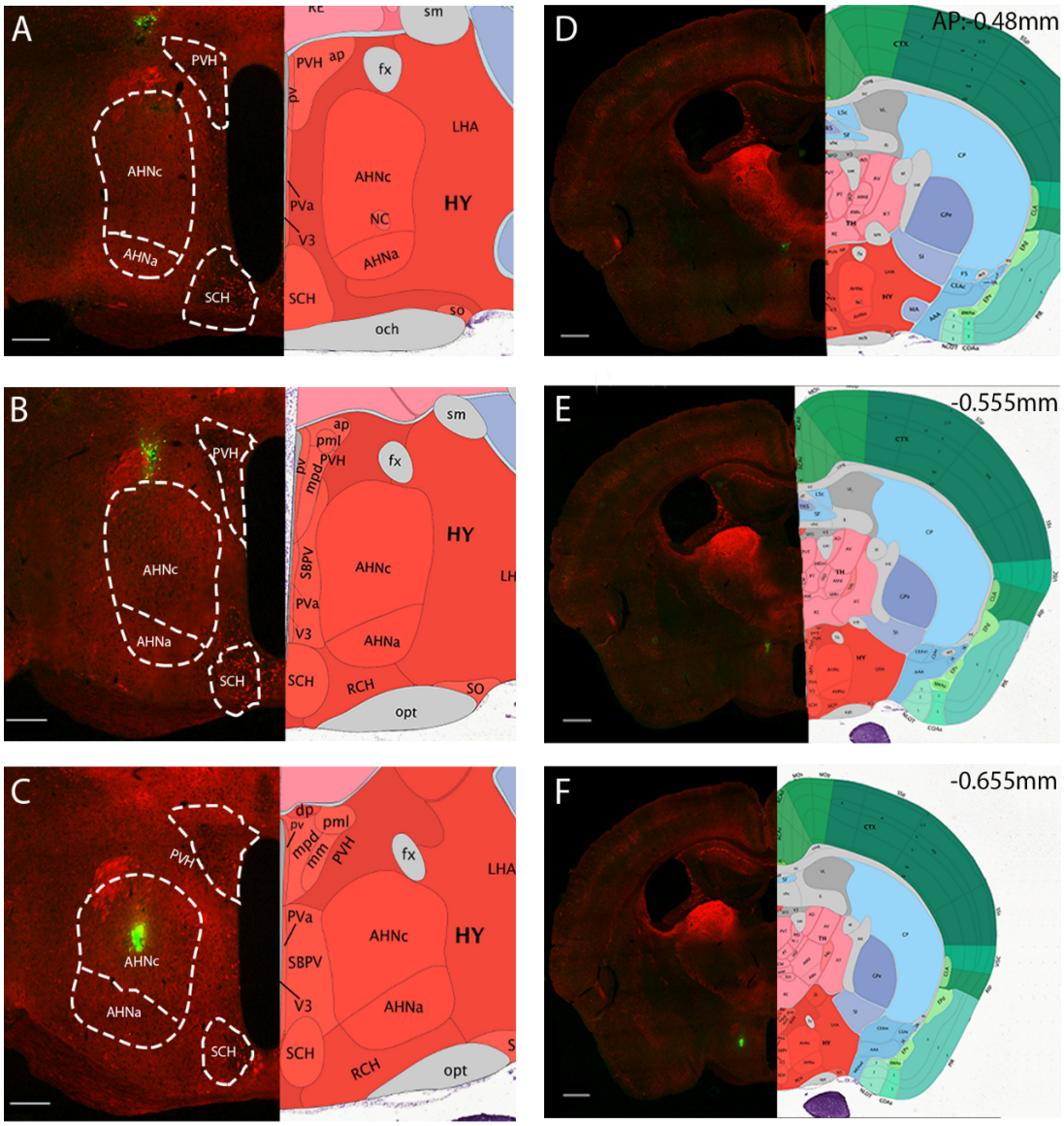


**Figure 6: Stereotactic delivery of green fluorescent latex particles in the hypothalamic peri-PVN region of BAC-CCK-Cre$^{tg/+}$;Ai9 mice.** 200nl of 0.1% w/v latex particles (0.04µm diameter, Invitrogen, cat no:F-8795) were injected unilateraly to the AHNc at the stereotactic coordinates AP:-0.5mm, DV:-5.8mm (from dura), VL: ±0.5mm. Tile images of 20µm thick coronal sections spaced 100µm between them from -0.48mm to -0.655mm from bregma. (a-c) Images emphasizing the region of hypothalamus showing green fluorescence co-localising with td-tomato positive CCK neurons in AHN and VMH nuclei with DMH also in proximity (scale bar 200µm) or (d-f) whole brain images showing green fluorescence exclusively in the hypothalamic regions anterior to PVN (scale bar 500µm) alongside atlas reference images (from ©2014 Allen Institute for Brain Science, Allen Mouse Brain Atlas [Internet])

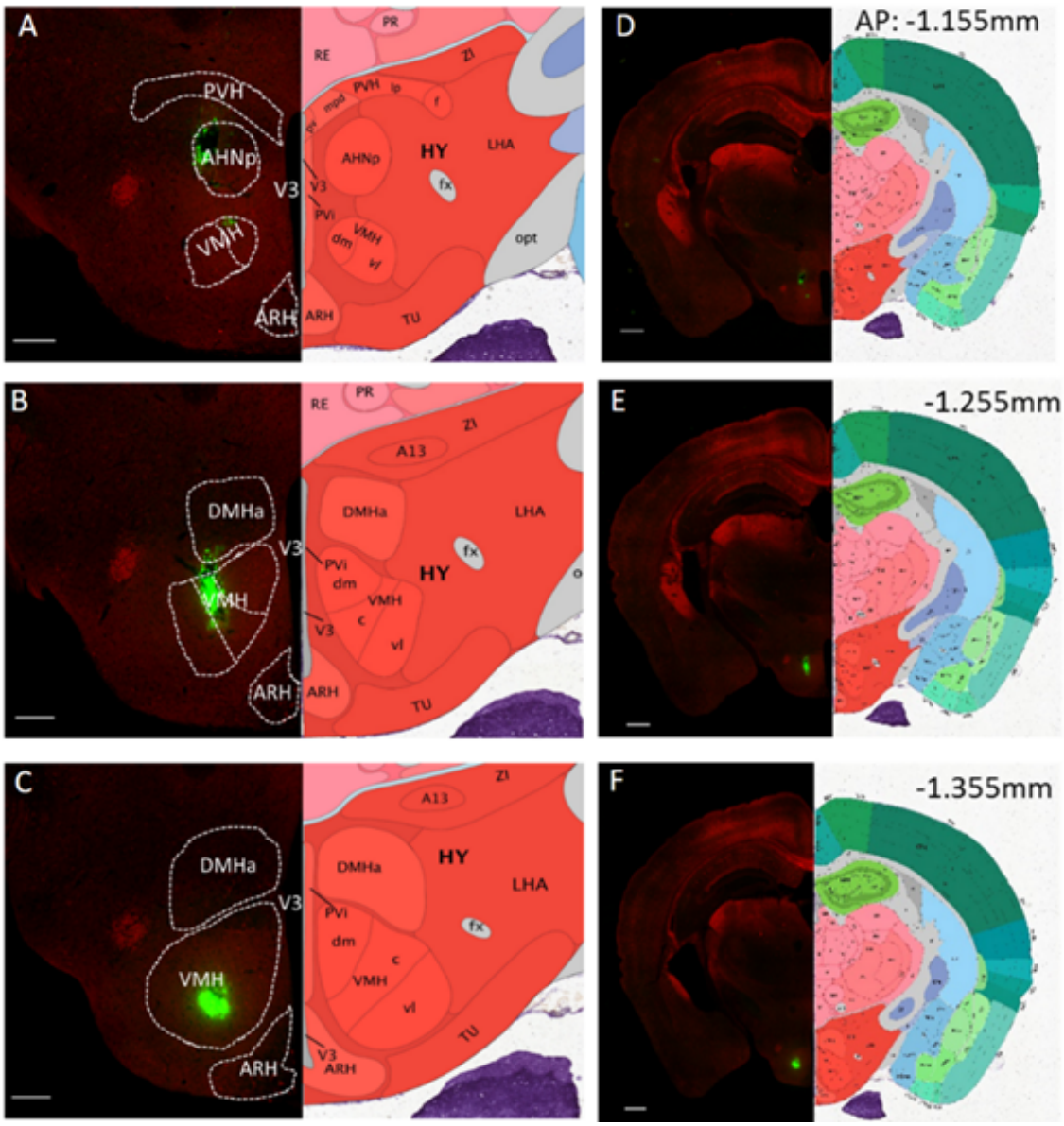


**Figure 7: Stereotactic delivery of green fluorescent latex particles in the hypothalamic peri-PVN region of BAC-CCK-Cre$^{tg/+}$; Ai9 mice.** 200nl of 0.1% w/v latex particles (0.04µm diameter, Invitrogen, cat no:F-8795) were injected unilateraly to the VMHvl at the stereotactic coordinates AP:-1.28mm, DV:-6.25mm (from dura), VL: ±0.5mm. Tile images of 20µm thick coronal sections spaced 100µm between them from -1.155mm to -1.355mm from bregma. (a-c) Images emphasizing the region of hypothalamus showing green fluorescence co-localising with td-tomato positive CCK neurons in AHN and VMH nuclei with DMH also in proximity (scale bar 200µm) or (d-f) whole brain images showing green fluorescence exclusively in the hypothalamic regions posterior to PVN (scale bar 500µm) alongside atlas reference images (from ©2014 Allen Institute for Brain Science, Allen Mouse Brain Atlas [Internet])

## 3.3 Pharmacogenetic inhibition of $CCK^{VMH}$ neurons: Expression of DREADDs and CNO-mediated silencing of CCK neurons

The short-term role of $CCK^{VMH}$ neurons in homeostatic regulation was assessed by acute inhibition of their neurotransmission by utilising a pharmacogenetics approached called DREADDs (Designer Receptors Exclusively Activated by Designer Drugs) originally developed by Prof. Brian Roth (Roth, Hill and Carolina, 2013) (Figure 8A). The neuronal silencing is achieved upon activation of the DREADD receptor with the otherwise inert (for mice) clozapine-n-oxide (CNO) drug that can be delivered systemically. Firstly, we successfully established a stable expression of the inhibitory DREADD receptor in the $CCK^{VMH}$ neurons by stereotactic delivery of the AAV2/5-hSyn-DIO-hm4D-mcherry bilaterally at the coordinates we previously established for targeting the VMH nucleus (Figure 8B). A group of BAC-CCK-Cre animals was injected bilaterally with 200nl of the AAV at a titre of $5.1 \times 10^{12}$ GC/ml. The animals were sacrificed after 3 weeks for assessing the expression levels of DREADDs by visualising the mcherry fluorescent protein fused to the C terminus of the hm4D receptor (Figure 8C). The endogenous mcherry expression was found at the VMH nucleus without the need to use an a-dsred antibody to enhance the fluorescent signal. On a higher magnification, the mcherry puncta can be seen mostly on the somata and axons of the $CCK^{VMH}$ neurons. Following their successful expression, we validated the ability of CNO to successfully inhibit their neurotransmission by electrophysiological recordings of their firing rate upon CNO administration. We injected another group of animals but this time unilaterally with DREADDs and on the other hemisphere we injected a control AAV-DIO-GFP virus (data not shown). Upon CNO bath application at coronal slices of the VMH, the mcherry positive CCK neurons reduced significantly their

firing relative to pre-CNO recordings while there was no firing change to the GFP positive control CCK neurons of the other hemisphere (data not shown). The recordings and analysis were done by Dr Tommas Ellender. Collectively, we optimised and successfully developed a protocol to in vivo modulate the activity of the hypothalamic CCK neurons with the established technique of inhibitory DREADDs. We achieved high expression of the receptor, capable of silencing these neurons upon CNO application.

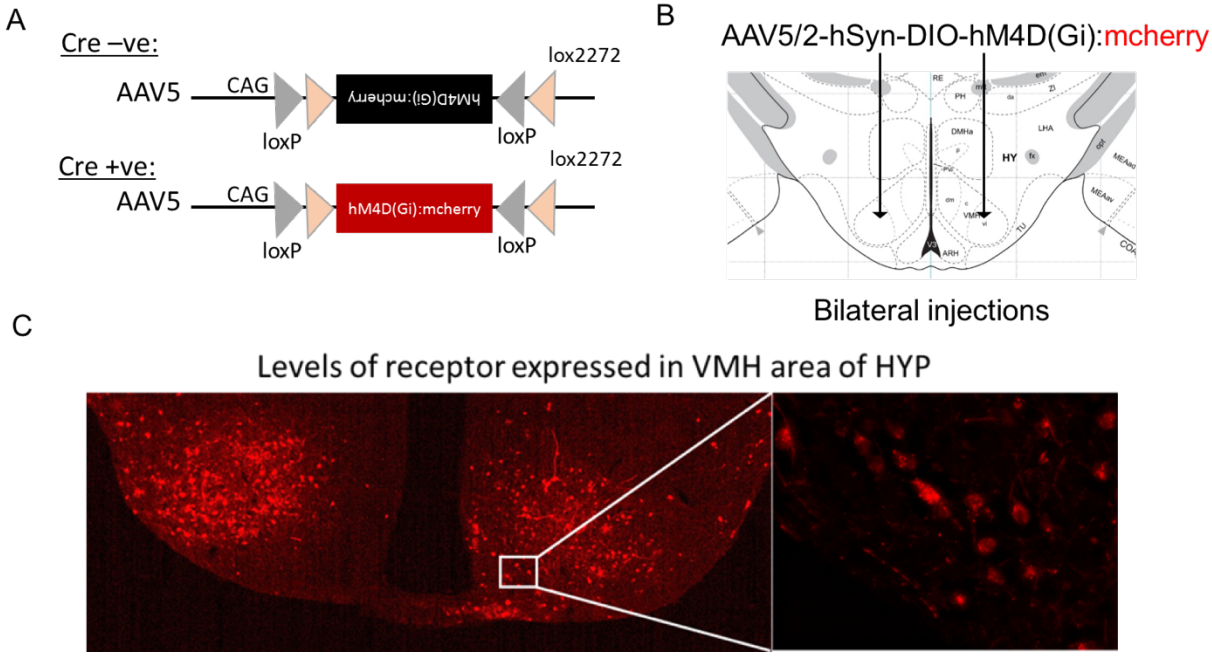


**Figure 8: CCK$^{VMH}$ neuronal expression of inhibitory hM4D Designer Receptor Exclusively Activated by Designer Drugs (DREADD) which confers inhibition of neurotransmission upon CNO application.** A) schematic of cre-inducible DREADD viral construct AAV2/5-hSyn-DIO-hm4D-mcherry. B) Schematic of the stereotactic delivery of the AAV-DREADD at VMH coordinates. BAC-CCK-Cre animals were injected bilaterally with 200nl of the AAV at a titre of 5.1 x $10^{12}$ GC/ml. C) DREADD expression after 3 weeks from the surgery visualised by the mcherry fluorescence.

## 3.4 Assessing the long-term role of $CCK^{VMH}$ neurons by diphtheria toxin ablation strategy

### 3.4.1 Generation of a double recombinase mediated diphtheria toxin receptor mouse line: BAC-CCK-Cre; $Rosa26^{LxP\text{-}FRT\text{-}iDTR}$

The long-term role of $CCK^{VMH}$ neurons in homeostatic regulation was examined by cell and region-specific ablation. The ablation was achieved by expressing diphtheria toxin receptor (DTR) only to this cell type in the VMH nucleus and systemically administering diphtheria toxin (DT). We therefore generated a double recombinase inducible diphtheria toxin receptor (iDTR) transgenic mouse in which Cre- and Flp- mediated excision of two consecutive STOP cassettes allows the expression of DTR fused to green fluorescent protein (GFP) (iDTR-GFP). The conditional DTR cassette was inserted into the ubiquitously expressed Rosa26 promoter, resulting in the Rosa26LxP-FRT-iDTR mouse line. Crossing this line to the BAC-CCK-Cre line will result in the CCK-iDTR line which will allow expression of the DTR in the CCK-Cre neurons upon region-specific transduction with AAV-mediated FLPo recombinase expression (VMH nucleus in this case). Only in the CCK neurons, Cre recombinase will excise the first stop cassette that is flanked by loxP sites and allow the mcherry to be expressed. Mcherry expression will act as a reporter for the CCK positive neurons. The mcherry and a second stop cassette are flanked by FRT sites which will get excised upon stereotactic delivery of AAV-FLPo. Subsequently, only CCK neurons in the regions transduced by the AAV-FLPo, will switch from mcherry to GFP positive neurons, indicating the successful expression of DTR. An IP injection of DT will lead to specific ablation of the hypothalamic CCK neurons of the VMH (Figure 9).

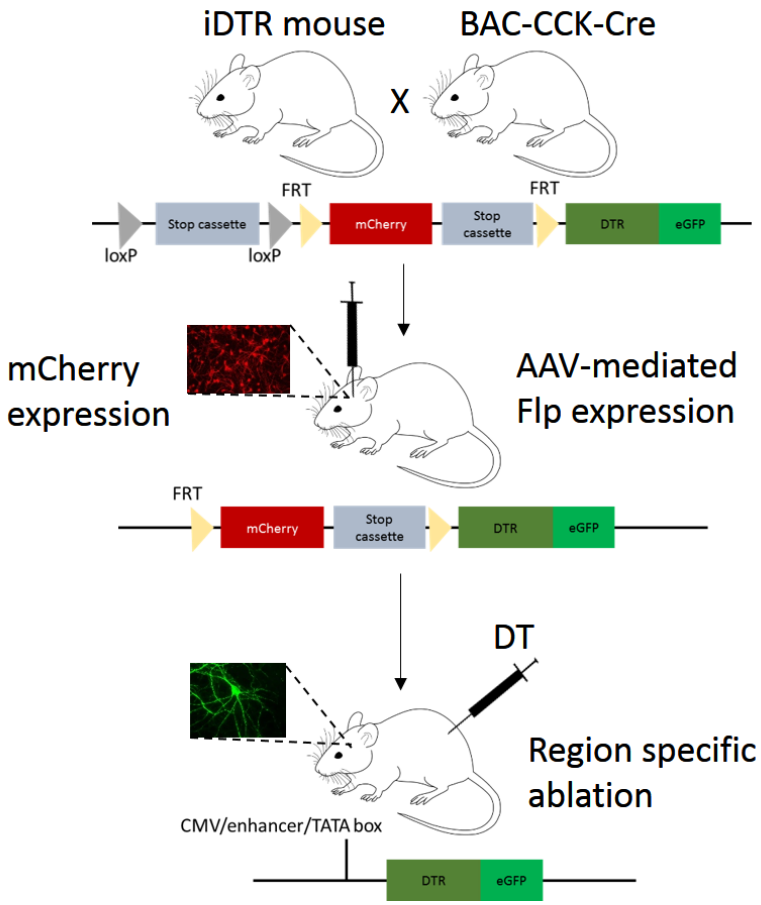


**Figure 9: Schematic summary of region-specific ablation of CCK neurons by diphtheria toxin administration.** AAV transduction of Flp recombinase allows regional specific ablation. CCK specific cre-mediated recombination removes the floxed stop cassette and mcherry is expressed. Stereotactic injection of AAV expressing FLPo recombinase removes the second stop cassette and the mcherry gene, allowing the expression of iDTR fused to eGFP at the C terminus. The CCK neurons infected by the AAV will be ablated upon systemic delivery of DT.

To generate the CCK-iDTR mouse strain (Figure 9), a construct containing the elements depicted in Figure 10 was inserted by homologous recombination into embryonic stem cells (ESCs) by a mouse genetic service. I then screened 144 clones by southern blot to identify clones in which the iDTR construct was successfully inserted by homologous recombination in the Rosa26 locus. The correct clone would show two bands of distinct different sizes in base pairs, one for the wild type allele of Rosa26 locus and the other one for the iDTR knock-in allele, by digesting the genomic DNA of each ESC clone with different restriction endonuclease enzymes and hybridizing radioactive probes at either 5' or 3' end of the targeted region. The 3' probe would give 2 bands at 19.2 and 11 kbp and the 5' probe would give 13.2 and 10.4 kbp size band, respectively (Figure 10). I amplified the respective sequences for the two probes from plasmids by PCR and purified the probes after gel electrophoresis using a commercially available nucleotide purification column. The purified probe was run on an agarose gel to be quantified and verified that it is the correct size (Figure 11A). The probes were then used as a template to incorporate $^{32}$P-CTP and the radioactive probes were used for hybridisation of the PVDF membrane. Firstly, by screening with the 3' probe, I identified 3 positive clones for the iDTR knock-in, a representative southern blot with clone 5A3 is shown (Figure 11B) with a distinct band of 11 kbp indicating successful integration of iDTR. The three positive clones were subsequently probed with 5' probe to verify the iDTR construct is incorporated correctly into the locus. The clones 4D9, 5A3 and 5E6 all gave the expected bands when blotted with both probes (Figure 11C), whereas other clones were negative. Following the screening, two positive clones were sent to be injected into blastocysts and implanted into pseudo-

pregnant mice towards the generation of chimaeras. The germline-positive mice were bred to establish homozygosity for iDTR.

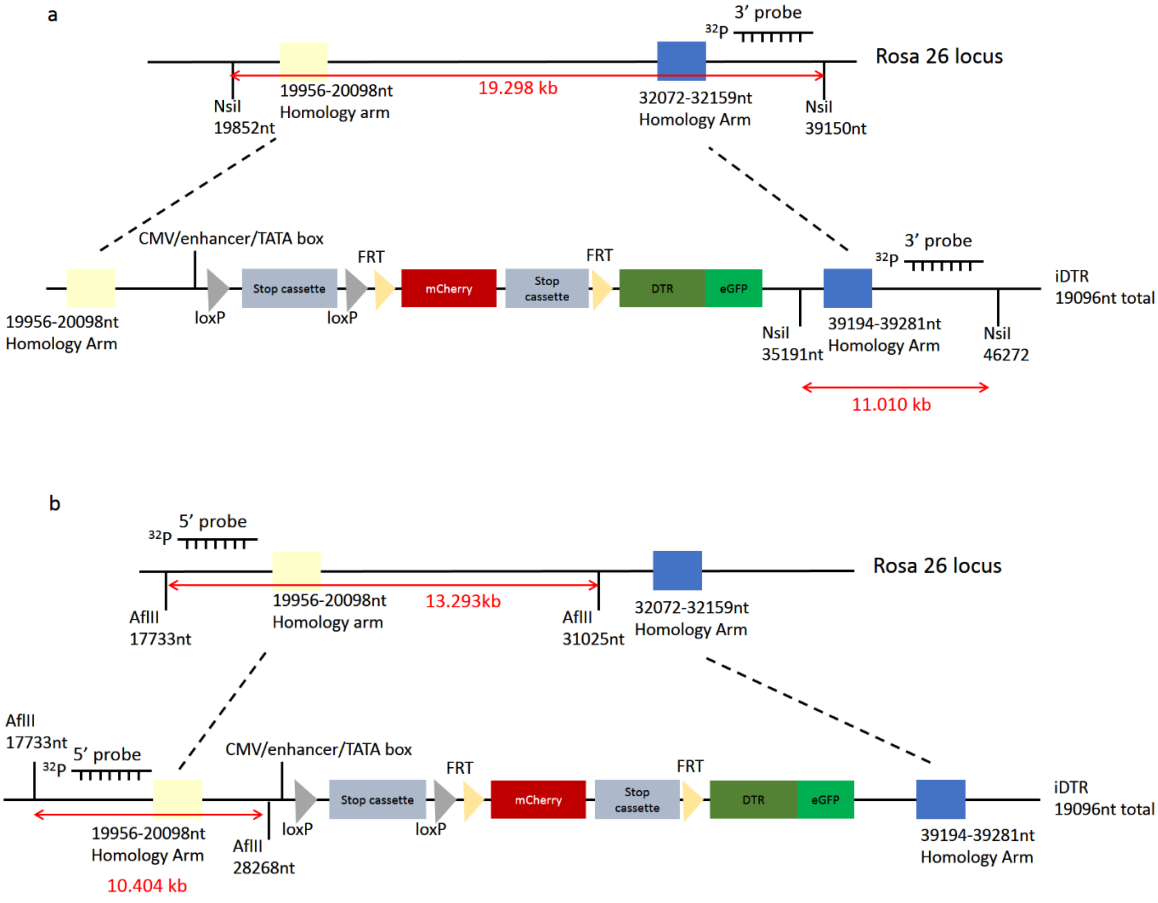


**Figure 10: Schematic representation of southern blot screening of ESCs transfected with the iDTR construct.** Rosa26 locus has been targeted by homologous recombination at the homology arms depicted for introducing the iDTR cassette downstream of regulatory elements. The iDTR construct contains the two stop cassettes flanked by loxP and FRT sites respectively and the DTR sequence fused with eGFP at the C terminus. a) Digestion of wild type allele with NsiI generates 19.3 kbp fragment whereas the knock-in introduces another unique digestion site, resulting in 11 kbp band identified by a radioactive 3’ probe. b) Digestion with AflII generates a 13.3 kbp fragment for wild type allele whereas the knock-in introduces another unique site, resulting in 10.4 kbp identified by a radioactive 5’ probe.

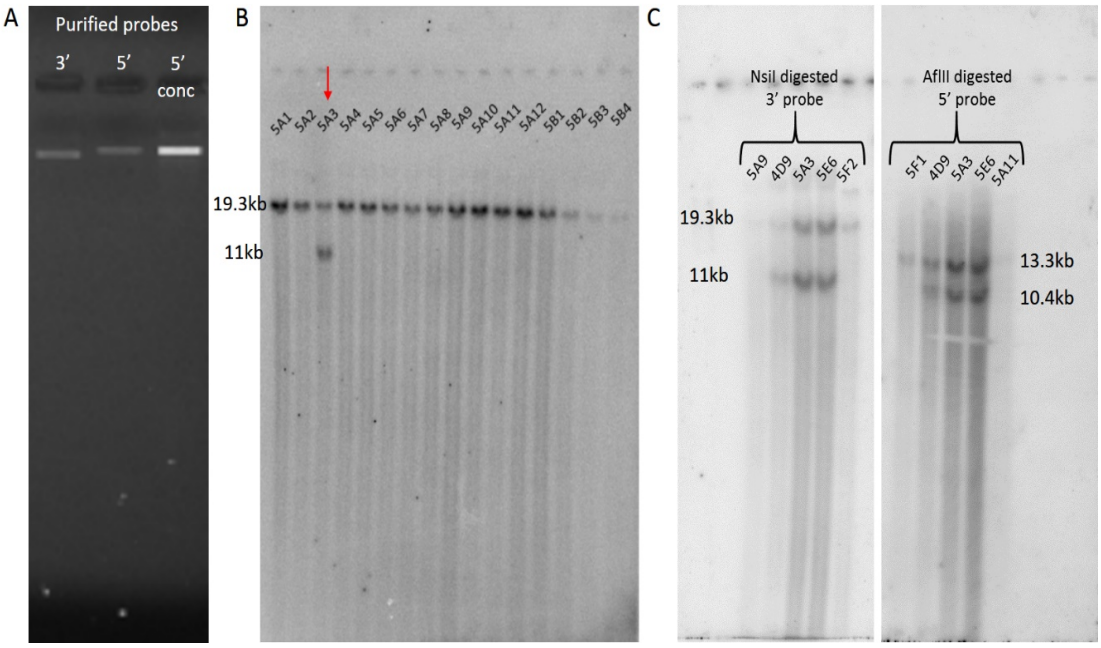


**Figure 11: Positive ESC clones with iDTR construct for generating the Rosa26LxP-FRT-iDTR mouse line**. a) 1 µl of 3' and 5' probe for Rosa26 locus and last lane 5 µl of 5' probe was run in 1% TAE agarose gel for quantification and integrity check. b) Representative of a southern blot with samples digested with NsiI and hybridised with 3' probe showing the positive 5A3 clone (red arrow) with 11kb band size. c) Southern blot with both probes showing all three positive ESC clones identified (4D9, 5A3 and 5E6) in comparison to other negative clones.

### 3.4.2 Characterisation of the CCK-iDTR mouse line

The homozygous for the iDTR cassette mice were then crossed to BAC-CCK-Cre tg+ animals to obtain the CCK-iDTR line. Firstly, we wanted to characterise the ability of the line to excise both stop cassettes and ultimately allow the expression of the DTR-GFP so that CCK ablation will be possible upon DT administration. We chose to analyse the desired functionality of the construct on a genomic and protein level. For these sets of experiments, we crossed the CCK-iDTR line to a deleter FLP line (del-FLP) that expresses FLP ubiquitously. The resulting animals should excise the mcherry- 2$^{nd}$ stop cassette in every cell due to FLP expression while the 1$^{st}$ stop cassette would only be excised in CCK cell which are Cre positive. The ability of the two recombinases (Cre and FLP) to excise in vivo the two stop cassettes was tested on a genomic level by a PCR strategy designed to assess if the said recombination occurred successfully (Figure 12A and B). We designed 3 primers, a forward primer (labelled as fwd1) upstream of the first stop cassette, another one (fwd2) within the 1$^{st}$ stop cassette and a reverse (rev) primer downstream of the 2$^{nd}$ stop cassette, at the DTR sequence. Each set of fwrd-rev primers amplify DNA fragments of a specific base pair length, implying the recombination that has taken place. The fwd2-rev primer set would amplify a 797bp long DNA fragment if the FLP had excised the mcherry 2$^{nd}$ stop cassette. The fwd1-rev primer set would amplify a 407bp long DNA fragment if both Cre and FLP had excised the respective elements from the construct. If the recombination-excision events hadn't taken place, the designed primers would be far apart, making it impossible to amplify any DNA fragment due to the very long length. DNA was extracted and purified from brain and tail clip lysates from animals that were positive for both Cre and FLP and from control FLP only animals (Cre -ve) and the PCR

reactions were run on an agarose gel. Both DNA bands were found on the samples from CCK-iDTR;del-FLP indicating that both recombinases excise the respective stop cassettes of the iDTR line (sample 2, lanes 2 and 4) (Figure 12A). In the cre-ve samples, only the 797bp band was amplified due to the expression of the FLP recombinase. On a protein level, we performed western blotting of protein lysates from brains of Cre+/FLP-ve, Cre/FLP -ve and Cre/FLP+ animals. A BCA assay was done for normalising the total protein levels of all samples. We blotted with a-GFP and identified the presence of the fused DTR-GFP in the Cre/FLP+ animals (Figure 12B). A protein band with molecular weight 53KDa was only observed in samples with both recombinases. Taken together, these results show the ability of the iDTR mouse line to express the DTR-GFP since the upstream stop cassettes can be excised by Cre/FLP and the GFP can be detected in brain protein lysates by western blot.

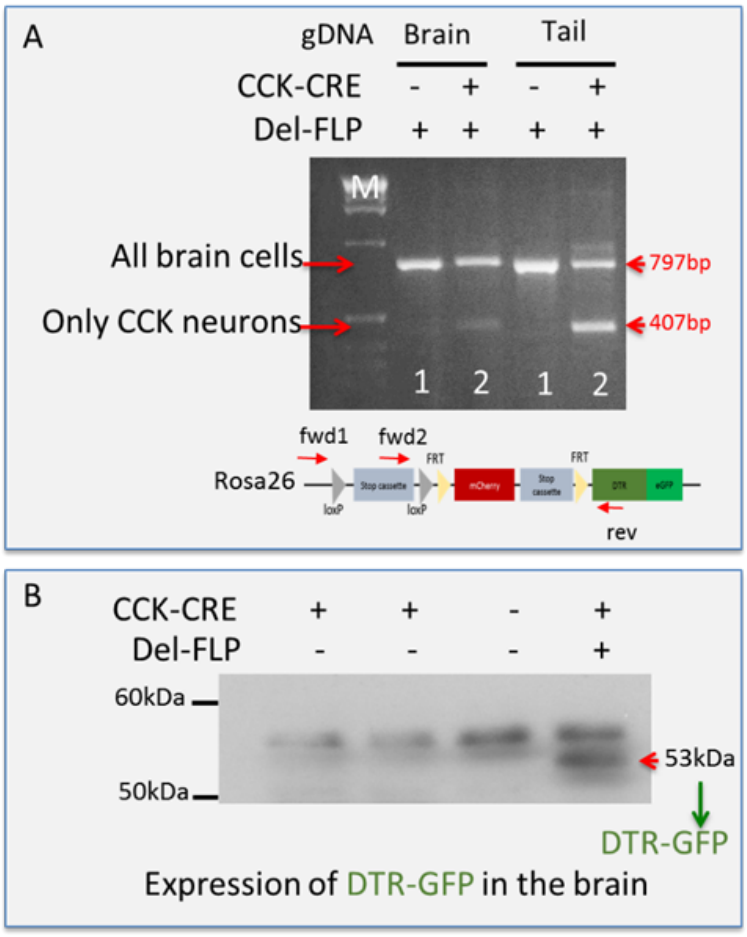


**Figure 12: Successful excision of mCherry stop cassette and expression of iDTR-GFP cassette shown by PCR and western blot analysis of R26ds-iDTR mouse line.** BAC-CCK-Cre;R26ds-iDTR crossed to a Deleter-FLP line was analysed by PCR and western blot for verifying the excision of the first stop by Cre and the excision of mCherry/stop by FLP and the subsequent expression of DTR-GFP. A) PCR analysis of brain and tail genomic DNA of mice positive or negative for Cre in the presence of FLP shows successful excision of stop cassettes. Sample 1 shows the upper band which indicates the excision of mCherry by FLP in all tissues as expected. Sample 2 has both the upper and lower band. The lower band can only be amplified in the presence of Cre and FLP. B) Western blot analysis of brain lysates from mice of different genotypes using antibodies against GFP. First three samples do not have FLP and Cre alone cannot remove the last stop. The last sample has both Cre and FLP and hence an extra band of the fusion of DTR with GFP is detected. This result has been confirmed with two antibodies.

### 3.4.3 Successful expression of mcherry in all the CCK positive neurons

The brains of the CCK-iDTR animals were analysed by a-dsred immunofluorescence to verify the recombination pattern compared to the published characterisation of the BAC-CCK-Cre line. The pattern of recombination was identical to the characterisation of the Cre line as seen by a representative sagittal section compared to the BAC-CCK-Cre crossed to a reporter line (R26R-EYFP$^{yfp/+}$) (Figure 13).

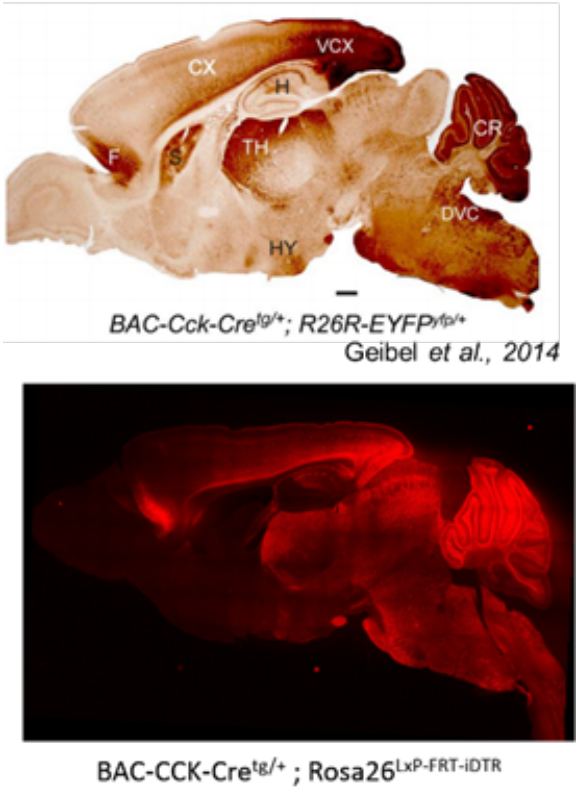


**Figure 13: Identical recombination pattern between the newly generated R26ds-iDTR mouse line crossed to BAC-CCK-Cre$^{tg/+}$ strain and the previously published BAC-CCK-Cre line crossed with a R26-EYFP reporter line.** A) Sagittal section of BAC-CCK-Cre$^{tg/+}$ ; R26RLxP-FRT-iDTR mouse immunostained with anti-dsred depicting the mCherry-positive CCK neurons in the same anatomical locations seen in panel (B). B) Adult sagittal brain section of BAC-Cck-Cre$^{tg/+}$;R26R-EYFPyfp/+ stained with anti-G(Y)FP specific antibodies. Cre-mediated EYFP-expression is detected in cortex (CX), particularly frontal cortex (F) and visual cortex (VCX), hippocampus (H), striatum (S), thalamus (TH), hypothalamus (HY), cerebellum (CR), dorsal vagal complex (DVC) in the brainstem, published in Geibel et al. Nat Commun. 5, 3427 (2014).

### 3.4.4 Second stop cassette removal mediated by stereotactic delivery of AAV-FLPo in the hypothalamic nuclei allows DTR-GFP to be expressed

The CCK-iDTR mouse line expresses mcherry at the expected pattern according to published BAC-CCK-Cre characterisation which means that the first stop cassette is excised in the Cre positive neurons (CCK in this case). We also needed to characterise the ability of the construct to excise the second stop cassette (indicated by the loss of mcherry signal) so that the expression of DTR-GFP can occur as it has been designed (details above). We stereotactically injected a group of animals with AAV-FLPo or saline (sham injection) at the VMH nucleus of the hypothalamus to assess the mcherry signal loss at the region (Figure 14). The animals were sacrificed and their brains harvested 3 weeks after the surgery, to allow adequate expression of the AAV in the region. Upon FLPo expression, the mcherry expression was lost in the CCK neurons of the VMH nucleus while other regions such as dorsal hypothalamic and thalamic areas retained their mcherry expression in their respective CCK populations.

After the excision of the mcherry cassette, the DTR-GFP can now be expressed only on the CCK neurons transduced with AAV-FLPo. However, no endogenous GFP could be detected on any animals injected with AAV-FLPo. We also performed immunohistochemical analysis with three a-GFP antibodies in adult CCK-iDTR brains injected with AAV-FLPo and in neonatal and adult CCK-iDTR;del-FLP brains. The conditions of the protocol were also changed for optimisation, including epitope heat retrieval, methanol/Triton permeabilization and varying degrees of fixation. A summary of the attempts performed are listed in table 1. Even though we couldn't visualise the DTR-GFP, its presence on genomic and protein level was adequate for proceeding with ablating the CCK neurons of the

hypothalamus and demonstrating with other experiments that the CCK neurons are ablated after DT administration on AAV-FLPo injected CCK-iDTR animals. The ablation strategy by DT administration and its efficiency is described on the respective chapter of the CCK ablation.

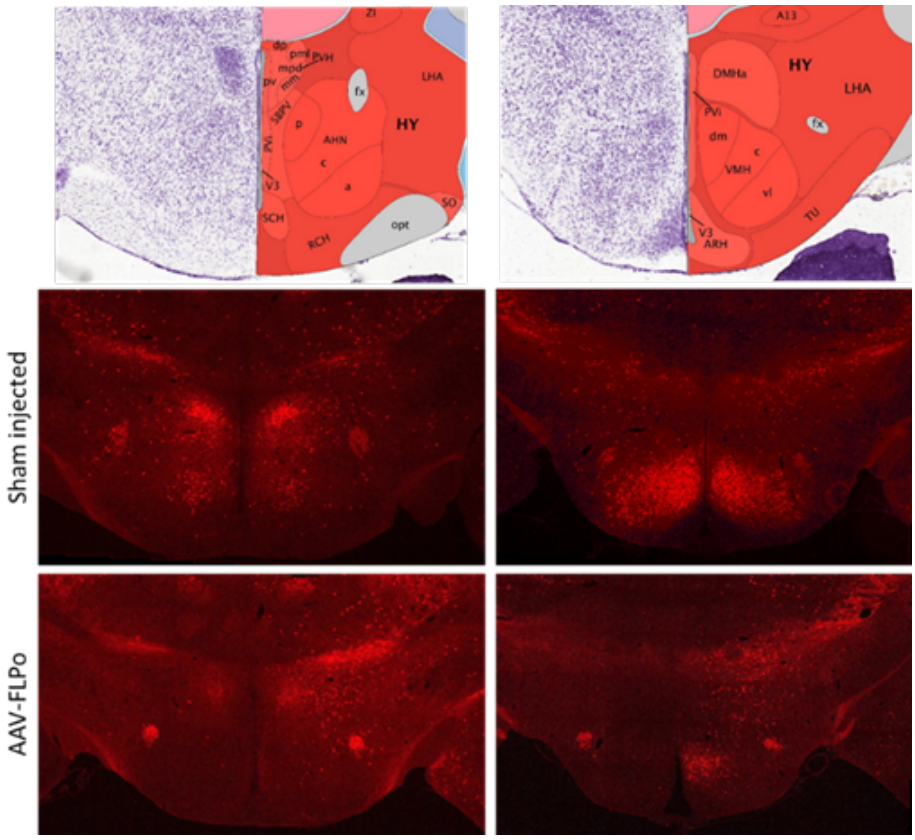


**Figure 14: Targeted ablation of mcherry-positive CCK neurons in the hypothalamic regions around PVN.** CCK-R26ds-iDTR mice were stereotactically injected with AAV-FLPo or saline.A) Atlas images of hypothalamic regions shown in DT treated mice, B) Control immuno-fluorescent images of 20µm-thick coronal sections from CCK-R26ds-iDTR injected with saline in hypothalamus and showing mcherry-expressing CCK neurons around PVN. The CCK neurons are unaffected from the DT administration. C) Significant ablation of mcherry-expressing CCK neurons due to systemic DT, shown in immuno-fluorescent images of 20µm-thick coronal sections from CCK-R26ds-iDTR injected with AAV-FLPo in hypothalamus.

| Animals | Histological analysis | Antibodies | Conditions(buffers,pH,temperature etc) |
|---|---|---|---|
| CCK-iDTR with AAV-FLPo | Immunofluorescence<br>3,3′-Diaminobenzidine (DAB) | Chicken a-GFP (Ab13970)<br>Rabbit a-GFP (Ab290) | Standard protocol<br>" " |
| CCK-iDTR;del-FLP | Immunofluorescence<br>3,3′-Diaminobenzidine (DAB) | Chicken a-GFP (Ab13970)<br>Rabbit a-GFP (Ab290)<br>Rabbit a-GFP (A-11122) | " "<br>" "<br>" " |
| | Immunofluorescence | Chicken a-GFP (Ab13970)<br>Rabbit a-GFP (Ab290)<br>Rabbit a-GFP (A-11122) | **a) Methanol permeabilsation**<br>i)with Triton<br>ii)without Triton<br>**b) Heat retrieval**<br>i)10mM sodium citrate at pH6<br>ii)50mM sodium citrate pH9<br>iii)10mM citric acid at pH6 + 0.05% Tween-20<br>**c) Over-fixation 2h 4%PFA with 0.3/0.1% Triton** |

**Table 1: Immunohistological assays and their respective conditions in a congenital DTR-expressing CCK line and in FLPo-injected mice that express DTR in CCK$^{VMH}$ neurons.**

# Chapter 4: Pharmacogenetic inhibition of $CCK^{VMH}$ neurons by DREADDs results in increased food intake and meal pattern changes

## 4.1 Expression of DREADDs in the CCK neurons of the VMH

To silence specifically the Cre expressing neurons, we utilised a DIO AAV construct that expresses the genetically engineered GPCR receptor hM4D(Gi) and the mcherry fluorescent protein for easier identification of the successfully targeted neurons. The loxP and lox2272 sites are flanking the DREADD:mcherry cassette, which is in inverted orientation, and can allow irreversible recombination by Cre recombinase (Figure 15A).

Stereotactic surgery was performed in BAC-CCK-Cre animals, injecting bilaterally 200nl of the AAV-DREADD at coordinates for targeting the CCK neurons of the VMH (Figure 15B). The animals were allowed to recover from the surgery for 3 weeks prior the start of any experiments. Adequate DREADD expression in the CCK neurons of the VMH was assessed by immunohistochemical analysis by detecting the mcherry fluorescent protein with an anti-dsred antibody. The low volume of the virus and its serotype, restricted the spread of the virus to the VMH region (Figure 15C). Most CCK neurons were successfully targeted throughout the VMH as assessed quantitatively compared to the reporter Ai9-CCK line (Figure 15D-G). Out of 2908 ± 184 Ai9-CCK neurons counted in the VMH, 2209 ± 60 were mcherry positive in the BAC-CCK-Cre animals injected with DREADDs which equates to 76 ± 2 % of the CCK population of the VMH (Figure 15D and E). The density of CCK neurons expressing DREADDs was 904 ± 38 neurons/$mm^2$

compared to 1282 ± 58 CCK neurons in the Ai9-CCK, which accounts for 70.7 ± 2.7 % of the CCK density of the VMH nucleus (Figure 15F and G).

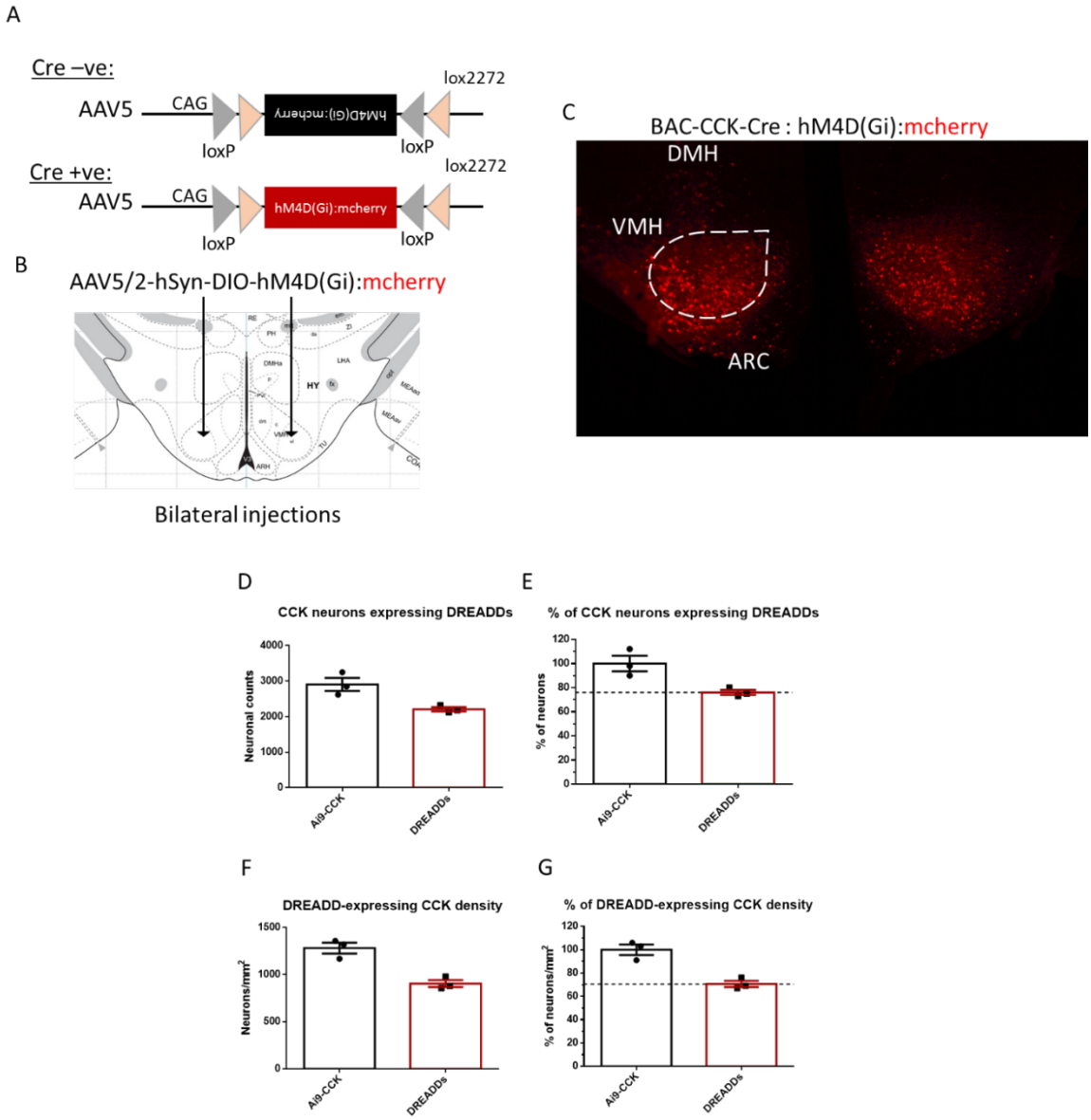


**Figure 15: Cre-dependent expression of inhibitory DREADDs in CCK$^{VMH}$ neurons for assessing their role in food intake regulation.** A) Diagram of the Double-floxed Inverted Orientation (DIO) AAV construct depicting the Cre-dependent recombination/inversion of the hM4D(Gi):mcherry cassette into sense orientation to allow its expression in Cre positive cells. B) Drawing of the bilateral stereotactic injection of the AAV-DIO-hM4Di(Gi):mcherry in the VMH region. C) Successful expression of hM4Di(Gi):mcherry in the CCK neurons of the VMH two weeks after surgery. D,E) Quantification of neurons expressing DREADDs compared to the CCK neurons of the Ai9-CCK reporter line. F,G) Neuronal density of DREADD expressing CCK neurons compared to Ai9-CCK. (n=3 mice per group)

## 4.2 Eating behaviour is not affected by the experimental protocol used to activate DREADDs

We sought to silence the CCK neurons of the VMH in a timely manner and assess the effect of these neurons in the regulation of food intake, the DREADD receptor needs to be activated by CNO, its exclusive designer drug. CNO has been shown to be inert in rodents with no obvious effects in studies used so far and with biochemical analysis showing that it is not activating other receptors. The most reliable route of administration of CNO is by intraperitoneal injection. This CNO administration has been used before in food intake studies with no reported effect of the drug alone. However, sequential ip injections spanning across multiple days could cause a degree of stress to a singly housed animal, hence a habituation protocol is required. For this purpose, we initially assessed the effect of the protocol in food intake of BAC-CCK-Cre animals previously injected stereotactically with DREADDs. The animals were habituated in handling prior of being singly housed in metabolic cages for the period of the experiment. After 2 days of monitoring their food intake they received twice daily (10am and 6pm) ip injections of saline for 10 days. Following habituation to ensure that food intake readings have been stabilised, saline was replaced with CNO (Figure 16A). Their daily food intake indicated that indeed in the first 3 days of saline injections the measurements fluctuated but then remained stable across the rest of the days with each animal approaching the mean (Figure 16B). In the first 2 days of singly housing, the animals consumed on average 3.078 ± 0.307g of pellets cumulatively throughout the day but the variation within the group was high due to the change in their environment. Upon the first 2 days of ip injections, the food intake was reduced to 2.728g due to the novel and intrusive nature of the procedure. However, during the habituation, the

food intake was stabilised to a mean of 3.368 ± 0.114g (last 3 days of saline ip). This observed decreased variability was quantified by assessing the coefficient of variation (coef.var.: % standard deviation/mean) for each day within the experimental group (Figure 16C). The coef.var dropped from an average of 22% in the first 5 days to an average of 8.4% in the last 3 days of ip injections indicating that the variability in food intake measurements within the group decreased. Collectively, these results show that the protocol chosen for DREADD activation with CNO by ip injections is not interfering with food intake as the values remain constant and the within group variability decreased in satisfactory levels.

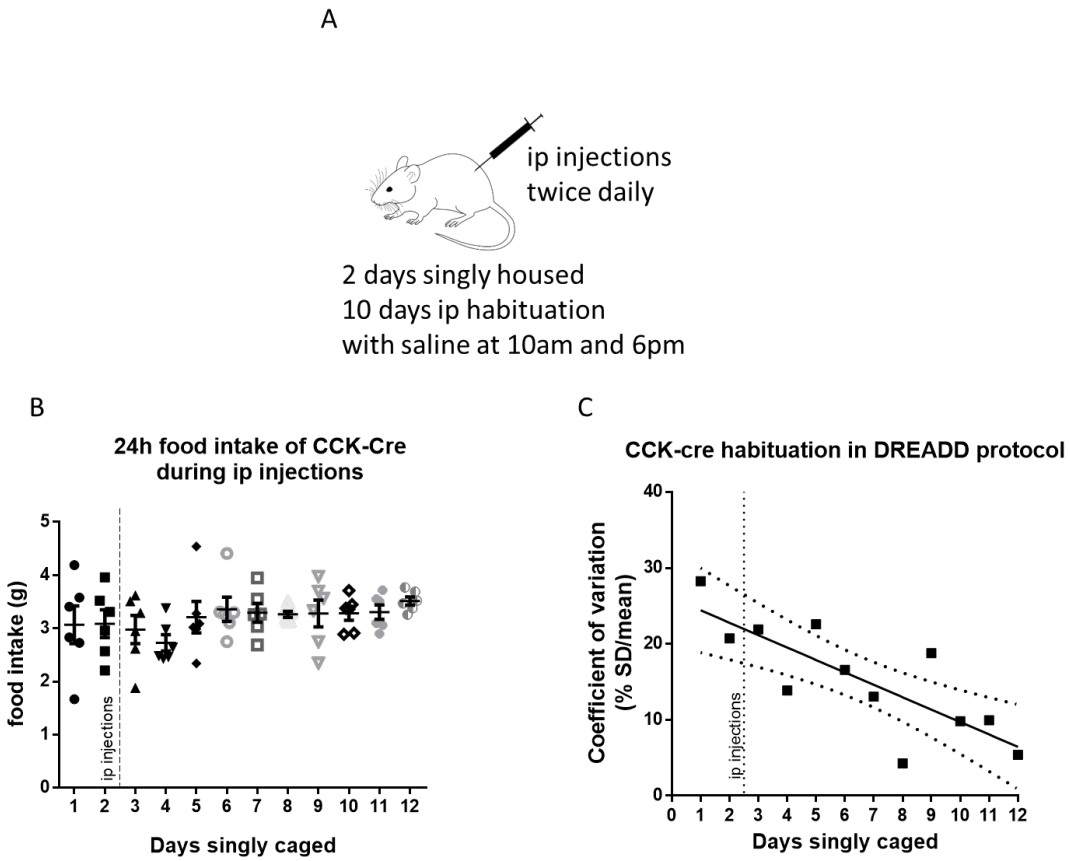


**Figure 16: Establishing a daily administration protocol by intraperitoneal injection for monitoring food intake that does not affect their eating behaviour.** A) Protocol to assess food intake and meal patterns. Animals were singly housed for 2 days and then habituated for 10 days with saline ip injections twice daily every 10am and 6pm. B) 24h food intake of CCK-Cre animals 2 days before and 10 days after receiving the saline ip injections. C ) The protocol for habituation is sufficient to reduce variability in the feeding data as revealed by the coefficient of variation of their daily food intake before and after the saline ip injections. (n=6 male mice)

## 4.3 Acute inhibition of CCK neurons of the VMH increases food intake

Since we established that the experimental protocol of singly housing and daily ip injections did not affect food intake in the DREADD injected BAC-CCK-Cre animals, we initiated the CNO injections immediately following the saline habituation.

Given the variation in CNO doses reported in recent publications, we decided to experimentally titrate the dose in a range that is biologically appropriate for *in vivo* DREADD applications. In detail, animals were habituated for 10 days in ip injections as described above and then received incremental doses of CNO concentration. Each dose (0.75/1.5/2 and 3 mg/Kg BW) was given twice daily at 10am and 6pm for 3 consecutive days (Figure 17A). The average daily food intake for each CNO dose was recorded in BAC-CCK-Cre mice 4 weeks after stereotactic injection of DREADDs (hM4Di-CCK$^{VMH}$) and in non-injected control littermates (Figure 17B and C). As expected, CNO had no effect in the amount of food consumed in control BAC-CCK-Cre littermates apart from 2mg/Kg BW that food intake slightly decreased but did not reach statistically significant levels (Figure 17B). Upon activation of DREADDs with 3mg/Kg BW in the hM4Di-CCK$^{VMH}$ animals, daily food intake significantly increased compared to the average consumption with saline injections from

3.125 ± 0.135g to 3.693 ± 0.143g of chow pellets. There wasn't any significant effect at lower CNO doses (Figure 17C). Food intake after CNO administration was also analysed as a percentage change from the baseline intake during saline injections (Figure 17D). Direct comparison of the food intake percentage changes between controls and hM4Di-CCK$^{VMH}$ at each dose highlights a significant increase in food intake of the hM4Di-CCK$^{VMH}$ group compared to controls at CNO doses of 2 and

3mg/Kg BW but not at lower doses tested (2mg:92 ± 4 vs 106 ± 4%, 3mg:103 ± 3 vs 120 ± 9% for controls and hM4Di-CCK$^{VMH}$ respectively, $P< 0.01$).

Since any response elicited by CNO activation should be temporal, a time window immediately following administration was studied. It has been shown that CNO activation of DREADDs in neurons can persist for 6 to 8h. As expected, the control group's food intake was not affected by CNO administration 6h following the evening injection. Surprisingly, hM4Di-CCK$^{VMH}$ animals had unaltered cumulative food intake 6h after CNO administration (Figure 17E and F). Similar results were also observed 6h after the morning injection (data not shown). These results so far, show that CNO (3mg/Kg BW) activation of inhibitory DREADD receptors in CCK$^{VMH}$ neurons increases the daily cumulative food intake significantly, albeit not with an acute and immediate effect in the amount of food consumed in the first 6h following the injection. This intriguing finding sparked interest for further research into the food intake regulation of animals with their CCK$^{VMH}$ neurons silenced.

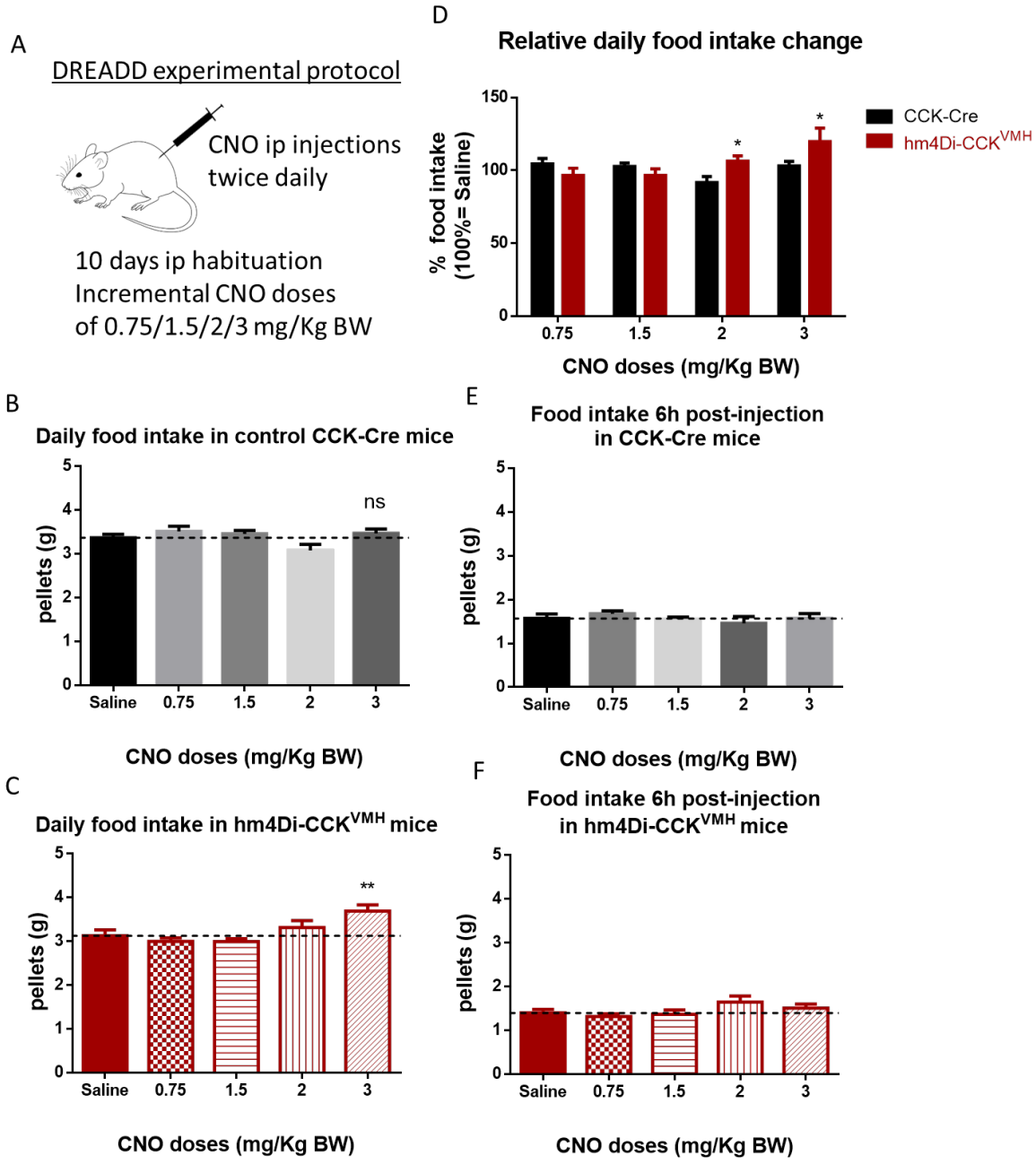


**Figure 17: Acute inhibition of CCK neurons of the VMH causes a gradual increase in total food intake that is not significant at 6 hours after CNO activation.** A) Protocol to assess food intake and meal patterns. Animals were singly housed for 2 days and then habituated for 10 days with saline ip injections twice daily every 10am and 6pm. They were then injected with increasing doses of CNO (0.75/1.5/2/3 mg/kg body weight (BW) ), with each dose continued for 3 days. B,C) Daily total food intake of CCK-Cre animals injected with DREADDs in VMH (hM4Di-CCK$^{VMH}$) or CCK-Cre controls and subjected to ip injections as described in the first panel of this figure. D) Percentage change of daily total food intake of hM4Di-CCK$^{VMH}$ animals compared to the control CCK-Cre group. Each group normalised to their own ip saline baseline, E,F) Cumulative food intake 6h post-injection with saline/CNO of hM4Di-CCK$^{VMH}$ animals and CCK-Cre controls. Data are given as means±s.e.m. (n=5-6 male mice per group). *P<0.05, **P<0.01, as compared with the corresponding saline injection (B,C,E,F Repeated measures (RM) one-way analysis of variance followed by Dunnett's post hoc test. D, two-way analysis of variance followed by Fisher's LSD test).

## 4.4 Meal frequency is increased in response to CNO-mediated inhibition of $CCK^{VMH}$ neurons

We could show that silencing $CCK^{VMH}$ neurons by administering CNO injections in hM4Di-$CCK^{VMH}$ animals increased their daily food intake without an immediate change in consumption within 6h from the injection. Food intake as a behaviour can be further analysed in parameters that define in detail the meal patterns and characteristics. Therefore, we sought to consider these parameters and identify any changes due to the silencing of $CCK^{VMH}$ neurons. In detail, the analysis was focused on the meal frequency based on the amount of meals and time between each meal (intermeal time) as well as the properties of each meal such as the size, duration and consumption rate. First, we tracked the meal patterns immediately following CNO administration (3mg/Kg BW) to explore the possibility of any changes resulting in the reported daily increased food intake of hM4Di-$CCK^{VMH}$ animals. Direct comparisons were made within each experimental group between saline and CNO injections. The meal frequency was found to be increased in the DREADD animals with total meal numbers increased from an average of 5.802 ± 0.4904 to 7.266 ± 0.6439 meals and the intermeal time reduced from 57.80 ± 5.652 mins to 43.80 ± 2.615 mins (Figure 18A and C, $P<0.05$). Control animals that were given the same CNO dose had same numbers of meals (Figure 18B) and a longer intermeal time from 51.33 ± 5.057 to 59.17 ± 5.997 mins (Figure 18D, $P<0.05$). Regarding each meal's characteristics, both groups did not show any statistically significant changes in meal size (Figure 18E, F and G), meal duration (Figure 18H and I) or meal rate (not shown). However, it is worthwhile to note that with an exception of two hM4Di-$CCK^{VMH}$ animals (individual symbols assigned), there was a trend for shorter meal sizes 6h after CNO administration that is not observed in

control littermates. A between group comparison indeed shows significant reduction in average meal size (Figure 18G, ctrl: 0.2878 ± 0.01689g ; DREADDs: 0.2138 ± 0.01599g, *P*<0.05). It is apparent that silencing CCK$^{VMH}$ neurons can immediately increase the meal frequency while the food intake remains unaltered. Concomitantly, there was a trend for smaller meal sizes with shorter duration, albeit not significant, which could explain why there was no change in the cumulative food intake results 6h after the CNO injection. In hindsight, increasing the experimental group number could statistically elucidate further any shift in meal parameters.

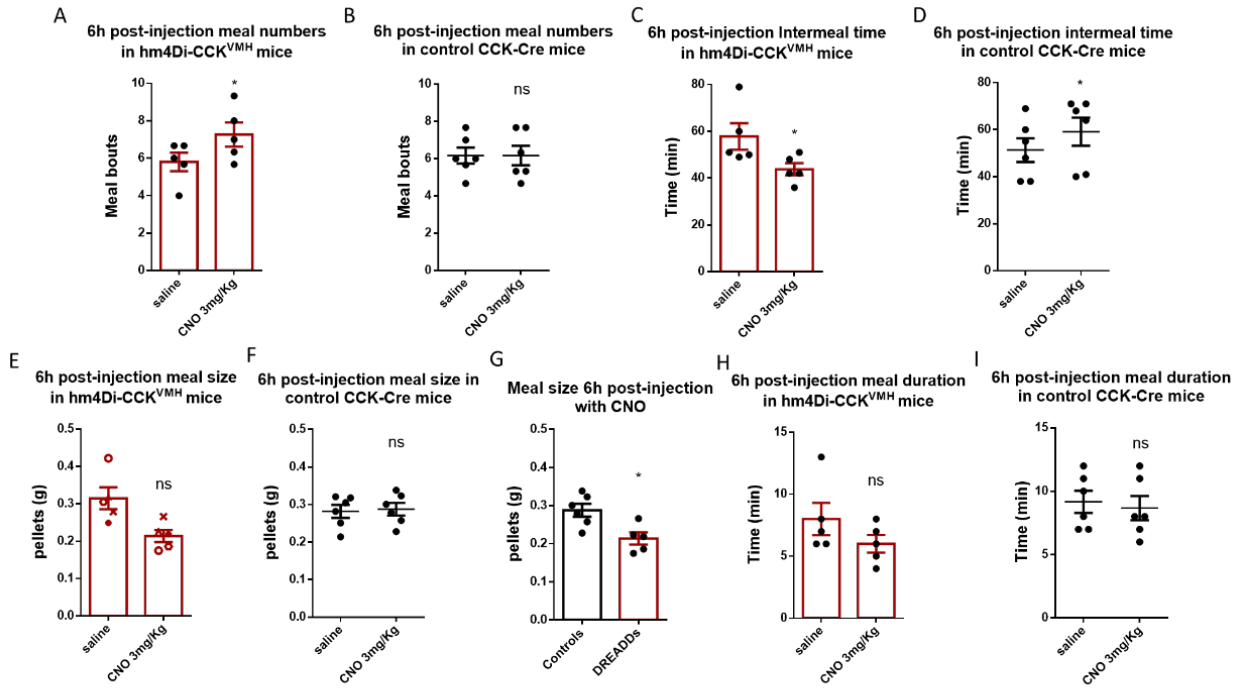


**Figure 18: Acute inhibition of CCK$^{VMH}$ neurons by CNO injection results in increased meal frequency and a decreased meal size while any meal duration changes are not significant at 6 hours post-injection of CNO.** A,B) Total number of meals consumed by hM4Di-CCK$^{VMH}$ and CCK-Cre control animals subjected to ip injections as described. C,D) Intermeal time of hM4Di-CCK$^{VMH}$ and CCK-Cre control animals. E,F) Meal size of hM4Di-CCK$^{VMH}$ and CCK-Cre control animals. G) Meal size direct comparison between the two animal groups. H,I) Meal duration of hM4Di-CCK$^{VMH}$ animals and CCK-Cre control. Data are given as means±s.e.m. (n=5-6 male mice per group). *P<0.05, as compared with the corresponding saline injection (two-tailed paired student t test apart from G) unpaired student t test).

## 4.5 Meal frequency changes persist throughout the day

Interestingly, we could identify similar results in the meal patterns that persisted throughout the day when CNO injections were administered. CNO usually lasts for a maximum of 8h to activate the DREADD receptors in vivo and induce any changes in behaviour related to the neuronal type in question. There are however reports of long-term effects occurring beyond the activation window that CNO provides. These have mostly been hypothesised to derive from the extensive activation of DREADD receptor and the GPCR downstream signalling cascades that have been activated which can elicit long lasting effects specific to the cell type in question. The meal frequency of hM4Di-CCK$^{VMH}$ animals increased during the whole day under CNO administration with meal numbers significantly increased from 14.87 ± 1.181 to 18.53 ± 1.514 (Figure 19A, $P$<0.05) and intermeal time reduced from 91.60 ± 7.580 to 72.80 ± 6.143 mins (Figure 19C, $P$< 0.01). There were no changes observed in the control BAC-CCK-Cre littermates (Figure 19B and D). The average daily meal size did not change significantly and the trend towards smaller meals, at 6h following CNO injections, was attenuated (Figure 19E). Likewise, daily meal duration (Figure 19G) and meal consumption rates (not shown) did not change. Meal characteristics of control littermates also remained unchanged (Figure 19F and H). In summary, meal pattern changes persist throughout the day during CNO activation of the inhibitory DREADDs that are expressed in CCK$^{VMH}$ neurons. The meal frequency is significantly increased while there is no significant change in the size, duration or rate by which each meal is consumed. These results are in alignment with the significantly increased cumulative food intake during the whole day.

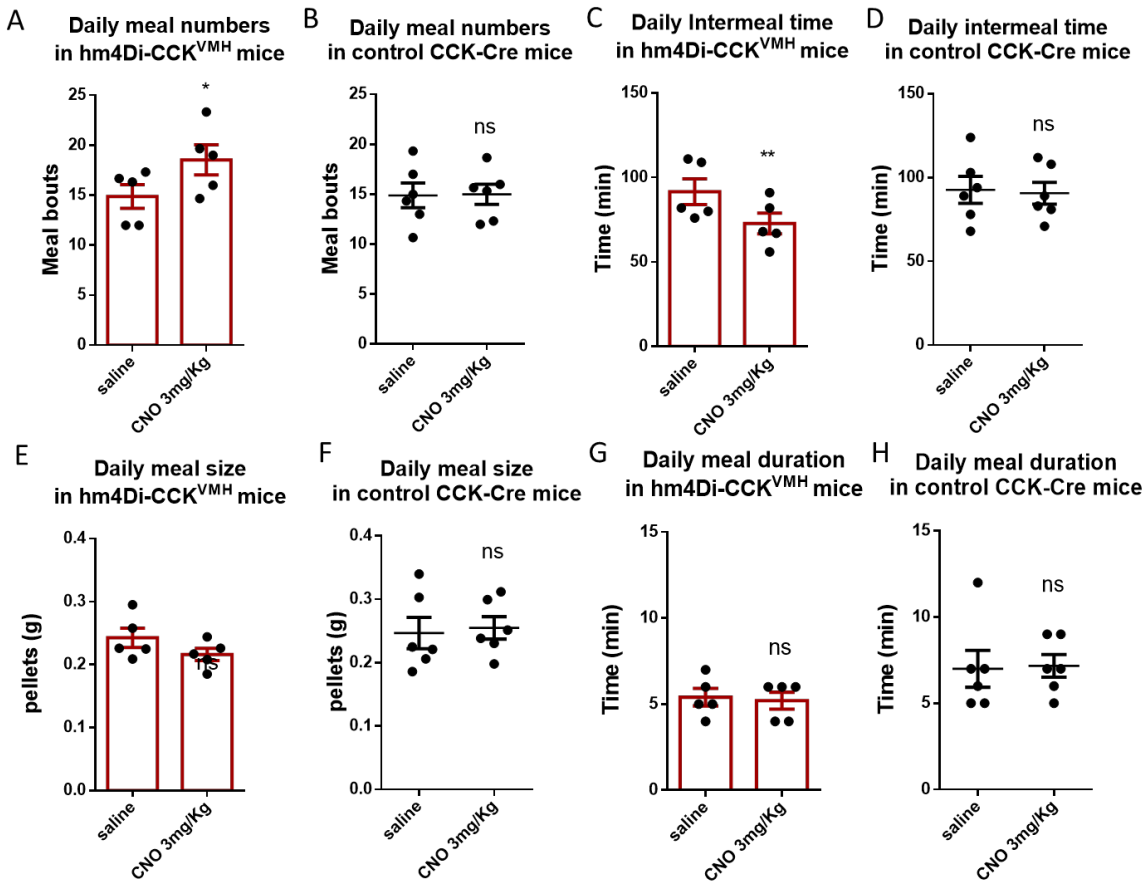


**Figure 19: Acute inhibition of CCK$^{VMH}$ neurons by CNO injection results in increased daily meal frequency while meal size and duration remain unaltered.** A,B) Daily total number of meals consumed by hM4Di-CCK$^{VMH}$ and CCK-Cre control animals subjected to ip injections as described. C,D) Daily intermeal time of hM4Di-CCK$^{VMH}$ and CCK-Cre control animals. E,F) Daily meal size of hM4Di-CCK$^{VMH}$ and CCK-Cre control animals. G,H) Daily meal duration of animals hM4Di-CCK$^{VMH}$ and CCK-Cre control animals. Data are given as means±s.e.m. (n=5-6 male mice per group). *P<0.05, **P<0.01, as compared with the corresponding saline injection (two-tailed paired student t test).

# Chapter 5: Ablation of $CCK^{VMH}$ neurons results in obesity due to hyperphagia

## 5.1 Cell-type and region-specific ablation of $CCK^{VMH}$ neurons in the CCK-iDTR mouse line

### 5.1.1 Establishing a tolerable DT dose for in vivo administration

After the first attempt of using higher dose of DT ip injections, which resulted in malaise and even death in control and experimental animals (not shown), we set out to establish a dose that can be tolerated by the control animals while it can also successfully ablate the CCK neurons. Female CCK-iDTR tg-ve animals were randomly allocated to two groups. The first group received DT ip injections of 30ng/g BW twice with the two injections 72 hours apart while the second group received just saline ip injections. This protocol of DT injections did not have an impact in their overall health as assessed by individual animal observation of their health and by monitoring the weight as an indicator. Both animal groups increased their weight as they aged without any significant fluctuations during the monitoring time of about three and a half months (Figure 20A). Having a closer look at the first two weeks of the protocol, both groups' weights are inseparable during the ip injections of DT/saline and the days after the administration (Figure 20B). In addition, plotting the percentage change in body weight for each day in relation to their starting weight before the ip injections, highlights a slight reduction in body weight during the DT injection days that is not significant and is immediately restored to the control group levels on the following days (Figure 20C). Taken together, we could successfully administer DT systemically at a dose of 30ng/g BW twice without any noticeable effect in animals' health or weight regulation. This resolved the issue we previously

had with higher published DT dose and protocol of three total injections. Following the establishment of a tolerable dose, we were not restrained by ethical and welfare considerations to proceed in assessing the effectiveness of this dose in ablating the DTR-expressing neurons of the VMH nucleus.

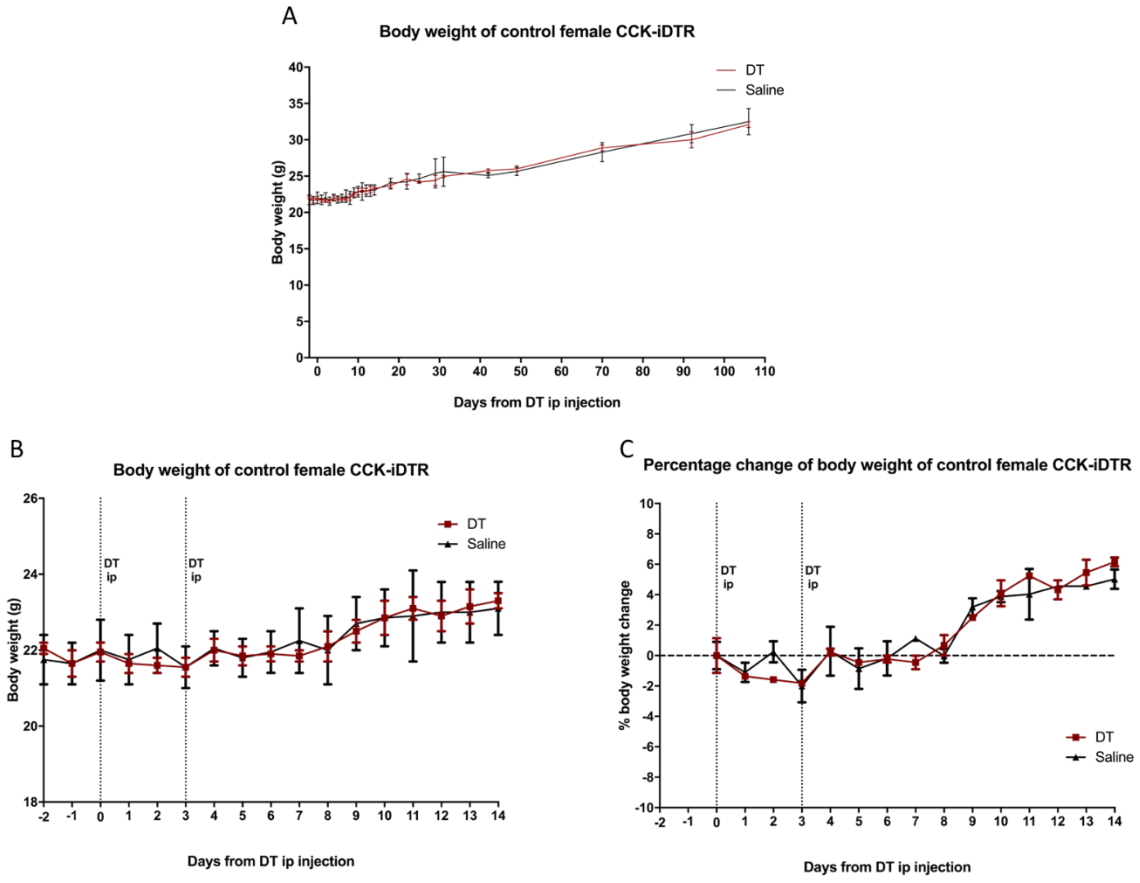


**Figure 20: Intraperitoneal administration of 30ng/g BW of diphtheria toxin is tolerable in female control CCK-iDTR mice without any effect in body weight regulation.** A) Body weight recorded for a total of 3.5 months was not significantly changed from 30ng/g BW of DT administration compared to animals injected with saline. B) Body weight for the last 2 days before and after the administration of DT. DT was ip injected at day 0 and day 3 as shown on the graph. C) Percentage change of body weight relative to their weight at day 0 before the first DT injection. Data are given as means±s.e.m. (n=3 female mice per group)

### 5.1.2 Partial ablation of CCK$^{VMH}$ neurons from systemic DT administration

The previous section describes the establishment of a tolerable systemic administration protocol of DT in the CCK-iDTR animals. This revised protocol apart from being tolerable to the animals, it is essential for DT to be able to reach the desired location where the DTR is being expressed, in our case the VMH nucleus of the hypothalamus. Since it was not possible to visualise the GFP that is linked to the C terminus of the DTR receptor (refer to chapter 3 for details) after the FLPo stop cassette excision, we revised a protocol for indirectly assessing the CCK ablation in the VMH nucleus of the hypothalamus. We decided to essentially introduce the GFP expression in a cre-dependent manner together with the AAV-FLPo intracranial injection. This will allow expression of GFP in CCK neurons in the region while at the same time the AAV-FLPo will excise the stop cassette which expresses the mcherry protein. The successfully targeted neurons will be devoid of mcherry while also expressing GFP. Upon systemic DT administration with the protocol revised earlier, GFP expressing/ mcherry negative neurons will be targeted and subsequently get ablated. This strategy can effectively assess the extent and success rate of ablation in the CCK neurons expressing DTR. Subsequently, we expected to find a mixture of populations that express either mcherry, GFP or both which will reveal the percentage of ablation achieved by our strategy. A group of CCK-iDTR animals were injected bilaterally at the coordinates previously established for targeting the VMH nucleus of the hypothalamus (Figure 21A). On one hemisphere, a mixture of AAV-FLPo and AAV-DIO-GFP was injected. The AAV-FLPo will excise the mcherry-stop cassette while the AAV-DIO-GFP will express GFP on any Cre+ CCK neurons in the area. On the other hemisphere, only AAV-DIO-GFP was injected to act as a control injection with Cre+ CCK neurons

expressing both mcherry and GFP. The animals were left to recover from the surgery for 4 weeks to allow adequate expression of the AAVs and were then injected with DT and perfused 3 weeks later. The brains were analysed immunohistochemically with a-dsred to visualise the mcherry expression and the endogenous strong signal of the cre-dependent GFP expression (Figure 21B). The absence of mcherry expression unilaterally at the VMH region indicated the successful FLPo mediated excision of the STOP cassette. However, in the mcherry devoid regions of the brain, albeit less, there were still GFP+/mcherry-ve neurons which failed to ablate by our DT protocol. Around the targeted area, there were also GFP+/mcherry+ neurons indicating the CCK neurons which did not get targeted by either of the AAVs. A very few of these were also found within the VMH area. We counted these as GFP+ since they still survived the overall ablation technique but because they were not transduced by the AAV-FLPo and failed to excise the stop cassette. Quantitative analysis of this experiment could show how many CCK neurons were successfully ablated in the CCK-iDTR line (Figure 21B-E). We compared CCK counts from the VMH nucleus of the reporter line Ai9-CCK to the remaining GFP+ neurons from the ablated hemisphere in our DT treated mice. From 1500 Ai9+ CCK neurons in the area, there were 900 GFP+ remaining after DT treatment (Figure 21D) which equates to 59% of CCK neurons not being ablated (Figure 21E). In terms of the density of the CCK population, from 1300 neurons/$mm^2$, 700 neurons/$mm^2$ were still alive in the DT treated animals (Figure 21F). The density of the spared CCK neurons represents the 51% of the CCK density of the VMH nucleus (Figure 21G). In summary, we established a DT protocol that can be tolerable to the animals without any effect in their welfare or in results related to their energy homeostasis, such as weight regulation. Moreover, we

successfully manage to ablate around 40% of the CCK neurons of the VMH nucleus. However, it should be noted that there is a fine balance between administering the DT in tolerable concentrations and achieving a desirable extent of CCK ablation. Further titration of potentially higher doses of DT or different administration route was significantly restricted as the welfare of the animals was of higher priority.

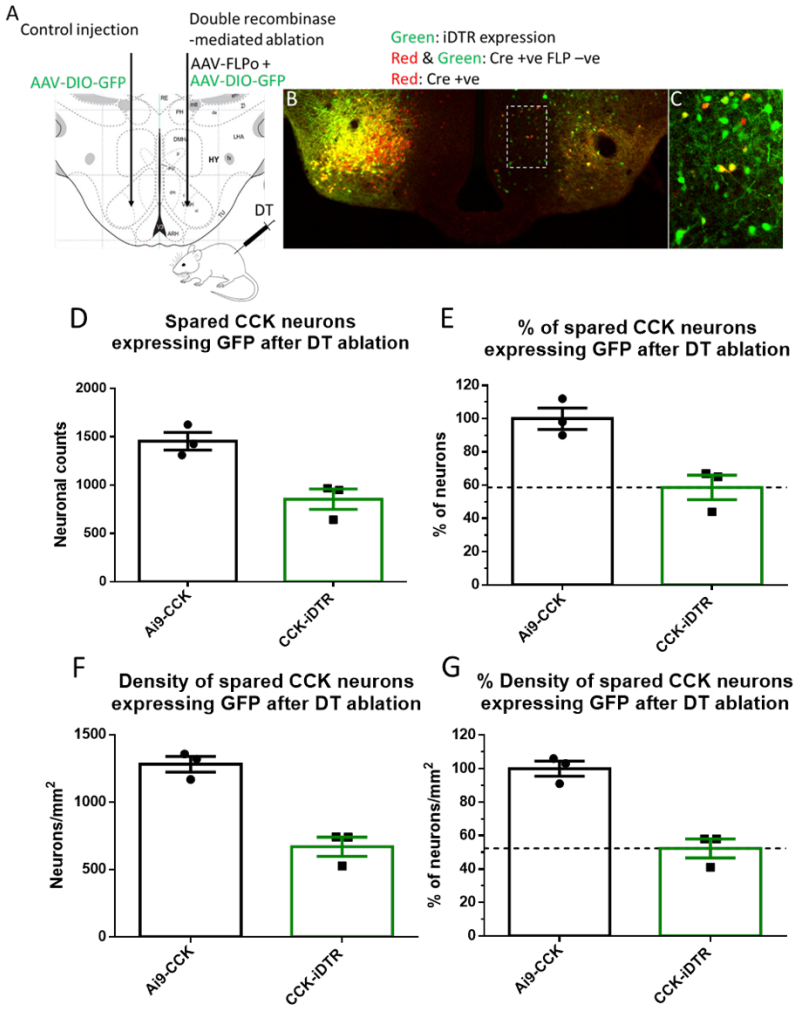


**Figure 21: Systemic administration of diphtheria toxin in virally injected BAC-CCK-Cre$^{tg/+}$ ; R26RLxP-FRT-iDTR induces partial ablation of hypothalamic CCK$^{VMH}$ neurons.** A) Schematic of the experimental protocol for visualising the extent of CCK ablation. Left hemisphere was injected with a cre-dependent AAV expressing GFP only in CCK neurons (mCherry expressing). Right hemisphere was injected with a mixture of AAV-FLP (removal of mCherry stop cassette) and AAV-DIO-GFP for visualising any remaining CCK neurons after systemic DT ablation with 30ng/g BW of DT ip as described previously. B) Representative image of the VMH region showing the extent of CCK ablation after unilateral AAV-FLP and systemic DT. mCherry stop-cassette is removed in all CCK+ neurons that got infected by AAV-FLPo and iDTR cassette is expressed leading to ablation of CCK neurons. C) Higher magnification reveals partial removal of CCK neurons visualised by GFP positive CCK neurons remaining alive in the region. D-G) Quantification of CCK GFP+ neurons spared by the DT-mediated ablation in the VMH region compared to reporter line Ai9-CCK. D,E) Neuronal counts and percentage difference of CCK neurons GFP+ in the VMH region of DT ablated brains compared to Ai9 positive CCK neurons of the reporter line at the same region. F,G) Neuronal density and percentage difference of GFP+ CCK neurons compared to Ai9-CCK reporter line. Data are given as means±s.e.m. (n=3 female mice per group)

### 5.1.3 Body weight regulation is not significantly affected by DT-mediated partial ablation

Although our previous results of DREADD-mediated inhibition of $CCK^{VMH}$ neurons were based on around 76% of CCK neurons expressing DREADDs, it could still be feasible to investigate the potential long-term effects of a smaller percentage of the CCK population by ablating them. Therefore, a group of female CCK-iDTR animals were stereotactically injected on both hemispheres with AAV-FLPo and after 4 weeks of recovery, they were injected with the previously described DT protocol. In brief, two ip injections of 30ng/g BW with 72 hours apart from each other. CCK-iDTR tg-ve littermates stereotactically injected with either vehicle (saline) or FLPo were used as controls. The animals were monitored regularly after the DT injections and their weights were recorded for a total of 3 months following the DT injection (Figure 22A). Both groups started with indistinguishable weights for the first month. We observed a slight increase of the weight of the CCK-iDTR tg+ animals at 60 days after the DT administration but the weight values were not significant compared to the control group (Figure 22B). However, when assessing the percentage change of their body weight relative to their weight prior the DT injections, the tg+ animals had significantly increased their weight by around 30% at the 60 days' time point, compared to a 17% increase in the control group (Figure 22C). Hence, ablating the CCK neurons of the VMH area did cause a rapid increase of weight at the time point examined. A month later, this increase proved to be transient as the control group reached similar weight increases with the tg+ group, 90 days after the DT administration. To conclude, the ablation of around 40% of the $CCK^{VMH}$ neurons, by expressing DTR followed by systemic administration of DT, resulted in a transient increase in body weight after 2 months from the DT injections.

Overall body weight was not significantly affected by the ablation perhaps due to the low ablation efficiency of our systemic DT administration which could not be further titrated due to welfare considerations mentioned above.

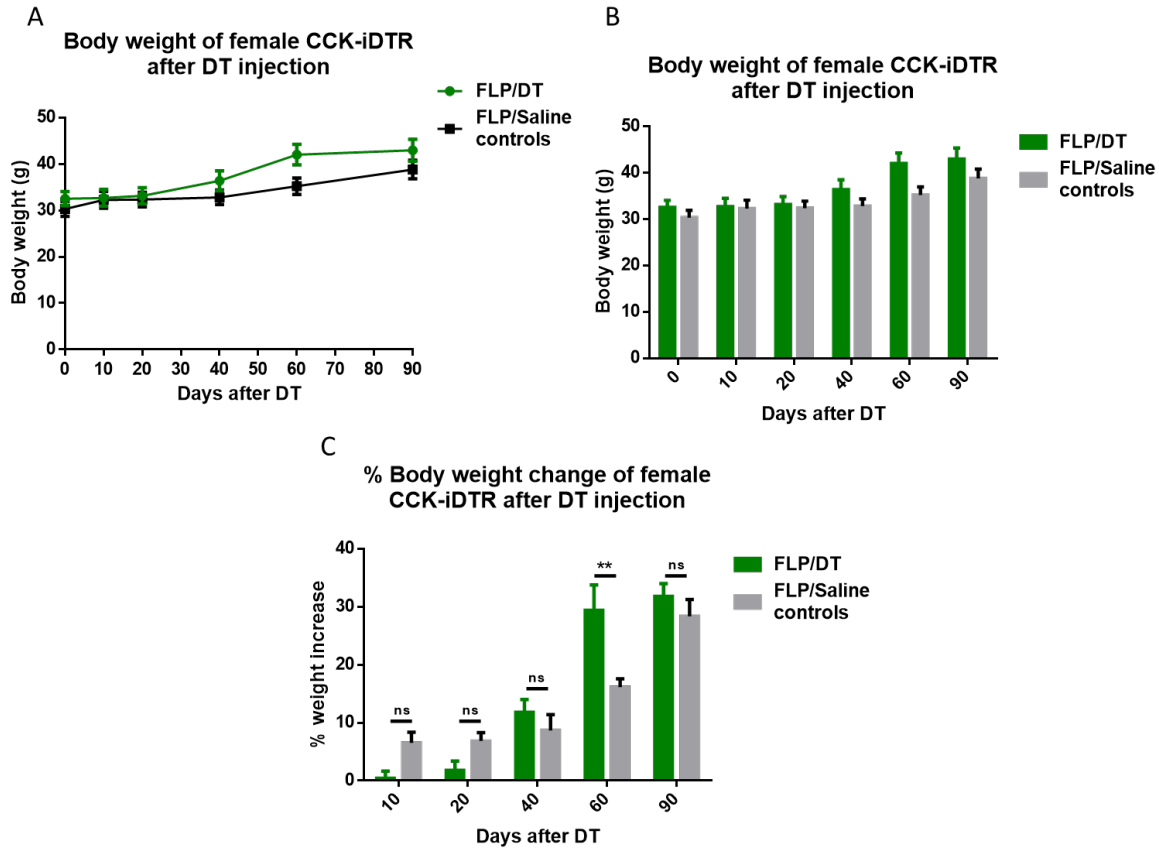


**Figure 22: Ablation of around 40% of CCK$^{VMH}$ neurons in FLPo and DT injected BAC-CCK-Cre$^{tg/+}$ ; R26RLxP-FRT-iDTR does not significantly affect their body weight regulation.** Female CCK-iDTR animals were stereotactically injected bilaterally with AAV-FLPo and then received DT or saline intraperitoneally and their body weight was recorded. A) Plot of their body weight which was recorded for a total of 90 days after DT-mediated ablation. B) Bar chart highlighting any differences in body weight between DT and saline injected groups. C) Percentage increase of each groups body weight relative to their initial weight before DT administration. At timepoint of 60 days after DT ip, the DT ablated group shows a transient increase in weight gain relative to saline group but this change is abolished at 90 days after DT. Data are given as means±s.e.m. (n=5-6 female mice per group) ( A) multiple student t test, B,C)Repeated measures (RM) two-way analysis of variance followed by Sidak's post hoc test, $^{**}P<0.01$)

## 5.2 Complete ablation of $CCK^{VMH}$ neurons increases their body weight and food intake

### 5.2.1 Successful complete ablation of $CCK^{VMH}$ neurons by AAV-mediated cre-dependent expression of diphtheria toxin A subunit

We were impeded to progress further with titration and optimisation experiments with the aforementioned systemic DT ablation strategy due to welfare concerns. Moreover, ablation of only 40% of $CCK^{VMH}$ neurons did not show any significant effect in weight regulation. However, the transient percentage increase observed, was in agreement with the food intake dysregulation detected with DREADD-mediated inhibition of a higher percentage of these neurons in the VMH nucleus. We therefore deployed an alternative strategy to directly ablate these neurons in a spatiotemporal manner by expressing the diphtheria toxin A subunit (DTA) via AAV-DIO-mediated expression (Figure 23). We stereotactically injected CCK-iDTR animals to utilise them as a reporter line because of the cre-dependent mcherry cassette of the construct. The injection site for the AAV was identical to the previous experiments reported, bilaterally injecting 300nl of $2.32 \times 10^{13}$ GC/ml AAV titre, targeting the CCK neurons of the VMH. The animals were allowed to recover for a month before immunohistochemical assessment of the CCK ablation. CCK-iDTR animals injected with the AAV-DIO-DTA had very few, to almost none, mcherry positive CCK neurons in the VMH region that survived the cre-dependent DTA expression (Figure 23A and B). Representative images show CCK neurons expressing mcherry in the VMH of control non-injected animals whereas injected animals lack mcherry in the same region of the hypothalamus. Since we successfully demonstrated that the technique can ablate most $CCK^{VMH}$ neurons, we proceeded in assessing the effect of the ablation on weight regulation. We

stereotactically injected with AAV-DIO-DTA tg+ CCK-iDTR animals. To control for the AAV-DTA virus and its titre we also injected tg-ve animals with DTA. To control for the surgery per se, tg+ animals were injected with the vehicle virus that expresses mcherry instead of DTA to allow detection of successful injection in the region (AAV-mcherry) and a group of tg-ve littermates was left untreated. Their body weight was recorded for a total of 3 months following stereotactic injection (Figure 23C and D). All experimental groups underwent surgery at 2-3 months of age and had a weight ranging from 25 to 35g with DTA injected animals deviating significantly from control groups starting from 3 weeks after surgery with their weight increase reaching a plateau at 7 to 9 weeks after DTA surgery. DTA expression had a profound and rapid effect in each group's percentage change of body weight in a matter of weeks, with significant changes as early as 3 weeks which lasted throughout the recorded period and plateaued at 7 to 9 weeks after the surgery (Figure 23D). CCK-iDTR tg+ animals showed 40% increase in body weight while control groups had only a 10% increase at 3 weeks following the surgery. The difference in percentage of BW increase reached a remarkable 70% compared to AAV-mcherry and non-injected controls at the 9 weeks' time point. Unfortunately, the control group of CCK-iDTR tg-ve animals were similar to tg+ve animals and had equally significant increase in body weight relative to injected or non-injected controls. This non-cre dependent DTA effect was also observed in WT C57BL/6J animals injected with the same virus. Post-hoc immunohistochemical analysis of their brains confirmed successful targeting of the VMH region and no mcherry expression, while PCR analysis confirmed their lack of Cre (not shown). Consideration was also given on the effect of surgery and the rare possibility of lesioning the VMH area in this group, there were no signs of physical lesion in these

animals and the AAV-mcherry group as well as previous experimental groups injected with AAV-FLPo or AAV-DREADDs, neither did they have such a dramatic weight increase in the weeks following the surgery. However, further analysis showed that the two groups' weight increase was associated with profound hyperphagia with more than double the pellets consumed from AAV-mcherry injected controls (Figure 23E). Food intake regulation could be affected by no cell-type specific cytotoxicity or changes in the local environment of the nucleus, potentially triggered by the AAV-DIO-DTA. These results were surprising and had not been previously reported by the literature regarding the use of commercially available and highly used AAV viruses, including ours. We therefore suspected that an increased viral load could be responsible for the BW changes we observed. In succession from these results, we then focused into titrating the virus to the VMH as an attempt to resolve the non-specific phenotype while still being able to utilise the high efficiency of $CCK^{VMH}$ ablation that we had successfully achieved.

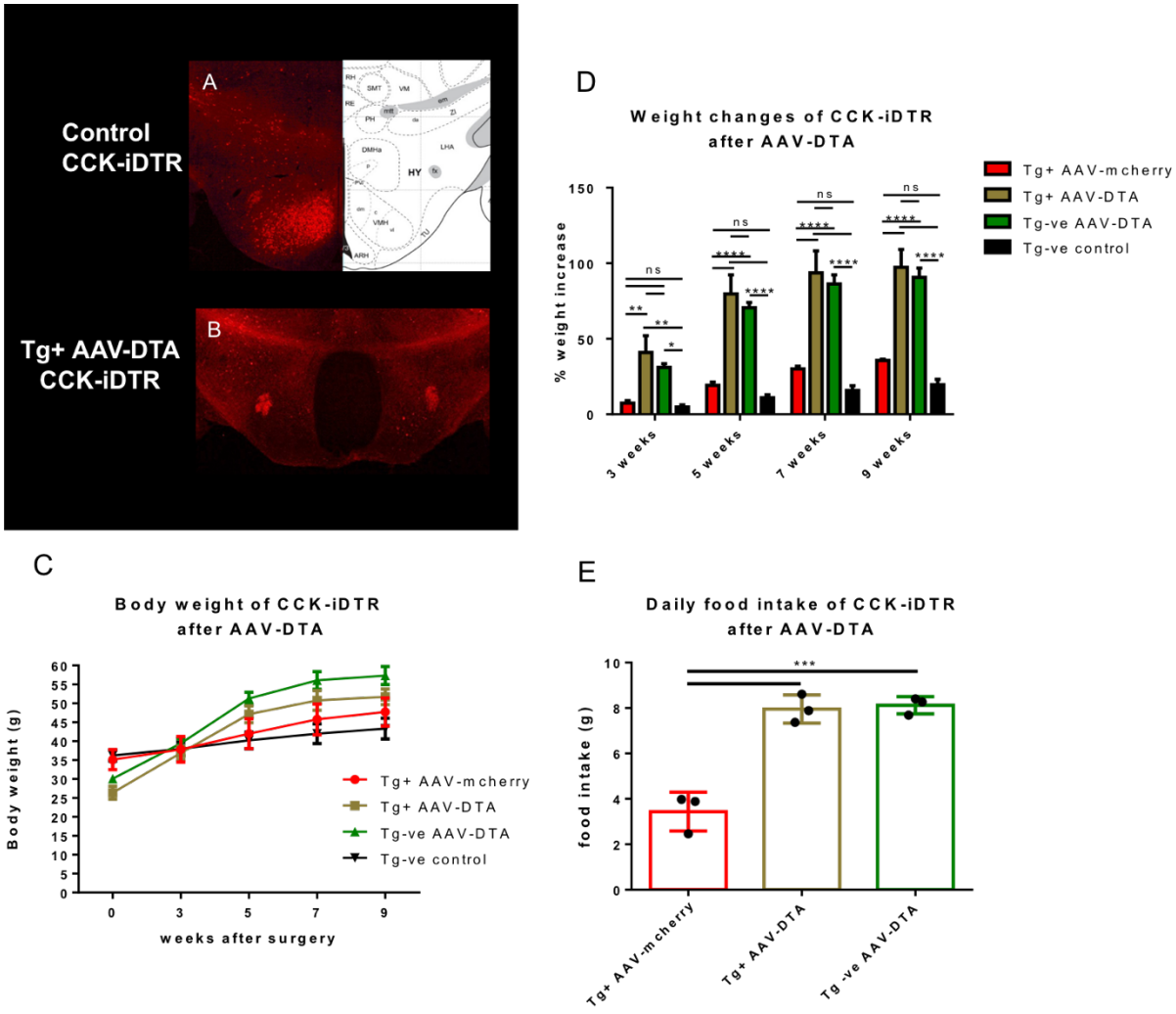


**Figure 23: Stereotactic injection of AAV-DIO-DTA successfully ablates the CCK$^{VMH}$ neurons but it also results in non-specific hyperphagic obesity in the control group.** A-B) Representative coronal section of CCK-iDTR tg+ with or without DTA C) Body weight plot of female CCK-iDTR animals tg+/-ve injected with DTA or mcherry or non-injected controls, weights were recorded for 9 weeks after surgery. D) Bar chart of the percentage increase in body weight relative to each groups baseline at various weeks after surgery. AAV-DTA significantly increases body weight in controls and tg+ animals. AAV-mcherry injection does not affect their weight significantly, compared to non-injected controls. E) Weight increase is due to hyperphagia for all groups injected with DTA. Average daily food intake was recorded a month after surgery for a period of two weeks. Data are given as means±s.e.m. (n=3 female mice per group apart from n=4 for Tg-ve AAV-DTA) ( D) Ordinary one-way analysis of variance followed by Tukey's post hoc test E)Repeated measures (RM) two-way analysis of variance followed by Tukey's post hoc test, *$P$<0.05, **$P$<0.01, ***$P$<0.001, ****$P$<0.0001)

### 5.2.2 Optimisation of the AAV delivery by establishing an appropriate titre

The titration of the AAV-DIO-DTA virus was performed in a group of tg-ve Ai9-CCK animals. The animals were stereotactically injected in both hemispheres at the VMH region as previously described with increasing dilutions of the AAV titre (not shown) and the titre of 2.32 x $10^{11}$ GC/ml was selected as the most tolerable. The non-specific increase in weight that was previously shown at higher AAV titres was abolished in animals that were monitored up to 6 months from the surgery (Figure 24A). The body weight of tg+ animals did not deviate from the non-injected controls apart from a peak at 75 days after surgery which was not statistically significant. We also assessed the ablation efficiency of the AAV titre to ensure adequate ablation levels of the $CCK^{VMH}$ neurons. We analysed Ai9-CCK brains injected with AAV-DIO-DTA, a month after surgery. The absence of tdtomato endogenous fluorescent signal in the VMH region indicates that the CCK neurons were successfully ablated (Figure 24B). The tdtomato signal intensity is significantly reduced compared to non-ablated control Ai9-CCK brains.

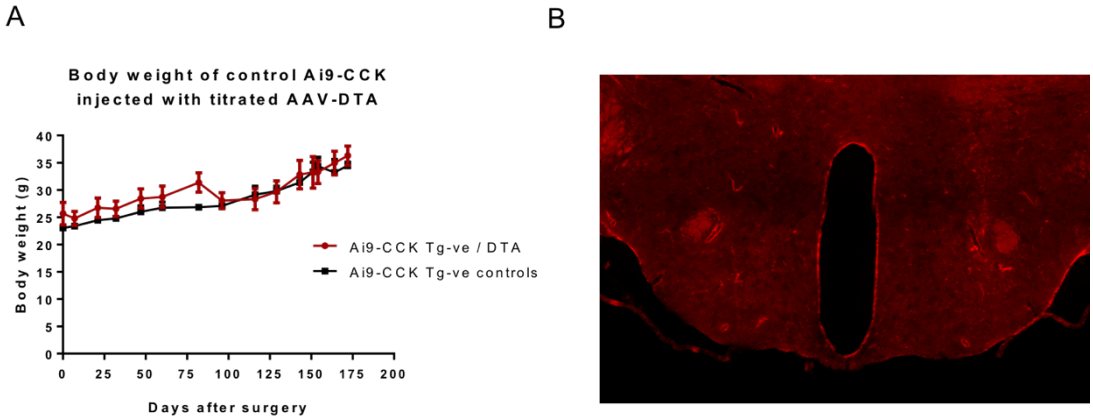


**Figure 24: Stereotactic injection of the titrated AAV-DIO-DTA at titre 2.32 x $10^{11}$ GC/ml abolishes the non-specific weight increase while it efficiently ablates the CCK neurons of the VMH nucleus in Ai9-CCK animals.** A) Body weight plot of control tg-ve Ai9-CCK animals injected with AAV-DIO-DTA compared to non-injected controls. The groups were monitored for a total of 6 months and there was no significant change in body weight between the two groups. B) Ai9-CCK tg+ animals injected with AAV-DIO-DTA. Ai9 fluorescent signal is significantly decreased in the injected VMH region. Female mice, n=4 injected with DTA and n=3 controls

### 5.2.3 DTA-mediated ablation results in obesity and hyperphagia

Upon establishing a tolerable AAV-DIO-DTA titre, we stereotactically injected tg+ Ai9-CCK animals and tg-ve controls at the VMH region. The injectate for the controls contained AAV-mcherry to aid the identification of successful viral delivery in the targeted location during the post-hoc analysis. The body weight of both groups was recorded for a total of 3 months after the surgery (Figure 25A). Tg+ animals had their body weight increased, starting at day 50, compared to controls and their weight continued to increase at days 75 and 90 while the injected controls did not change their weight significantly compared to their starting weight. The effect of CCK ablation on body weight regulation is further highlighted by comparing each group's percentage of body weight change at 3 months after the surgery (Figure 25B). The body weight of tg+ animals increased by around 38% since the AAV injection. In contrast, the injected tg-ve control group, only increased its weight by around 10%. We therefore conclude that the ablation of CCK neurons affects the homeostatic energy regulation and results in a body weight increase of around 28% in a period of 3 months. These long-term weight changes after the ablation could be due to several factors, such as food intake and meal pattern changes, which could result in a hyperphagic phenotype.

Ai9-CCK tg+ and tg-ve animals injected with AAV-DIO-DTA where singly caged in metabolic cages a month after the surgery and their food intake was monitored in real time. The animals were habituated to their new environment for 10 days and their food intake was recorded for the next 5 days and the measurements averaged. The daily food intake was significantly increased in the tg+ animals compared to the injected tg-ve controls (Figure 25C).

The meal frequency was found to be significantly decreased in the tg+ animals with daily meal numbers decreased from an average of 18 to 14 meals and the daily intermeal time increased from 70 mins to 90 mins (Figure 25D and E). Regarding each meal's characteristics, the average meal size was significantly increased in tg+ animals from 0.2 to 0.35 g (Figure 25F), the average meal duration was also increased from 5 to 9 mins (Figure 25G). The average rate of food consumption remained relatively unchanged with meal rates slightly dropping from 0.15g/min to 0.10g/min with no statistical significance. Collectively, the ablation of CCK neurons of the VMH region impacts body weight regulation with long-term increases in body weight due to hyperphagia characterised by longer and larger meals occurring less frequently throughout the day.

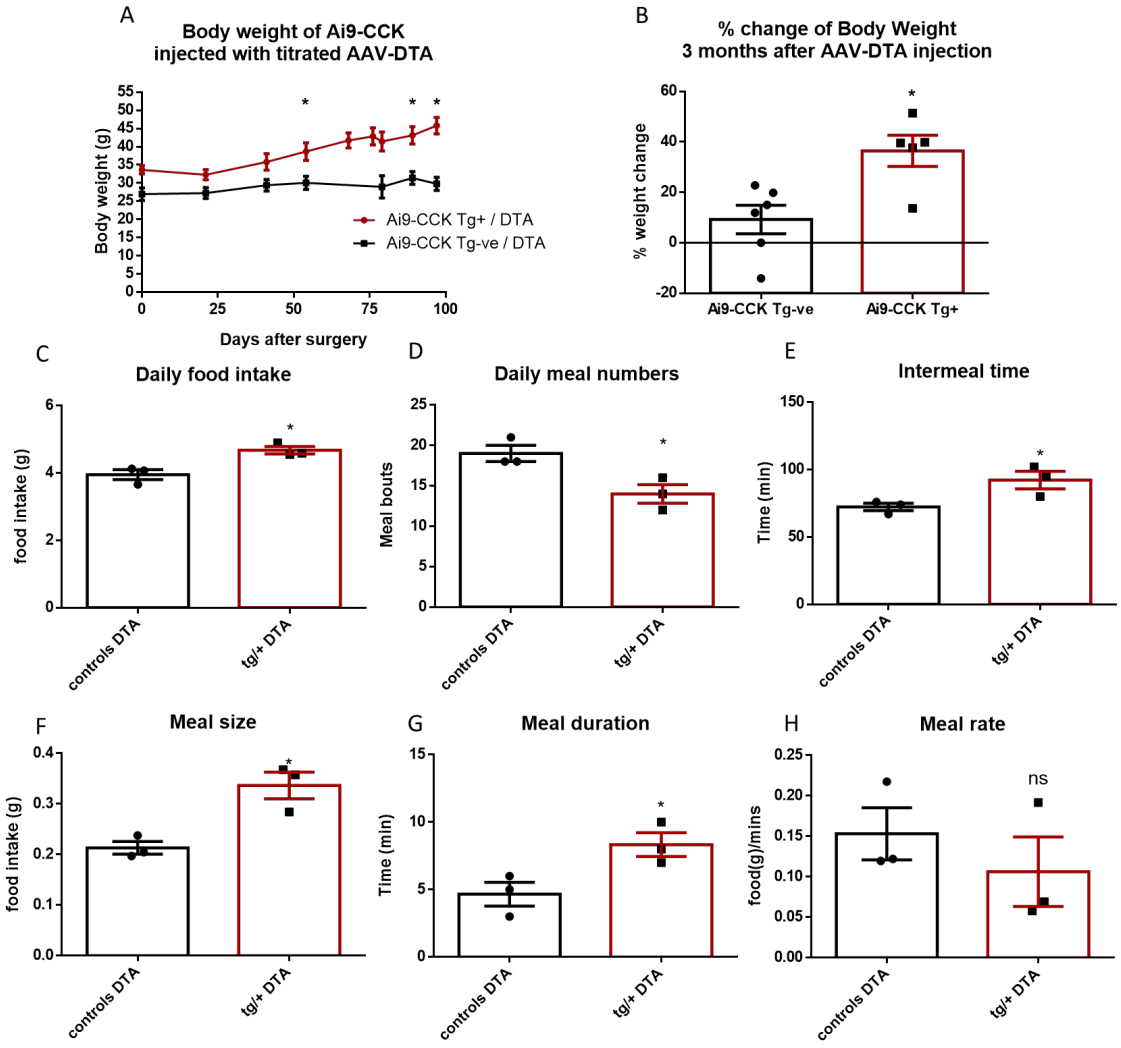


**Figure 25: DTA-mediated ablation of CCK$^{VMH}$ neurons in female Ai9-CCK mice induces chronic weight increase due to hyperphagia and meal pattern dysregulation.** Ai9-CCK animals were split in tg+ and tg-ve animals and all injected with AAV-DIO-DTA in the VMH. Body weight, food intake and meal pattern analysis were recorded and analysed. After 10 days of habituation singly housed in metabolic cages, 5 days of feeding sensor data was recorded and averaged. A) Body weight recorded for a total of 3 months after surgery. Tg+ animals significantly increased their BW compared to tg-ve group injected with DTA. B) Percentage weight change 3 months after surgery for each group based on its starting weight before the surgery. C-H) Food intake and meal pattern analysis between the two groups reveals tg+ animals injected with DTA increased food intake with longer and bigger meals while decreasing their meal frequency. C ) Average daily food intake of the two groups shows increased food intake in tg+ animals with DTA. D) Daily meal numbers decreased in tg+ group over the tg-ve group. E) Intermeal time increased in tg+ animals compared to tg-ve group. F) Meal size increased in tg+ animals over the tg-ve animals. G) Meal duration increased in tg+ compared to tg-ve animals. H) Meal rate remained relatively similar between the two groups. Data are given as means±s.e.m. ( A,B) n=5-6 female mice per group, C-H) n=3 female mice per group), ( A) multiple student t test, B-H) unpaired student t test , *$P$<0.05)

### 5.2.4 Animals devoid of $CCK^{VMH}$ neurons are hyperglycaemic and glucose intolerant

The VMH is a region that exerts control over glucose homeostasis. There is strong association between body weight and food intake dysregulations that are connected to blood glucose regulation. We therefore subjected groups of tg+ve and tg-ve Ai9-CCK animals injected with AAV-DIO-DTA in glucose tolerance test (GTT) 3 months after the stereotactic surgery. Both groups were fasted overnight (16h) with their food removed at the onset of their active period (18:00) which minimises any variation from individual food consumption from each animal. Blood glucose measurements were obtained with a handheld whole blood glucometer and blood was withdrawn from the tail vain. Their baseline blood glucose levels were measured the next morning at the beginning of their resting period. The tg+ animals were found hyperglycaemic with average glucose levels of 8.5 mmol/L compared to the injected controls of 6.5 mmol/L (Figure 26A). We subsequently performed a GTT assay by injecting the animals with an ip dose of glucose and following up their ability to clear the glucose from their bloodstream (Figure 26B and C). In the first 30mins after glucose injection, both animal groups had significantly raised their blood glucose levels to 30 mmol/L with no differences between the groups. Blood glucose remained significantly at higher levels for the tg+ animals while the controls reduced their blood glucose to almost baseline levels at 3 hours after the glucose challenge (Figure 26B). These results are also displayed as individual data points from each animal in each group for every time point that measurements were taken (Figure 26C).

**Figure 26: DTA-mediated ablation of CCK$^{VMH}$ neurons results in hyperglycaemia after 16h of fasting and glucose intolerance.** Glucose tolerance test (GTT) of Ai9-CCK tg+ and tg-ve groups injected with AAV-DIO-DTA. They were fasted for 16h overnight after 3 months from stereotactic injection and whole blood glucose measurements were recorded before and after intraperitoneal (ip) injection of 2g/Kg BW glucose. A) Baseline glucose levels after overnight fasting prior to glucose ip injection shows that tg+ animals are hyperglycaemic. B, C) GTT of the two groups in plot and individual data points graph that shows similar increase in blood glucose levels 30mins after ip injection but glucose intolerance in the tg+ group compared to the tg-ve group. Data are given as means±s.e.m. (n=4-5 female mice per group). ( A) unpaired student t test B-C ) two-way analysis of variance followed by Sidak's post hoc test, *$P$<0.05)

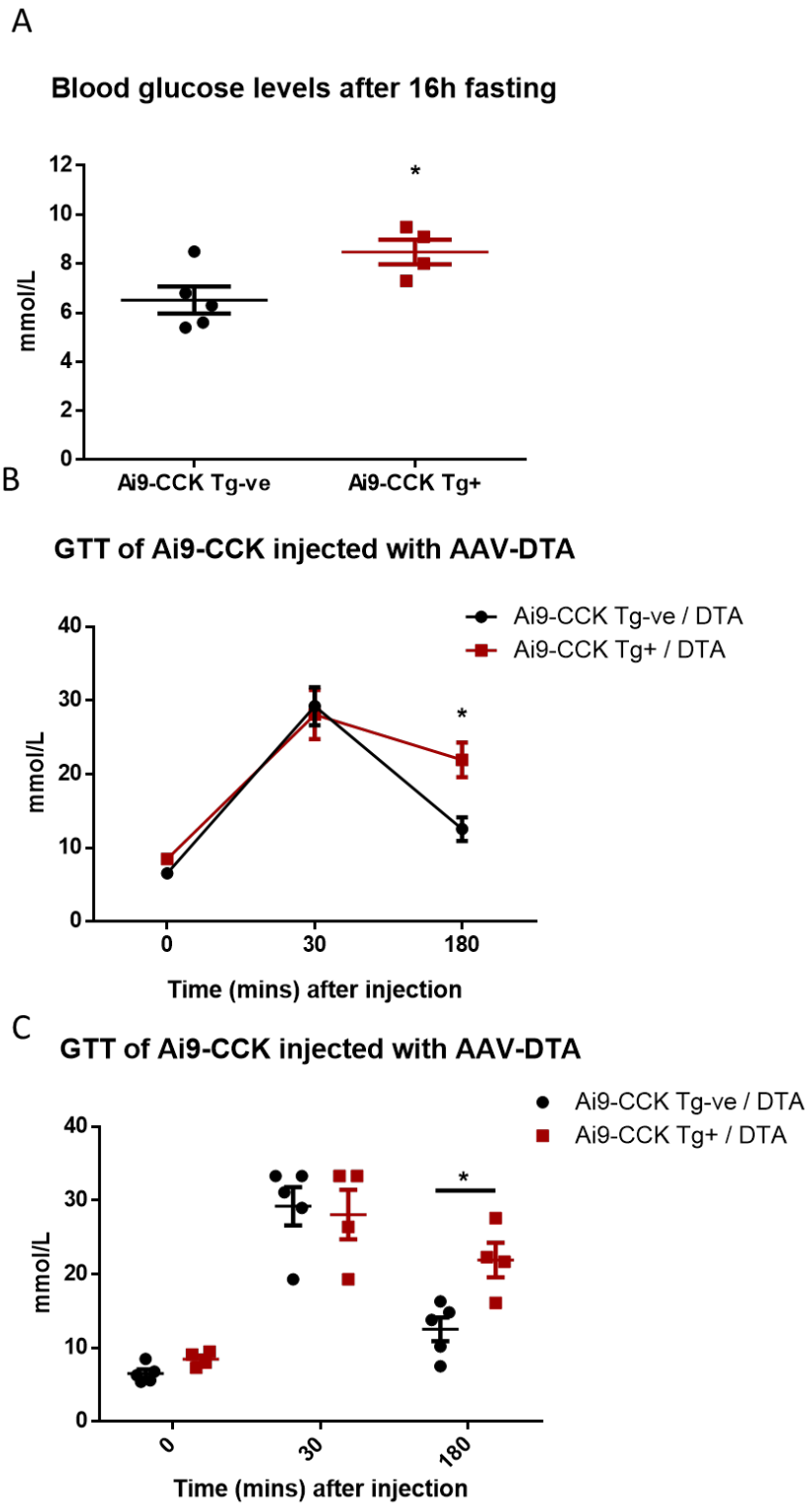

# Chapter 6: Discussion

The hypothalamus is one of the most important regulators of food intake and energy homeostasis. The VMH nucleus of the hypothalamus has a central role in energy homeostasis through the control of food intake, energy expenditure and glucose homeostasis (Choi *et al.*, 2013a). However, the cellular and molecular correlates of its functions are poorly understood (Kim *et al.*, 2011). There have been some attempts to identify genes enriched and distinct regional expression patterns in the VMH (Liu, Kishi, Aaron G Roseberry, *et al.*, 2003; Kurrasch *et al.*, 2007). It's anatomical location near the median eminence and 3$^{rd}$ ventricle allows the integration of satiety signals from the periphery (Rodríguez, Blázquez and Guerra, 2010) while also participating in neuronal circuits in the local hypothalamic circuitry as well as distant direct or indirect connections such as the NTS and other hindbrain nuclei (Morrison, 1999). VMH neurons are also projecting to other hypothalamic nuclei such as the ARC and its POMC neurons which are participating in food intake regulation (Sternson, Shepherd and Friedman, 2005; Krashes *et al.*, 2014).

SF-1, a nuclear receptor expressed only in the VMH of the brain, is required for VMH development and normal regulation of energy balance (Majdic *et al.*, 2002). SF-1 neurons are a representative population of the VMH, yet SF-1 is not expressed in the entire nucleus. Deletion of long form 3UTR′ BDNF in the VMH leads to hyperphagia and obesity in mice (Liao *et al.*, 2012). Moreover, deletion of ERα in the entire VMH leads to hyperphagia and severe obesity while deleting ERa only from SF-1 neurons has an attenuated effect (Musatov *et al.*, 2007; Xu *et al.*, 2011). BDNF and ERα are abundantly expressed in the ventro-lateral area of the VMH (Xu *et al.*, 2003; Musatov *et al.*, 2007) whereas SF-1 is not expressed in this area but rather in the dorsomedial part of the VMH (Cheung *et al.*, 2013). Furthermore, the

VMH is a dense site of expression of receptors for several humoral factors involved in energy regulation, including receptors for ghrelin, leptin and insulin (Mercer *et al.*, 1996; Spanswick *et al.*, 2000; Zigman *et al.*, 2006b).

Moreover, the VMH has a role in the control of glucose levels and counterregulatory response (CRR) (Borg *et al.*, 1994). VMH contains high numbers of glucose sensing neurons which they are heterogeneous in terms of their signalling, glucose levels required for activation and sensing satiety signals received (Song and Routh, 2006; Fioramonti *et al.*, 2013). VGLUT2 has been demonstrated to be important in SF-1 neurons for mounting CCR. SF-1 specific knock out exhibited impaired glucose homeostasis in the fasted condition together with blunted counterregulatory responses to insulin-induced hypoglycaemia (Tong *et al.*, 2007). Leptin, insulin, and their downstream effectors are also regulators of glucose homeostasis in the SF-1 neurons. Leptin-PI3K-FoxO1 pathway is a potential signalling pathway for glycaemic homeostasis in SF-1 neurons (Morton *et al.*, 2005; Kim *et al.*, 2012). The leptin-phosphorylated signal transducer and activator of transcription 3 (pSTAT3) pathway is also associated with glycaemic control in SF-1 neurons of the VMH (Zhang *et al.*, 2008). Deletion of SIRT1 in SF-1 neurons impairs their orexin induced activation and decreases insulin sensitivity (Ramadori *et al.*, 2011).

CCK mRNA is found in many brain areas including many hypothalamic nuclei such as the VMH (Hökfelt *et al.*, 1985; Schiffmann and Vanderhaeghen, 1991; Giacobini and Wray, 2008). CCK immunoreactivity has been shown for hypothalamus by our recent study of CCK TrkB signalling and its role in HPA axis (Geibel *et al.*, 2014). It has also been shown recently to be expressed in the hypothalamus by single cell RNA sequencing analysis exploring cell diversity of the

region (Chen *et al.*, 2017). Direct applications of CCK in the hypothalamus has been shown to supress feeding in rats. (Blevins, Stanley and Reidelberger, 2000). Rats with CCK1 receptor deficiency become hyperphagic due to disrupted function of NPY/AgRP-expressing neurons in the ARC and DMH (Bi *et al.*, 2001, 2004). Injection of CCK to the DMH has been shown to increase the c-Fos immunoreactivity in the medial part of the ARC but does not activate the NTS region where the vagally-mediated CCK signals are inhibiting food intake (Chen *et al.*, 2008). Moreover, restoring CCK1 receptors by viral transduction in receptor deficient animals, partially attenuated the disrupted feeding activity and enhanced glucose tolerance (Zhu *et al.*, 2012). Also, electrophysiologically distinct subpopulations of VMH are predominantly inhibited by systemic CCK administration (Sabatier and Leng, 2010). Additionally, it was shown in rats that CCK is released from DMH neurons from the somata and dendrites in response to repeated postsynaptic depolarisations and acts in an autocrine fashion on CCK2R to enhance NMDA receptor function and release nitric oxide (NO) ultimately enhancing GABA release (Crosby *et al.*, 2015). Recently, it was described how peripheral CCK administration directly causes a rapid but transient reduction in AgRP neuron activity in the ARC in fasted animals (Beutler *et al.*, 2017). They establish that CCK is required for the inhibition of AgRP neurons by fat but not glucose, consistent with fat being the most potent stimulus for CCK secretion from the gut (Tolhurst, Reimann and Gribble, 2012). The vagal afferent pathway cannot be excluded in the AgRP activation by CCK and raises the possibility of hypothalamic CCK release to be able to potentiate and enhance the ascending satiety signals directly at the AgRP population. Furthermore, activation of CCK neurons of the NTS was shown to

suppress appetite and decrease body weight possibly by innervating the MC4R expressing neurons of the PVN (D'Agostino *et al.*, 2016).

Despite increasing evidence of the presence and role of CCK in the hypothalamus and given the central role of the region to the regulation of energy homeostasis, there has not been a functional characterisation of the role of CCK-expressing neurons. Also, the VMH nucleus, which is a relatively molecularly uncharacterised nucleus, is particularly rich in CCK neurons and has extensive local connectivity while being integral in energy and glucose homeostasis. Thus, the VMH CCK neurons appear to be ideally located among already explored pathways and neuronal circuits that regulate food intake, body weight and glucose homeostasis.

## 6.1 Pharmacogenetic inhibition of $CCK^{VMH}$ neurons results in hyperphagia

We set out to assess the short-term role of $CCK^{VMH}$ neurons in homeostatic regulation and identifying their role in modulating food intake in a controlled and acute manner. Considering the inhibitory satiety signal of CCK directly in hypothalamus and its vagally-mediated modulation, we chose to pharmacogenetically inhibit the $CCK^{VMH}$ neurons in order to assess if their role is in energy regulation is inhibitory (i.e. increasing energy intake). We chose to use DREADDs (hM4D-mcherry) (Roth, Hill and Carolina, 2013) for their acute inhibition of their neurotransmission. DREADDs have been used extensively in hypothalamic studies for assessing neuronal circuits implicated in food intake (Krashes *et al.*, 2011; Garfield *et al.*, 2014; Koch *et al.*, 2015; Nakajima *et al.*, 2016). Activation of hM4Di induces neuronal silencing by coupling to Gi protein and stimulating calcium release and ERK1/2 activation, inhibits forskolin-induced cAMP formation, and, in cultured neurons, it was shown to activate GIRK, thereby causing hyperpolarization and inhibition of basal action potential firing (Roth, Hill and Carolina, 2013). At the time of this experimental work, DREADDs were thought to be activated exclusively by the otherwise inert ligand CNO. Recently, a study has found that it is indeed a metabolite of CNO, clozapine, that activates DREADDs in vivo (Gomez *et al.*, 2017). CNO was unable to be detected binding or activating the DREADD receptors unless used at very high doses. While CNO is inert at low concentrations, it was shown that at high concentrations it can activate other receptors such the muscarinic and adrenergic receptors. Ultimately, CNO's ability to activate DREADDs expressed in the brain is through its conversion to clozapine. Hence, high doses of CNO that are usually used in vivo have the risk for non-specific undesired effects and phenotypes

due to binding in other receptors. However, there have been previous reports suggesting that CNO can have non-specific effects and should be appropriately controlled (MacLaren *et al.*, 2016; Raper *et al.*, 2017). Our study has been appropriately controlled by applying the same experimental protocol to animals with no surgery and no DREADD expression in order to assess CNO's effects in food intake and meal patterns and act as a comparable control to the DREADD injected animals in order to assess the role of CCK inhibition.

### 6.1.1 Inhibitory DREADDs expression and silencing of $CCK^{VMH}$ neurons

Firstly, we wanted to establish a stable expression of inhibitory DREADDs only in the VMH region and only in the CCK neurons. We injected a small volume of high titer of AAV that expresses the hM4Di (inhibitory DREADD) in a cre-dependent manner in the VMH region of BAC-CCK-Cre animals. After 3 weeks, there was significantly high expression of the hM4Di in the $CCK^{VMH}$ neurons that was visualised fluorescently by the mcherry fusion to the C terminus of the receptor. We successfully expressed the hM4Di receptor bilaterally to around 76% of CCK positive neurons of the VMH.

We also assessed the ability of the receptor to silence the CCK neurons upon activation with CNO in electrophysiological slices. For this purpose, we injected on one hemisphere DREADDs and on the other a control AAV-DIO-GFP for cre dependent GFP expression in the CCK neurons of the VMH. Recordings performed by Dr Ellender, verified that upon CNO bath application, CCK neurons expressing hM4Di-mcherry reduced their firing compared to their firing pattern prior CNO. GFP expressing CCK neurons did not show any signs of inhibition after CNO application. Even though there are limitations in bath application of CNO and in vitro electrophysiology, it is frequently used as a practical way to assess DREADD

inhibition after intracranial injection and in vivo expression of the receptors (Garfield *et al.*, 2015). This validation method does not directly assess the ability of certain doses of CNO to reach the VMH and inhibit the CCK neurons of the area successfully. However, it is sufficient evidence for the presence of functional DREADD receptors in the CCK neurons of the VMH which indeed recruit the Gi-mediated downstream signalling to silence the neuron. Therefore, we could continue to assess the in vivo role of CCK neurons in the VMH by inhibiting them with DREADDs.

### 6.1.2 Experimental protocol for food intake studies

The experimental design for CNO-mediated activation of inhibitory DREADDs was based on earlier studies of hypothalamic DREADD modulation and food intake monitoring. It was important to establish a protocol for CNO delivery that would minimise any non-specific effect to their food intake. Even though there have been a few studies of repeated CNO dosing via drinking water (MacLaren *et al.*, 2016), most studies deliver CNO by ip injection with some of them injecting CNO twice a day spaced by 6-8 hours. The time is chosen empirically by assessing the time window the CNO is in blood circulation, onset of behavioural effects and neuronal recordings of DREADD modulated neurons with peaks in activity at around 5-6 hours after CNO injection. Drinking water delivery has benefits, such as being less intrusive, but the disadvantages outweigh them. There would be less control over the drinking amount at any given time point or short period and that would introduce variability within the group. Also, the bitter taste of CNO would require extensive habituation with risk of dehydration or addition of sweeteners which could interfere with food intake behaviour. Logistically, constant daily replacements with

fresh CNO was also undesirable as this could also increase the disturbance to the animals during the experiment.

However, CNO ip injections require meticulous extensive habituation prior the onset of the experiment in order to establish if there is any effect to the animal's feeding behaviour due to the disturbance from handling and ip injections. Thus, we designed the experiment to allow a couple of days of handling and cage habituation followed by 10 days of saline vehicle ip injections. We initially used a control group of animals to monitor the variability of their food intake from day to day and establish the right amount of days for the habituation phase of the protocol. As expected, the daily average food intake was transiently affected in the first two days of ip administration. The variability within the group was also high as every animal responded differently to the injection and handling as a form of stressor. After the 5$^{th}$ day of twice daily ip injections, the animals normalised their feeding to values comparable to the ones prior the injections and the variability within the group got reduced greatly. Food intake of the last 3 days of saline ip injections was almost identical to the average food intake before the injections while the food intake within the group was normalised. As a quantification of the magnitude of the habituation protocol established, we plotted the coefficient of variation, which is the percentage of standard deviation divided by the mean for each day. The coef.var dropped from an average of 22% in the first 5 days to an average of 8.4% in the last 3 days of ip injections indicating that the variability in food intake measurements within the group decreased. The habituation part of the protocol ensures that the food intake within the experimental group is not affected by the repeated ip injections, the single housing and the frequent handling and establishes an accurate baseline for food intake in a relative long period of observation prior CNO activation of DREADDs.

### 6.1.3 Food intake and meal pattern changes upon $CCK^{VMH}$ inhibition

The doses of CNO given on similar studies ranges from 0.3 - 5mg/Kg BW so we decided to experimentally titrate the dose in a biologically appropriate range that has already been administered in previous studies (Zhan *et al.*, 2013; Garfield *et al.*, 2015; Koch *et al.*, 2015; Nakajima *et al.*, 2016; Zséli *et al.*, 2017). Each group of animals received incremental doses of CNO (0.75/1.5/2 and 3 mg/Kg BW) and their daily total food intake analysed. Inhibition of $CCK^{VMH}$ neurons with lower CNO doses did not change their food intake significantly, whereas 3 mg/Kg BW CNO increased their food intake compared directly to controls as a percentage increase as well as within the group compared to the saline food intake measurement that acted as a baseline. The controls receiving CNO did not change their food intake. This dose-dependent response identified the optimal CNO concentration that is sufficient at this dosing frequency to reach the VMH nucleus and activate the percentage of CCK neurons expressing adequate levels of hM4Di receptor. Interestingly, food intake 6h after CNO administration did not affect food intake, implying that the mechanism and the neuronal circuit that CCK neurons are part of does not act immediately to modulate food intake for an effect to be observed at such a short time window despite the short delay in a matter of minutes and hours reported for CNO mediated DREADD inhibition of hypothalamic neurons.

Food intake can be further analysed in parameters that define in detail the meal patterns and characteristics (Zorrilla *et al.*, 2005). Therefore, we analysed these parameters and identified any changes due to the silencing of $CCK^{VMH}$ neurons. In detail, we focused on the meal frequency based on the amount of meals and time elapsed between each meal (intermeal time) as well as the properties of each meal such as the size, duration and the consumption rate. The inhibition of

$CCK^{VMH}$ neurons increased the meal frequency even at 6h after the CNO injection which did not affect the total food intake. The increased meal frequency was due to an increase in the meal numbers while intermeal time got significantly reduced. There was a trend for decreased meal sizes within the hM4Di-$CCK^{VMH}$ group that was not significant for the number of animals assessed. However, the meal size reduction was significant when directly compared to the control group. Taking into consideration that meal duration was not affected, it can be hypothesised that changes in meal frequency are counteracted temporarily by a mild reduction in meal size, possibly explaining the unchanged cumulative food intake at 6h after the inhibition. Extensive activation of DREADD receptor and the resulting GPCR signalling cascades downstream of the receptor, could elicit long lasting effects specific to the cell type in question. Indeed, inhibition of $CCK^{VMH}$ neurons resulted in increased meal frequency which persisted throughout the day. The meal sizes remained unchanged in the 24h data analysis, indicating that the compensatory mechanism in response to increased meal frequency is abolished after continued inhibition for prolonged time. It could be possible for other nodes of the satiety neuronal circuitry to fine tune the sensitivity of the VMH neuronal circuit that CCK neurons are part of (see introduction for details e.g receiving nutrient derived satiety signals). Taken together, CCK inhibition increases meal frequency, while meal size is initially adjusted to prevent excess energy intake. However, sustained inhibition leads to attenuation of meal size reduction which results in increased total food intake due to increased meal frequency.

## 6.2 Ablation of $CCK^{VMH}$ neurons leads to hyperphagia-mediated obesity and hyperglycaemia

We could not progress further with the titration and optimisation experiments with the systemic DT ablation strategy due to welfare concerns. Moreover, ablation of only 40% of $CCK^{VMH}$ neurons did not show any significant effect in weight regulation. The partial ablation of the CCK neurons resulted in a hypomorphic phenotype from which the animals were able to recover possibly through system redundancy. However, the temporal (at 2 months) percentage increase observed, was in alignment with the food intake increase and meal pattern changes observed with DREADD-mediated inhibition of a higher percentage (76%) of these neurons in the VMH nucleus. We, therefore, proceeded with an alternative strategy to ablate these neurons with higher efficiency (higher percentage of neurons ablated) by expressing the diphtheria toxin A subunit (DTA) via AAV-DIO-mediated expression.

### 6.2.1 Stereotactic delivery of tolerable titres of AAV-DIO-DTA

The successful expression of AAV-DIO-DTA in Ai9-CCK animals proved to be challenging as previously reported viral high titers ended up causing complications possibly due to cytotoxicity, resulting in control animals gaining weight similar to the Cre positive group. A control group injected with AAV-mcherry in the VMH bilaterally had similar weight with non-injected animals and were not hyperphagic, indicating that the AAV-DIO-DTA in particular is causing an undesired and non-specific effect in the region. One possible explanation could be a sensitisation of the microglial population in and around the hypothalamic nuclei leading to neuroinflammation which is linked to metabolic syndromes and changes in energy expenditure (Thaler *et al.*, 2013). Internal or external factors (diet) that result in inflammation of hypothalamus (such as in the ARC or VMH), are associated

with obesity. These factors are highly correlated with neuronal loss in the region. A possible mechanism by which AAV-DIO-DTA is triggering microglia activation could be the engulfment of the particles and the subsequent display of DTA fragments on the membrane of macrophages and microglia further priming their activation and recruitment to the VMH (Li *et al.*, 2004; Koizumi *et al.*, 2007). In any case, we were able to resolve the issue by titrating the dose to a tolerable dilution. Control animals injected with the titrated particles did not increase their weight compared to a non-injected group. Most importantly, the efficiency of CCK ablation in the VMH remained similar after titrating down the AAV-DIO-DTA which is expected given the high potency of DTA in inducing apoptosis, as one single molecule is adequate for triggering apoptosis to a single neuron (Yamaizumi *et al.*, 1978)

### 6.2.2 Increased body weight due to hyperphagia, and hyperglycaemia after the loss of $CCK^{VMH}$ neurons

Following the optimisation of the DTA injections, we set out to assess the long-term role of $CCK^{VMH}$ neurons in energy homeostasis by ablating them. DTA-mediated ablation resulted in increased body weight of 28% compared to DTA-injected controls 3 months after intracranial delivery of the AAV-DIO-DTA. The obese phenotype was apparent at around a month after injection, coinciding with the usual time for optimal expression reported for AAV viral expressions and the time it takes for complete ablation of neurons with DTA. The obesity observed was due to hyperphagia characterised by increased individual meal sizes with longer meal duration. Interestingly, the meal numbers and time between meals were both reduced significantly in the absence of $CCK^{VMH}$ neurons. Presumably reflecting compensatory mechanisms that are attempting to compensate for the increased food intake with larger and longer meals. Also, peripheral satiety signals might be

increased due to energy surplus, leading to activation of hindbrain intake inhibitory neuronal circuits. It should be noted that the food intake dysregulation resulting from the complete ablation of $CCK^{VMH}$ neurons has key differences from the one observed with the DREADD inhibition. DTA ablation removed almost all the CCK positive neurons from the VMH, effectively disengaging the CCK expressing population from the local circuitry. During DREADD-mediated inhibition, the neurons are still intact and are participating in their network, they may receive presynaptic inputs and they may still engage in the processing and integration of satiety signals (such as glucose sensing, leptin/insulin or ghrelin) that does not require synaptic neurotransmission which is being inhibited by DREADDs. DREADD inhibition is also dependent on the presence of its ligand, which creates a temporal window of maximal inhibition with varying degrees of inhibition throughout the day according to the injection protocol, in this case twice per day at the onset of their resting and active period. Therefore, $CCK^{VMH}$ neurons are likely to modulate food intake with more than one mechanism. Inhibition of their neurotransmission results in increased meal frequency, suggesting that their postsynaptic partners are participating in satiety signals that adjust the energy intake according to meal consumption. In the absence of CCK input, meal consumption is disturbed with an early effect in decreased meal size and as the inhibition of CCK continues, the meal size normalises but the onset of meals is dysregulated as it occurs more frequently. On the other hand, ablation of the neurons results in prolonged meals with increased meal size, suggesting a role in the integration of neurohormonal satiety signals that are independent of synaptic communication. It is possible that meal termination mechanisms could be impacted by the absence of CCK neurons. The increased meal sizes are probably triggering compensatory satiety circuits emanating from the

GI tract and vagally-mediated to the brain (such as nutrient-dependent peptide release and gastric tension) which ultimately decrease the meal frequency (see introduction). However, irrespectively of the type of modulation CCK neurons are exerting on the satiety circuit, both inhibition and ablation leads to increased food intake. Moreover, it should be noted that the DREADD modulation was performed in male animals while the ablation in females. Male-female sex differences in the physiology of eating involve both organizational and activation effects of androgens and oestrogens (Roepke, 2009; Asarian and Geary, 2013). Therefore, the possibility of a gender difference between the two experiments cannot be excluded and the observed phenotype in either of the experiments cannot be inferred to be true for the other gender.

Since the VMH is dense in glucose sensing neurons and has a central role in glucose homeostasis and CRR, we wanted to assess the response to a glucose challenge in the absence of $CCK^{VMH}$ neurons. We therefore subjected DTA-ablated animals to a glucose tolerance test (GTT) 3 months after surgery. $CCK^{VMH}$ ablation led to hyperglycaemia as the baseline blood glucose levels were higher than the controls after 16h of fasting. The animals were also glucose intolerant upon glucose administration since blood glucose levels remained higher than the controls up to 2.5 hours after glucose administration. However, the identified phenotype could be secondary to changes in body weight and not a direct effect of CCK ablation. Future work can look at glucose homeostasis prior to the obese phenotype. These results indicate that CCK neurons could have a role in glucose sensing and homeostasis of the VMH and in their absence blood glucose levels remain high.

## 6.3 Peripheral and central CCK signalling compared to $CCK^{VMH}$ inhibition or ablation

The pharmacogenetic inhibition of the CCK neurons of the VMH increased food intake by increasing the meal frequency without an effect in meal size or duration while the CCK ablation from the VMH resulted in a different phenotype of hyperphagia characterised by reduced meal frequency but with larger meals with longer duration.

Intraperitoneal administration of CCK significantly reduces food intake (Garlicki *et al.*, 1990; Weatherford *et al.*, 1993; Goebel-Stengel *et al.*, 2012). Chronic administration of CCK at meal onset results in chronic decreases in meal size but an increase in meal frequency such that overall food intake is not affected (West, Fey and Woods, 1984). Upon administration at the onset of dark phase, CCK reduces the size, duration of the first meal while food intake was reduced in the first hour following the injection. Also, CCK was shown to delay the onset of the first meal and increase the intermeal intervals. The food intake reduction is accompanied with a reduction in eating-related behaviours such as approach and sniffing of the food, an increase in grooming and a reduction in locomotion (Goebel-Stengel *et al.*, 2012). CCK injection in different hypothalamic nuclei was shown to suppress food intake in the first 30mins after injection with the effect lasting for 4 hours and with no increase in food intake as a compensation mechanism for up to 18 hours after injection (Blevins, Stanley and Reidelberger, 2000). Hence, the meal frequency effect observed in CCK inhibition and ablation experiments is expected since the lack of CCK would lead to opposing effects from its administration.

The obesity rat model Otsuka Long Evans Tokushima Fatty (OLETF) is a CCK1R knockout model lacking CCK1R in both the gastrointestinal track and the

brain which is hyperphagic with increased meal sizes but reduced meal numbers but overall increased food intake (Moran *et al.*, 1998). OLETF rats also show higher preferences for high fat, sucrose and other sweet tastes (De Jonghe, Hajnal and Covasa, 2005). This phenotype shares similarities with the CCK ablation where food intake is increased due to larger meals but reduced meal numbers.

Administration of the specific CCK1R antagonist ,devazepide, attenuated the meal size reduction and prolonged intermeal intervals induced by duodenal fat infusions (Woltman, Castellanos and Reidelberger, 1995). However, centrally administered devazepide failed to induce any changes to food intake (Corp *et al.*, 1997). In contrast, intracerebroventricular injections of a CCKBR antagonist, CI988, reduces the cumulative food intake starting at 2h after injection with the effect lasting up to 11 hours post injection in fasted rats but with no effect in ad libitum animals. Systemic administration of a dopamine antagonist blocked the CI988 mediated reduction of food intake, indicating the involvement of dopamine signalling in the central effects of CCK in satiety (Frommelt *et al.*, 2013).

## 6.4 Concluding remarks

The hypothalamus has a central role in regulation of energy homeostasis. Within the hypothalamus the VMH nucleus is integrating satiety related information ascending from the hindbrain and limbic regions of the brain while also receiving direct signals from local hypothalamic networks and satiety signals from the leaky BBB from the median eminence. The VMH is not well characterised in its molecular components and cell types. However, the SF-1 is critical for the development and cytoarchitecture of the nucleus and has become a genetic identity of a large subpopulation of VMH neurons that are required for physiological energy expenditure, thermogenesis, body weight balance and glucose homeostasis. Other VMH neurons express ERa and BDNF and they are involved in food intake and body weight regulation. CCK as a gut neuropeptide, exerts its satiety control through the vagal nerve afferents to the hindbrain. However, there is an increasing amount of studies focusing on brain-derived CCK release in the hypothalamus which modulate food intake and glucose homeostasis through the CCK1R. But, the source of endogenous CCK in the hypothalamus and the role of CCK expressing neurons in energy homeostasis has remained elusive so far.

Hence, we spatiotemporally inhibited the $CCK^{VMH}$ neurons and have demonstrated their role in food intake. CCK inhibition increased meal frequency and total food intake. The long-term role of $CCK^{VMH}$ neurons was assessed by DTA ablation which triggered the onset of obesity with hyperphagia followed by hyperglycaemia and glucose intolerance. Further characterisation of the VMH nucleus and its heterogeneity will pave the research endeavours towards effective treatments of obesity and diabetes and CCK neurons could be a primary and attractive target for pharmacological interventions.

## 6.5 Outlook and future perspectives

CCK neurons of the VMH have a role in energy homeostasis by affecting food intake, body weight and glucose homeostasis. Given the complexity of the neuronal circuitry involved in these processes, it is important to understand their role in the network. Identifying the projections to and from the $CCK^{VMH}$ neurons will be useful for linking their role with other known hypothalamic neuronal types that are involved in energy homeostasis such as POMC neurons of the ARC that have been shown to be innervated by VMH neurons (Sternson, Shepherd and Friedman, 2005). Intracranial injections of AAV-DIO-GFP can assist in anterograde tracing of the $CCK^{VMH}$ neuronal projections. Moreover, their long-term effect in obesity glucose regulation could be studied by silencing the neurons permanently with AAV-DIO-Tetanus toxin expression as a complementary study to the ablation experiments. Furthermore, the bimodulation of food intake could be explored with the excitatory version of DREADDs (hM3Dq) where it would be interesting to see if the food intake will be reduced and induce an anorexic phenotype. Finally, the molecular identity of the neurons could be explored with single cell RNA seq analysis, which our laboratory is capable of producing. Those answers will be instrumental to design new therapies for obesity and obesity-related diseases.

# List of abbreviations

**A**

| | |
|---|---|
| AAV | Adeno-associated virus |
| ABC | peroxidase Vectastain ABC system |
| ACTH | adrenocorticotropic hormone |
| *AGRP* | Agouti-Related Peptide |
| AHN | Anterior Hypothalamic Nucleus |
| AMPK | AMP-activated protein kinase |
| ARC | Arcuate nucleus |
| ARH | Arcuate hypothalamus |

**B**

| | |
|---|---|
| BAC | Bacterial Artificial Chromosome |
| BAT | Brown Adipose Tissue |
| BBB | Blood Brain Barrier |
| BCA | bicinchoninic acid |
| BDNF | Brain Derived Neurotrophic factor |
| BLA | Basolateral Amygdala |
| BNST | Bed Nuclei of Stria Terminalis |
| BSA | Bovine Serum Albumin |
| BW | Body Weight |

**C**

| | |
|---|---|
| CAG | cytomegalovirus enhancer/chicken beta-actin promoter |
| CCK | Cholecystokinin |
| CCKAR | Cholecystokinin Receptor A |
| $CCK^{VMH}$ | Cholecystokinin neurons of the VMH |
| CGE | Caudal ganglionic eminence |
| CMV | Cytomegalovirus |
| CNO | Clozapine-N-Oxide |
| CNS | Central Nervous system |
| CORT | Cortisone |
| CRH | Corticotrophin hormone |

**D**

| | |
|---|---|
| DAB | 3’3-diaminobenzidine |
| DAPI | 4',6-diamidino-2-phenylindole |
| DIO | Double-floxed inverse Orientation |
| DMH | Dorso medial Hypothalamus |
| DMSO | Dimethyl sulfoxide |
| DMV | dorsal motor nucleus of the vagus nerve |
| DREADD | Designer Receptors Exclusively Activated by Designer Drug |
| DT | Diphtheria toxin |
| DTA | Diphtheria toxin A subunit |
| DTR | Diphtheria toxin Recepto |
| DTT | Dithiothreitol |
| DVC | Dorsal vagal complex |

**E**

| | |
|---|---|
| ECL | enhanced chemiluminescence |
| EDTA | Ethylenediaminetetraacetic acid |
| ESC | Embryonic stem cells |
| EYFP | Enhanced yellow fluorescent protein |

**F**

| | |
|---|---|
| FLP | Flippase recombinase |
| FRT | FLP recombinase target sequence |

**G**

| | |
|---|---|
| GABA | γ-aminobutyric acid |
| GFP | Green Fluorescent protein |
| GHSR | Growth hormone secretogue receptor |
| GI | Gastrointestinal |
| GIRK | G protein coupled inwardly rectifying potassium channel |
| GK | Glucokinase |
| GLP | Glucagon like protein |
| GPCR | G Protein Coupled Receptor |

**H**

| | |
|---|---|
| HGP | Hepatic glucose production |
| HPA | Hypothalamic Pituitary Adrenal axis |
| HRP | Horseradish peroxidase |

**I**

| | |
|---|---|
| IP | Intraperitoneal injection |
| IRES | internal ribosome entry site |
| IV | Intravenous injection |

**K**

| | |
|---|---|
| KATP | ATP sensitive potassium channel |

**L**

| | |
|---|---|
| LH | Lateral hypothalamic nucleus |

**M**

| | |
|---|---|
| MAPK | Mitogen-activated protein kinase |
| ME | Median eminence |
| MSH | Melanocortin stimulating hormone |

**N**

| | |
|---|---|
| NIRKO | Neuronal insulin-receptor knockout |
| NO | Nitric oxide |
| NPY | Neuropeptide Y |
| NTS | Nucleus Tractus solitarius |

**O**

| | |
|---|---|
| OCT | Optimal cutting temperature (compound for embedding tissue) |
| ORF | Open Reading Frame |

**P**

| | |
|---|---|
| PAGE | Polyacrylamide gel electrophoresis |
| PB | Phosphate buffer |

| | |
|---|---|
| PBN | Parabrachial nucleus |
| PBS | Phosphate buffer saline |
| PBST | Phosphate buffer saline Triton |
| PFA | Paraformaldehyde |
| PMSF | Phenylmethylsulfonyl fluoride |
| POMC | Pro-opiomelanocorticotrophin |
| PVDF | Polyvinylidene fluoride |
| PVN | Paraventricularnucleus |
| PYY | Peptide YY |

**R**

| | |
|---|---|
| ROI | Region of Interest |
| RT | Room Temperature |

**S**

| | |
|---|---|
| SCH | Suprachiasmatic nucleus |
| SDS | sodium dodecyl sulfate |
| SGLT | sodium glucose co-transporter |
| SSC | saline-sodium citrate buffer |

**T**

| | |
|---|---|
| TASK | Twik-related acid-sensitive potassium-like channel |
| TH | Thyroid hormone |
| TRH | Thyrotropin-releasing hormone |

**V**

| | |
|---|---|
| VCX | Visual Cortex |
| VIP | Vaso-intestinal peptide |
| VLM | Ventrolateral medulla |
| VMH | Ventromedial Hypothalamus |
| VTA | Ventral Tegmental Area |

**W**

| | |
|---|---|
| WPRE | Woodchuck Hepatitis Posttranscriptional Regulatory Element |
| WT | Wild type |

# References


Ahrén, B. (2000) 'Autonomic regulation of islet hormone secretion - Implications for health and disease', *Diabetologia*. Springer-Verlag, 43(4), pp. 393–410. doi: 10.1007/s001250051322.

Alhadeff, A. L., Rupprecht, L. E. and Hayes, M. R. (2012) 'GLP-1 Neurons in the Nucleus of the Solitary Tract Project Directly to the Ventral Tegmental Area and Nucleus Accumbens to Control for Food Intake', *Endocrinology*, 153(2), pp. 647–658. doi: 10.1210/en.2011-1443.

Anagnostides, A. A., Chadwick, V. S., Selden, A. C., Barr, J. and Maton, P. N. (1985) 'Human pancreatic and biliary responses to physiological concentrations of cholecystokinin octapeptide.', *Clinical science (London, England : 1979)*. Portland Press Limited, 69(3), pp. 259–63. doi: 10.1042/CS0690259.

Anand, B. K., Chhina, G. S., Sharma, K. N., Dua, S. and Singh, B. (1964) 'Activity of single neurons in the hypothalamic feeding centers: effect of glucose', *American Journal of Physiology-Legacy Content*, 207(5), pp. 1146–1154. doi: 10.1152/ajplegacy.1964.207.5.1146.

Andrew, S. F., Dinh, T. T. and Ritter, S. (2007) 'Localized glucoprivation of hindbrain sites elicits corticosterone and glucagon secretion', *American Journal of Physiology-Regulatory, Integrative and Comparative Physiology*, 292(5), pp. R1792–R1798. doi: 10.1152/ajpregu.00777.2006.

Arluison, M., Quignon, M., Nguyen, P., Thorens, B., Leloup, C. and Penicaud, L. (2004) 'Distribution and anatomical localization of the glucose transporter 2 (GLUT2) in the adult rat brain—an immunohistochemical study', *Journal of Chemical Neuroanatomy*, 28(3), pp. 117–136. doi: 10.1016/j.jchemneu.2004.05.009.

Asarian, L. and Geary, N. (2013) 'Sex differences in the physiology of eating', *American Journal of Physiology-Regulatory, Integrative and Comparative Physiology*. American Physiological Society Bethesda, MD, 305(11), pp. R1215–R1267. doi: 10.1152/ajpregu.00446.2012.

Atalayer, D. and Rowland, N. E. (2011) 'Structure of motivation using food demand in mice', *Physiology & Behavior*, 104(1), pp. 15–19. doi: 10.1016/j.physbeh.2011.04.042.

Atasoy, D., Betley, J. N., Su, H. H. and Sternson, S. M. (2012) 'Deconstruction of a neural circuit for hunger', *Nature*, 488(7410), pp. 172–177. doi: 10.1038/nature11270.

Bady, I., Marty, N., Dallaporta, M., Emery, M., Gyger, J., Tarussio, D., Foretz, M. and Thorens, B. (2006) 'Evidence From Glut2-Null Mice That Glucose Is a Critical Physiological Regulator of Feeding', *Diabetes*, 55(4), pp. 988–995. doi: 10.2337/diabetes.55.04.06.db05-1386.

Bake, T., Murphy, M., Morgan, D. G. A. and Mercer, J. G. (2014) 'Large, binge-type meals of high fat diet change feeding behaviour and entrain food anticipatory activity in mice.', *Appetite*. Elsevier, 77(100), pp. 60–71. doi: 10.1016/j.appet.2014.02.020.

Balthasar, N., Coppari, R., McMinn, J., Liu, S. M., Lee, C. E., Tang, V., Kenny, C. D., McGovern, R. A., Chua, S. C., Elmquist, J. K. and Lowell, B. B. (2004) 'Leptin Receptor Signaling in POMC Neurons Is Required for Normal Body Weight Homeostasis', *Neuron*. Cell Press, 42(6), pp. 983–991. doi: 10.1016/J.NEURON.2004.06.004.

Balthasar, N., Dalgaard, L. T., Lee, C. E., Yu, J., Funahashi, H., Williams, T., Ferreira, M., Tang, V., McGovern, R. A., Kenny, C. D., Christiansen, L. M., Edelstein, E., Choi, B., Boss, O., Aschkenasi, C., Zhang, C., Mountjoy, K., Kishi, T., Elmquist, J. K. and Lowell, B. B. (2005) 'Divergence of Melanocortin Pathways in the Control of Food Intake and Energy Expenditure', *Cell*, 123(3), pp. 493–505. doi: 10.1016/j.cell.2005.08.035.

Banihashemi, L. and Rinaman, L. (2006) 'Noradrenergic Inputs to the Bed Nucleus of the Stria Terminalis and Paraventricular Nucleus of the Hypothalamus Underlie Hypothalamic-Pituitary-Adrenal Axis But Not Hypophagic or Conditioned Avoidance Responses to Systemic Yohimbine', *Journal of Neuroscience*, 26(44), pp. 11442–11453. doi: 10.1523/JNEUROSCI.3561-06.2006.

Baver, S. B., Hope, K., Guyot, S., Bjorbaek, C., Kaczorowski, C. and O'Connell, K. M. S. (2014) 'Leptin Modulates the Intrinsic Excitability of AgRP/NPY Neurons in the Arcuate Nucleus of the Hypothalamus', *Journal of Neuroscience*, 34(16), pp. 5486–5496. doi: 10.1523/JNEUROSCI.4861-12.2014.

Beinfeld, M. C. (2001) 'An introduction to neuronal cholecystokinin.',

*Peptides*, 22(8), pp. 1197–200.

Belgardt, B. F. and Brüning, J. C. (2010) 'CNS leptin and insulin action in the control of energy homeostasis', *Annals of the New York Academy of Sciences*, 1212(1), pp. 97–113. doi: 10.1111/j.1749-6632.2010.05799.x.

Bellinger, L. L. and Bernardis, L. L. (2002) 'The dorsomedial hypothalamic nucleus and its role in ingestive behavior and body weight regulation: lessons learned from lesioning studies.', *Physiology & behavior*, 76(3), pp. 431–42.

Benarroch, E. (1998) 'The Lower Brainstem and Bodily Homeostasis. *By William Blessing Oxford, UK, Oxford University Press, 1997 579 pp, illustrated, $85.00*', *Annals of Neurology*. Wiley Subscription Services, Inc., A Wiley Company, 43(6), pp. 839–839. doi: 10.1002/ana.410430624.

Benoit, S. C., Air, E. L., Coolen, L. M., Strauss, R., Jackman, A., Clegg, D. J., Seeley, R. J. and Woods, S. C. (2002) 'The catabolic action of insulin in the brain is mediated by melanocortins.', *The Journal of neuroscience : the official journal of the Society for Neuroscience*, 22(20), pp. 9048–52.

Bernard, C. (1813-1878). A. du texte (1855) 'Leçons de physiologie expérimentale appliquée à la médecine, faites au Collège de France. T. 2, Cours du semestre d'été 1855 / par Claude Bernard,... ; publié par Henri Lefèvre'.

Berthoud, H.-R. and Münzberg, H. (2011) 'The lateral hypothalamus as integrator of metabolic and environmental needs: From electrical self-stimulation to opto-genetics', *Physiology & Behavior*, 104(1), pp. 29–39. doi: 10.1016/j.physbeh.2011.04.051.

Berthoud, H.-R., Sutton, G. M., Townsend, R. L., Patterson, L. M. and Zheng, H. (2006) 'Brainstem mechanisms integrating gut-derived satiety signals and descending forebrain information in the control of meal size.', *Physiology & behavior*, 89(4), pp. 517–24. doi: 10.1016/j.physbeh.2006.08.018.

Betley, J. N., Cao, Z. F. H., Ritola, K. D. and Sternson, S. M. (2013) 'Parallel, Redundant Circuit Organization for Homeostatic Control of Feeding Behavior', *Cell*, 155(6), pp. 1337–1350. doi: 10.1016/j.cell.2013.11.002.

Beutler, L. R., Chen, Y., Ahn, J. S., Lin, Y.-C., Essner, R. A. and Knight, Z. A. (2017) 'Dynamics of Gut-Brain Communication Underlying Hunger', *Neuron*,

96(2), p. 461–475.e5. doi: 10.1016/j.neuron.2017.09.043.

Bi, S. (2013) ‘Dorsomedial hypothalamic NPY modulation of adiposity and thermogenesis.’, *Physiology & behavior*, 121, pp. 56–60. doi: 10.1016/j.physbeh.2013.03.022.

Bi, S., Ladenheim, E. E., Schwartz, G. J. and Moran, T. H. (2001) ‘A role for NPY overexpression in the dorsomedial hypothalamus in hyperphagia and obesity of OLETF rats.’, *American journal of physiology. Regulatory, integrative and comparative physiology*, 281(1), pp. R254-60.

Bi, S., Scott, K. A., Kopin, A. S. and Moran, T. H. (2004) ‘Differential roles for cholecystokinin a receptors in energy balance in rats and mice.’, *Endocrinology*, 145(8), pp. 3873–80. doi: 10.1210/en.2004-0284.

Bjørbæk, C., Buchholz, R. M., Davis, S. M., Bates, S. H., Pierroz, D. D., Gu, H., Neel, B. G., Myers, M. G. and Flier, J. S. (2001) ‘Divergent Roles of SHP-2 in ERK Activation by Leptin Receptors’, *Journal of Biological Chemistry*, 276(7), pp. 4747–4755. doi: 10.1074/jbc.M007439200.

Blevins, J. E., Eakin, T. J., Murphy, J. A., Schwartz, M. W. and Baskin, D. G. (2003) ‘Oxytocin innervation of caudal brainstem nuclei activated by cholecystokinin’, *Brain Research*. Elsevier, 993(1–2), pp. 30–41. doi: 10.1016/j.brainres.2003.08.036.

Blevins, J. E., Schwartz, M. W. and Baskin, D. G. (2004) ‘Evidence that paraventricular nucleus oxytocin neurons link hypothalamic leptin action to caudal brain stem nuclei controlling meal size’, *American Journal of Physiology-Regulatory, Integrative and Comparative Physiology*, 287(1), pp. R87–R96. doi: 10.1152/ajpregu.00604.2003.

Blevins, J. E., Stanley, B. G. and Reidelberger, R. D. (2000) ‘Brain regions where cholecystokinin suppresses feeding in rats.’, *Brain research*, 860(1–2), pp. 1–10. doi: 10.1016/S0006-8993(99)02477-4.

Blouet, C., Jo, Y.-H., Li, X. and Schwartz, G. J. (2009a) ‘Mediobasal Hypothalamic Leucine Sensing Regulates Food Intake through Activation of a Hypothalamus-Brainstem Circuit’, *Journal of Neuroscience*, 29(26), pp. 8302–8311. doi: 10.1523/JNEUROSCI.1668-09.2009.

Blouet, C., Jo, Y.-H., Li, X. and Schwartz, G. J. (2009b) 'Mediobasal Hypothalamic Leucine Sensing Regulates Food Intake through Activation of a Hypothalamus-Brainstem Circuit', *Journal of Neuroscience*, 29(26), pp. 8302–8311. doi: 10.1523/JNEUROSCI.1668-09.2009.

Del Boca, C., Lutz, P. E., Le Merrer, J., Koebel, P. and Kieffer, B. L. (2012) 'Cholecystokinin knock-down in the basolateral amygdala has anxiolytic and antidepressant-like effects in mice', *Neuroscience*, 218, pp. 185–195. doi: 10.1016/j.neuroscience.2012.05.022.

Borg, W. P., During, M. J., Sherwin, R. S., Borg, M. A., Brines, M. L. and Shulman, G. I. (1994) 'Ventromedial hypothalamic lesions in rats suppress counterregulatory responses to hypoglycemia.', *Journal of Clinical Investigation*, 93(4), pp. 1677–1682. doi: 10.1172/JCI117150.

Bowers, M. E., Choi, D. C. and Ressler, K. J. (2012) 'Neuropeptide regulation of fear and anxiety: Implications of cholecystokinin, endogenous opioids, and neuropeptide Y.', *Physiology & behavior*. NIH Public Access, 107(5), pp. 699–710. doi: 10.1016/j.physbeh.2012.03.004.

Bragado, M. J., Tashiro, M. and Williams, J. A. (2000) 'Regulation of the initiation of pancreatic digestive enzyme protein synthesis by cholecystokinin in rat pancreas in vivo.', *Gastroenterology*, 119(6), pp. 1731–9.

Broberger, C., Johansen, J., Johansson, C., Schalling, M. and Hokfelt, T. (1998) 'The neuropeptide Y/agouti gene-related protein (AGRP) brain circuitry in normal, anorectic, and monosodium glutamate-treated mice', *Proceedings of the National Academy of Sciences*, 95(25), pp. 15043–15048. doi: 10.1073/pnas.95.25.15043.

Buffa, R., Solcia, E. and Go, V. L. (1976) 'Immunohistochemical identification of the cholecystokinin cell in the intestinal mucosa.', *Gastroenterology*, 70(4), pp. 528–32.

Burdakov, D., Gerasimenko, O. and Verkhratsky, A. (2005) 'Physiological Changes in Glucose Differentially Modulate the Excitability of Hypothalamic Melanin-Concentrating Hormone and Orexin Neurons In Situ', *Journal of Neuroscience*, 25(9), pp. 2429–2433. doi: 10.1523/JNEUROSCI.4925-04.2005.

Burgunder, J. M. and Young, W. S. (1990) ‘Cortical neurons expressing the cholecystokinin gene in the rat: distribution in the adult brain, ontogeny, and some of their projections.’, *The Journal of comparative neurology*, 300(1), pp. 26–46. doi: 10.1002/cne.903000104.

Cabrele, C., Langer, M., Bader, R., Wieland, H. A., Doods, H. N., Zerbe, O. and Beck-Sickinger, A. G. (2000) ‘The First Selective Agonist for the Neuropeptide YY $_5$ Receptor Increases Food Intake in Rats’, *Journal of Biological Chemistry*, 275(46), pp. 36043–36048. doi: 10.1074/jbc.M000626200.

Cai, X. J., Evans, M. L., Lister, C. A., Leslie, R. A., Arch, J. R., Wilson, S. and Williams, G. (2001) ‘Hypoglycemia activates orexin neurons and selectively increases hypothalamic orexin-B levels: responses inhibited by feeding and possibly mediated by the nucleus of the solitary tract.’, *Diabetes*, 50(1), pp. 105–12.

Canabal, D. D., Potian, J. G., Duran, R. G., McArdle, J. J. and Routh, V. H. (2007) ‘Hyperglycemia impairs glucose and insulin regulation of nitric oxide production in glucose-inhibited neurons in the ventromedial hypothalamus’, *American Journal of Physiology-Regulatory, Integrative and Comparative Physiology*, 293(2), pp. R592–R600. doi: 10.1152/ajpregu.00207.2007.

Canabal, D. D., Song, Z., Potian, J. G., Beuve, A., McArdle, J. J. and Routh, V. H. (2007) ‘Glucose, insulin, and leptin signaling pathways modulate nitric oxide synthesis in glucose-inhibited neurons in the ventromedial hypothalamus’, *American Journal of Physiology-Regulatory, Integrative and Comparative Physiology*, 292(4), pp. R1418–R1428. doi: 10.1152/ajpregu.00216.2006.

Cardoso, F. L., Brites, D. and Brito, M. A. (2010) ‘Looking at the blood–brain barrier: Molecular anatomy and possible investigation approaches’, *Brain Research Reviews*, 64(2), pp. 328–363. doi: 10.1016/j.brainresrev.2010.05.003.

Chaudhri, O., Small, C. and Bloom, S. (2006) ‘Gastrointestinal hormones regulating appetite’, *Philosophical Transactions of the Royal Society B: Biological Sciences*. Royal Society, 361(1471), pp. 1187–1209. doi: 10.1098/rstb.2006.1856.

Chen, D., Zhao, C.-M., Håkanson, R., Samuelson, L. C., Rehfeld, J. F. and Friis-Hansen, L. (2004) ‘Altered control of gastric acid secretion in gastrin-cholecystokinin double mutant mice.’, *Gastroenterology*, 126(2), pp. 476–87.

Chen, J., Scott, K. A., Zhao, Z., Moran, T. H. and Bi, S. (2008) 'Characterization of the feeding inhibition and neural activation produced by dorsomedial hypothalamic cholecystokinin administration.', *Neuroscience*, 152(1), pp. 178–88. doi: 10.1016/j.neuroscience.2007.12.004.

Chen, R., Wu, X., Jiang, L. and Zhang, Y. (2017) 'Single-Cell RNA-Seq Reveals Hypothalamic Cell Diversity.', *Cell reports*, 18(13), pp. 3227–3241. doi: 10.1016/j.celrep.2017.03.004.

Cheung, C. C., Kurrasch, D. M., Liang, J. K. and Ingraham, H. A. (2013) 'Genetic labeling of steroidogenic factor-1 (SF-1) neurons in mice reveals ventromedial nucleus of the hypothalamus (VMH) circuitry beginning at neurogenesis and development of a separate non-SF-1 neuronal cluster in the ventrolateral VMH', *Journal of Comparative Neurology*, 521(6), pp. 1268–1288. doi: 10.1002/cne.23226.

Choi, Y.-H., Fujikawa, T., Lee, J., Reuter, A. and Kim, K. W. (2013a) 'Revisiting the Ventral Medial Nucleus of the Hypothalamus: The Roles of SF-1 Neurons in Energy Homeostasis.', *Frontiers in neuroscience*. Frontiers Media SA, 7, p. 71. doi: 10.3389/fnins.2013.00071.

Choi, Y.-H., Fujikawa, T., Lee, J., Reuter, A. and Kim, K. W. (2013b) 'Revisiting the Ventral Medial Nucleus of the Hypothalamus: The Roles of SF-1 Neurons in Energy Homeostasis', *Frontiers in Neuroscience*, 7, p. 71. doi: 10.3389/fnins.2013.00071.

Ciriello, J., McMurray, J. C., Babic, T. and de Oliveira, C. V. R. (2003) 'Collateral axonal projections from hypothalamic hypocretin neurons to cardiovascular sites in nucleus ambiguus and nucleus tractus solitarius', *Brain Research*, 991(1–2), pp. 133–141. doi: 10.1016/j.brainres.2003.08.016.

Cohen, H., Kaplan, Z., Matar, M. A., Buriakovsky, I., Bourin, M. and Kotler, M. (2004) 'Different pathways mediated by CCK1 and CCK2 receptors: Effect of intraperitonal mrna antisense oligodeoxynucleotides to cholecystokinin on anxiety-like and learning behaviors in rats', *Depression and Anxiety*. Wiley Subscription Services, Inc., A Wiley Company, 20(3), pp. 139–152. doi: 10.1002/da.20032.

Cohen, R. S. and Pfaff, D. W. (1992) 'Ventromedial hypothalamic neurons in the mediation of long-lasting effects of estrogen on lordosis behavior.', *Progress in*

*neurobiology*, 38(5), pp. 423–53.

Corp, E. S., Curcio, M., Gibbs, J. and Smith, G. P. (1997) 'The Effect of Centrally Administered CCK-Receptor Antagonists on Food Intake in Rats', *Physiology & Behavior*. Elsevier, 61(6), pp. 823–827. doi: 10.1016/S0031-9384(96)00561-6.

Cota, D., Proulx, K., Smith, K. A. B., Kozma, S. C., Thomas, G., Woods, S. C. and Seeley, R. J. (2006) 'Hypothalamic mTOR Signaling Regulates Food Intake', *Science*, 312(5775), pp. 927–930. doi: 10.1126/science.1124147.

Cotero, V. E., Zhang, B. B. and Routh, V. H. (2010) 'The Response of Glucose-Excited Neurones in the Ventromedial Hypothalamus to Decreased Glucose is Enhanced in a Murine Model of Type 2 Diabetes Mellitus', *Journal of Neuroendocrinology*, 22(2), pp. 65–74. doi: 10.1111/j.1365-2826.2009.01938.x.

Cowley, M. A., Smart, J. L., Rubinstein, M., Cerdán, M. G., Diano, S., Horvath, T. L., Cone, R. D. and Low, M. J. (2001) 'Leptin activates anorexigenic POMC neurons through a neural network in the arcuate nucleus.', *Nature*, 411(6836), pp. 480–484. doi: 10.1038/35078085.

Crosby, K. M., Baimoukhametova, D. V., Bains, J. S. and Pittman, Q. J. (2015) 'Postsynaptic Depolarization Enhances GABA Drive to Dorsomedial Hypothalamic Neurons through Somatodendritic Cholecystokinin Release', *Journal of Neuroscience*, 35(38), pp. 13160–13170. doi: 10.1523/JNEUROSCI.3123-14.2015.

Cruciani-Guglielmacci, C., Hervalet, A., Douared, L., Sanders, N. M., Levin, B. E., Ktorza, A. and Magnan, C. (2004) 'Beta oxidation in the brain is required for the effects of non-esterified fatty acids on glucose-induced insulin secretion in rats', *Diabetologia*, 47(11), pp. 2032–2038. doi: 10.1007/s00125-004-1569-2.

Cui, R. J., Li, X. and Appleyard, S. M. (2011) 'Ghrelin Inhibits Visceral Afferent Activation of Catecholamine Neurons in the Solitary Tract Nucleus', *Journal of Neuroscience*, 31(9), pp. 3484–3492. doi: 10.1523/JNEUROSCI.3187-10.2011.

D'Agostino, G., Lyons, D. J., Cristiano, C., Burke, L. K., Madara, J. C., Campbell, J. N., Garcia, A. P., Land, B. B., Lowell, B. B., Dileone, R. J. and Heisler, L. K. (2016) 'Appetite controlled by a cholecystokinin nucleus of the solitary tract to

hypothalamus neurocircuit', *eLife*. eLife Sciences Publications Limited, 5, p. e12225. doi: 10.7554/eLife.12225.

Darling, R. A. and Ritter, S. (2009) '2-Deoxy- d -glucose, but not mercaptoacetate, increases food intake in decerebrate rats', *American Journal of Physiology-Regulatory, Integrative and Comparative Physiology*, 297(2), pp. R382–R386. doi: 10.1152/ajpregu.90827.2008.

Dhillon, H., Zigman, J. M., Ye, C., Lee, C. E., McGovern, R. A., Tang, V., Kenny, C. D., Christiansen, L. M., White, R. D., Edelstein, E. A., Coppari, R., Balthasar, N., Cowley, M. A., Chua, S., Elmquist, J. K. and Lowell, B. B. (2006) 'Leptin Directly Activates SF1 Neurons in the VMH, and This Action by Leptin Is Required for Normal Body-Weight Homeostasis', *Neuron*, 49(2), pp. 191–203. doi: 10.1016/j.neuron.2005.12.021.

Diggs-Andrews, K. A., Zhang, X., Song, Z., Daphna-Iken, D., Routh, V. H. and Fisher, S. J. (2010) 'Brain Insulin Action Regulates Hypothalamic Glucose Sensing and the Counterregulatory Response to Hypoglycemia', *Diabetes*, 59(9), pp. 2271–2280. doi: 10.2337/db10-0401.

Dodd, G. T., Decherf, S., Loh, K., Simonds, S. E., Wiede, F., Balland, E., Merry, T. L., Münzberg, H., Zhang, Z.-Y., Kahn, B. B., Neel, B. G., Bence, K. K., Andrews, Z. B., Cowley, M. A. and Tiganis, T. (2015) 'Leptin and Insulin Act on POMC Neurons to Promote the Browning of White Fat', *Cell*, 160(1–2), pp. 88–104. doi: 10.1016/j.cell.2014.12.022.

Dodd, P. R., Edwardson, J. A. and Dockray, G. J. (1980) 'The depolarization-induced release of cholecystokinin C-terminal octapeptide (CCK-8) from rat synaptosomes and brain slices', *Regulatory Peptides*. Elsevier, 1(1), pp. 17–29. doi: 10.1016/0167-0115(80)90003-8.

Dong, H.-W. and Swanson, L. W. (2006) 'Projections from bed nuclei of the stria terminalis, anteromedial area: Cerebral hemisphere integration of neuroendocrine, autonomic, and behavioral aspects of energy balance', *The Journal of Comparative Neurology*, 494(1), pp. 142–178. doi: 10.1002/cne.20788.

Dossat, A. M., Lilly, N., Kay, K. and Williams, D. L. (2011) 'Glucagon-Like Peptide 1 Receptors in Nucleus Accumbens Affect Food Intake', *Journal of Neuroscience*, 31(41), pp. 14453–14457. doi: 10.1523/JNEUROSCI.3262-11.2011.

Draper, S., Kirigiti, M., Glavas, M., Grayson, B., Chong, C. N. A., Jiang, B., Smith, M. S., Zeltser, L. M. and Grove, K. L. (2010) 'Differential gene expression between neuropeptide Y expressing neurons of the dorsomedial nucleus of the hypothalamus and the arcuate nucleus: microarray analysis study.', *Brain research*, 1350, pp. 139–50. doi: 10.1016/j.brainres.2010.03.082.

Dufresne, M., Seva, C. and Fourmy, D. (2006) 'Cholecystokinin and Gastrin Receptors', *Physiological Reviews*, 86(3), pp. 805–847. doi: 10.1152/physrev.00014.2005.

Dyck, W. P., Bonnet, D., Lasater, J., Stinson, C. and Hall, F. F. (1974) 'Hormonal Stimulation of Intestinal Disaccharidase Release in the Dog', *Gastroenterology*. Elsevier, 66(4), pp. 533–538. doi: 10.1016/S0016-5085(74)80041-7.

Egawa, M., Inoue, S., Sato, S., Takamura, Y., Murakami, N. and Takahashi, K. (1991) 'Restoration of circadian corticosterone rhythm in ventromedial hypothalamic lesioned rats.', *Neuroendocrinology*, 53(6), pp. 543–8.

Emson, P. C., Lee, C. M. and Rehfeld, J. F. (1980) 'Cholecystokinin octapeptide: Vesicular localization and calcium dependent release from rat brain in vitro', *Life Sciences*. Pergamon, 26(25), pp. 2157–2163. doi: 10.1016/0024-3205(80)90603-7.

Enriori, P. J., Sinnayah, P., Simonds, S. E., Garcia Rudaz, C. and Cowley, M. A. (2011) 'Leptin Action in the Dorsomedial Hypothalamus Increases Sympathetic Tone to Brown Adipose Tissue in Spite of Systemic Leptin Resistance', *Journal of Neuroscience*, 31(34), pp. 12189–12197. doi: 10.1523/JNEUROSCI.2336-11.2011.

Fan, W., Ellacott, K. L. J., Halatchev, I. G., Takahashi, K., Yu, P. and Cone, R. D. (2004) 'Cholecystokinin-mediated suppression of feeding involves the brainstem melanocortin system', *Nature Neuroscience*, 7(4), pp. 335–336. doi: 10.1038/nn1214.

Farley, C., Cook, J. A., Spar, B. D., Austin, T. M. and Kowalski, T. J. (2003) 'Meal Pattern Analysis of Diet-Induced Obesity in Susceptible and Resistant Rats', *Obesity Research*. Blackwell Publishing Ltd, 11(7), pp. 845–851. doi: 10.1038/oby.2003.116.

Farley, F. W., Soriano, P., Steffen, L. S. and Dymecki, S. M. (2000) 'Widespread recombinase expression using FLPeR (flipper) mice.', *Genesis (New York, N.Y. : 2000)*, 28(3–4), pp. 106–10.

Faulconbridge, L. F., Cummings, D. E., Kaplan, J. M. and Grill, H. J. (2003) 'Hyperphagic Effects of Brainstem Ghrelin Administration', *Diabetes*, 52(9), pp. 2260–2265. doi: 10.2337/diabetes.52.9.2260.

Fioramonti, X., Contie, S., Song, Z., Routh, V. H., Lorsignol, A. and Penicaud, L. (2007) 'Characterization of Glucosensing Neuron Subpopulations in the Arcuate Nucleus: Integration in Neuropeptide Y and Pro-Opio Melanocortin Networks?', *Diabetes*, 56(5), pp. 1219–1227. doi: 10.2337/db06-0567.

Fioramonti, X., Deak, A., Deshpande, S., Carneiro, L., Zhou, C., Sayed, N., Orban, B., Berlin, J. R., Pénicaud, L., Leloup, C., Beuve, A. and Routh, V. H. (2013) 'Hypothalamic S-Nitrosylation Contributes to the Counter-Regulatory Response Impairment following Recurrent Hypoglycemia', *PLoS ONE*. Edited by C. Gaetano, 8(7), p. e68709. doi: 10.1371/journal.pone.0068709.

Fioramonti, X., Lorsignol, A., Taupignon, A. and Pénicaud, L. (2004) 'A new ATP-sensitive K+ channel-independent mechanism is involved in glucose-excited neurons of mouse arcuate nucleus.', *Diabetes*, 53(11), pp. 2767–75.

Fioramonti, X., Marsollier, N., Song, Z., Fakira, K. A., Patel, R. M., Brown, S., Duparc, T., Pica-Mendez, A., Sanders, N. M., Knauf, C., Valet, P., McCrimmon, R. J., Beuve, A., Magnan, C. and Routh, V. H. (2010) 'Ventromedial Hypothalamic Nitric Oxide Production Is Necessary for Hypoglycemia Detection and Counterregulation', *Diabetes*, 59(2), pp. 519–528. doi: 10.2337/db09-0421.

Le Foll, C., Dunn-Meynell, A. A., Miziorko, H. M. and Levin, B. E. (2014) 'Regulation of Hypothalamic Neuronal Sensing and Food Intake by Ketone Bodies and Fatty Acids', *Diabetes*, 63(4), pp. 1259–1269. doi: 10.2337/db13-1090.

Freund, T. F. (2003) 'Interneuron Diversity series: Rhythm and mood in perisomatic inhibition.', *Trends in neurosciences*, 26(9), pp. 489–95. doi: 10.1016/S0166-2236(03)00227-3.

Freund, T. F. and Katona, I. (2007) 'Perisomatic inhibition.', *Neuron*, 56(1), pp. 33–42. doi: 10.1016/j.neuron.2007.09.012.

Frommelt, L., Lembke, V., Hofmann, T., Goebel-Stengel, M., Mönnikes, H., Wiedenmann, B., Klapp, B. F., Stengel, A. and Kobelt, P. (2013) 'The CCKB antagonist CI988 reduces food intake in fasted rats via a dopamine mediated pathway', *Peptides*, 39, pp. 111–118. doi: 10.1016/j.peptides.2012.11.012.

Fujimoto, S. (1980) 'The effect of prostaglandin E2 microinjected into the rat hypothalamus on urinary excretion of water and sodium.', *British journal of pharmacology*, 70(3), pp. 415–7.

Gage, G. J., Kipke, D. R. and Shain, W. (2012) 'Whole animal perfusion fixation for rodents.', *Journal of visualized experiments : JoVE*, (65), pp. 1–9. doi: 10.3791/3564.

Gao, S., Kinzig, K. P., Aja, S., Scott, K. A., Keung, W., Kelly, S., Strynadka, K., Chohnan, S., Smith, W. W., Tamashiro, K. L. K., Ladenheim, E. E., Ronnett, G. V., Tu, Y., Birnbaum, M. J., Lopaschuk, G. D. and Moran, T. H. (2007) 'Leptin activates hypothalamic acetyl-CoA carboxylase to inhibit food intake', *Proceedings of the National Academy of Sciences*, 104(44), pp. 17358–17363. doi: 10.1073/pnas.0708385104.

Garfield, A. S., Li, C., Madara, J. C., Shah, B. P., Webber, E., Steger, J. S., Campbell, J. N., Gavrilova, O., Lee, C. E., Olson, D. P., Elmquist, J. K., Tannous, B. A., Krashes, M. J. and Lowell, B. B. (2015) 'A neural basis for melanocortin-4 receptor–regulated appetite', *Nature Neuroscience*. Nature Publishing Group, 18(6), pp. 863–871. doi: 10.1038/nn.4011.

Garfield, A. S., Patterson, C., Skora, S., Gribble, F. M., Reimann, F., Evans, M. L., Myers, M. G. and Heisler, L. K. (2012) 'Neurochemical characterization of body weight-regulating leptin receptor neurons in the nucleus of the solitary tract', *Endocrinology*, 153(10), pp. 4600–4607. doi: 10.1210/en.2012-1282.

Garfield, A. S., Shah, B. P., Madara, J. C., Burke, L. K., Patterson, C. M., Flak, J., Neve, R. L., Evans, M. L., Lowell, B. B., Myers Jr., M. G., Heisler, L. K., Myers, M. G. and Heisler, L. K. (2014) 'A Parabrachial-Hypothalamic Cholecystokinin Neurocircuit Controls Counterregulatory Responses to Hypoglycemia', *Cell Metabolism*. Elsevier Inc., 20(6), pp. 1030–1037. doi: 10.1016/j.cmet.2014.11.006.

Garlicki, J., Konturek, P. K., Majka, J., Kwiecien, N. and Konturek, S. J.

(1990) ‘Cholecystokinin receptors and vagal nerves in control of food intake in rats’, *American Journal of Physiology-Endocrinology and Metabolism*, 258(1), pp. E40–E45. doi: 10.1152/ajpendo.1990.258.1.E40.

Geibel, M., Badurek, S., Horn, J. M., Vatanashevanopakorn, C., Koudelka, J., Wunderlich, C. M., Brönneke, H. S., Wunderlich, F. T. and Minichiello, L. (2014) ‘Ablation of TrkB signalling in CCK neurons results in hypercortisolism and obesity.’, *Nature communications*, 5, p. 3427. doi: 10.1038/ncomms4427.

Giacobini, P. and Wray, S. (2008) ‘Prenatal expression of cholecystokinin (CCK) in the central nervous system (CNS) of mouse’, *Neuroscience Letters*, 438(1), pp. 96–101. doi: 10.1016/j.neulet.2008.04.042.

Gibbs, J., Young, R. C. and Smith, G. P. (1973) ‘Cholecystokinin elicits satiety in rats with open gastric fistulas.’, *Nature*, 245(5424), pp. 323–5.

Goebel-Stengel, M., Stengel, A., Wang, L., Ohning, G., Taché, Y. and Reeve, J. R. (2012) ‘CCK-8 and CCK-58 differ in their effects on nocturnal solid meal pattern in undisturbed rats’, *American Journal of Physiology-Regulatory, Integrative and Comparative Physiology*, 303(8), pp. R850–R860. doi: 10.1152/ajpregu.00365.2011.

Gomez, J. L., Bonaventura, J., Lesniak, W., Mathews, W. B., Sysa-Shah, P., Rodriguez, L. A., Ellis, R. J., Richie, C. T., Harvey, B. K., Dannals, R. F., Pomper, M. G., Bonci, A. and Michaelides, M. (2017) ‘Chemogenetics revealed: DREADD occupancy and activation via converted clozapine.’, *Science (New York, N.Y.)*. American Association for the Advancement of Science, 357(6350), pp. 503–507. doi: 10.1126/science.aan2475.

González, J. A., Jensen, L. T., Doyle, S. E., Miranda-Anaya, M., Menaker, M., Fugger, L., Bayliss, D. A. and Burdakov, D. (2009) ‘Deletion of TASK1 and TASK3 channels disrupts intrinsic excitability but does not abolish glucose or pH responses of orexin/hypocretin neurons’, *European Journal of Neuroscience*, 30(1), pp. 57–64. doi: 10.1111/j.1460-9568.2009.06789.x.

Gonzalez, J. A., Jensen, L. T., Fugger, L. and Burdakov, D. (2008) ‘Metabolism-Independent Sugar Sensing in Central Orexin Neurons’, *Diabetes*, 57(10), pp. 2569–2576. doi: 10.2337/db08-0548.

Grill, H. J. and Hayes, M. R. (2012) 'Hindbrain Neurons as an Essential Hub in the Neuroanatomically Distributed Control of Energy Balance', *Cell Metabolism*. Cell Press, 16(3), pp. 296–309. doi: 10.1016/J.CMET.2012.06.015.

Gropp, E., Shanabrough, M., Borok, E., Xu, A. W., Janoschek, R., Buch, T., Plum, L., Balthasar, N., Hampel, B., Waisman, A., Barsh, G. S., Horvath, T. L. and Brüning, J. C. (2005) 'Agouti-related peptide–expressing neurons are mandatory for feeding', *Nature Neuroscience*, 8(10), pp. 1289–1291. doi: 10.1038/nn1548.

Gutierrez, R., Carmena, J. M., Nicolelis, M. A. L. and Simon, S. A. (2006) 'Orbitofrontal Ensemble Activity Monitors Licking and Distinguishes Among Natural Rewards', *Journal of Neurophysiology*, 95(1), pp. 119–133. doi: 10.1152/jn.00467.2005.

Hayes, M. R. and Covasa, M. (2005) 'CCK and 5-HT act synergistically to suppress food intake through simultaneous activation of CCK-1 and 5-HT3 receptors', *Peptides*, 26(11), pp. 2322–2330. doi: 10.1016/j.peptides.2005.03.045.

Hayes, M. R., Leichner, T. M., Zhao, S., Lee, G. S., Chowansky, A., Zimmer, D., De Jonghe, B. C., Kanoski, S. E., Grill, H. J. and Bence, K. K. (2011) 'Intracellular Signals Mediating the Food Intake-Suppressive Effects of Hindbrain Glucagon-like Peptide-1 Receptor Activation', *Cell Metabolism*, 13(3), pp. 320–330. doi: 10.1016/j.cmet.2011.02.001.

Hayes, M. R., Skibicka, K. P. and Grill, H. J. (2008) 'Caudal Brainstem Processing Is Sufficient for Behavioral, Sympathetic, and Parasympathetic Responses Driven by Peripheral and Hindbrain Glucagon-Like-Peptide-1 Receptor Stimulation', *Endocrinology*. Oxford University Press, 149(8), pp. 4059–4068. doi: 10.1210/en.2007-1743.

Hayes, M. R., Skibicka, K. P., Leichner, T. M., Guarnieri, D. J., DiLeone, R. J., Bence, K. K. and Grill, H. J. (2010) 'Endogenous Leptin Signaling in the Caudal Nucleus Tractus Solitarius and Area Postrema Is Required for Energy Balance Regulation', *Cell Metabolism*. Elsevier Ltd, 11(1), pp. 77–83. doi: 10.1016/j.cmet.2009.10.009.

Hendry, S. H., Jones, E. G., DeFelipe, J., Schmechel, D., Brandon, C. and Emson, P. C. (1984) 'Neuropeptide-containing neurons of the cerebral cortex are also GABAergic.', *Proceedings of the National Academy of Sciences of the United*

*States of America*, 81(20), pp. 6526–30.

Herman, J. P., Tasker, J. G., Ziegler, D. R. and Cullinan, W. E. (2002) 'Local circuit regulation of paraventricular nucleus stress integration: glutamate-GABA connections.', *Pharmacology, biochemistry, and behavior*, 71(3), pp. 457–468.

Hetherington, A. W. and Ranson, S. W. (1940) 'Hypothalamic lesions and adiposity in the rat', *The Anatomical Record*. Wiley Subscription Services, Inc., A Wiley Company, 78(2), pp. 149–172. doi: 10.1002/ar.1090780203.

Hill, J. W., Elias, C. F., Fukuda, M., Williams, K. W., Berglund, E. D., Holland, W. L., Cho, Y.-R., Chuang, J.-C., Xu, Y., Choi, M., Lauzon, D., Lee, C. E., Coppari, R., Richardson, J. A., Zigman, J. M., Chua, S., Scherer, P. E., Lowell, B. B., Brüning, J. C. and Elmquist, J. K. (2010) 'Direct Insulin and Leptin Action on Pro-opiomelanocortin Neurons Is Required for Normal Glucose Homeostasis and Fertility', *Cell Metabolism*, 11(4), pp. 286–297. doi: 10.1016/j.cmet.2010.03.002.

Himeno, S., Tarui, S., Kanayama, S., Kuroshima, T., Shinomura, Y., Hayashi, C., Tateishi, K., Imagawa, K., Hashimura, E. and Hamaoka, T. (1983) 'Plasma cholecystokinin responses after ingestion of liquid meal and intraduodenal infusion of fat, amino acids, or hydrochloric acid in man: analysis with region specific radioimmunoassay.', *The American journal of gastroenterology*, 78(11), pp. 703–7.

Hinney, A., Schmidt, A., Nottebom, K., Heibült, O., Becker, I., Ziegler, A., Gerber, G., Sina, M., Görg, T., Mayer, H., Siegfried, W., Fichter, M., Remschmidt, H. and Hebebrand, J. (1999) 'Several Mutations in the Melanocortin-4 Receptor Gene Including a Nonsense and a Frameshift Mutation Associated with Dominantly Inherited Obesity in Humans', *The Journal of Clinical Endocrinology & Metabolism*. Oxford University Press, 84(4), pp. 1483–1486. doi: 10.1210/jcem.84.4.5728.

Hisadome, K., Reimann, F., Gribble, F. M. and Trapp, S. (2010) 'Leptin Directly Depolarizes Preproglucagon Neurons in the Nucleus Tractus Solitarius', *Diabetes*, 59(8), pp. 1890–1898. doi: 10.2337/db10-0128.

Hisadome, K., Reimann, F., Gribble, F. M. and Trapp, S. (2011) 'CCK Stimulation of GLP-1 Neurons Involves $\alpha_1$-Adrenoceptor–Mediated Increase in Glutamatergic Synaptic Inputs', *Diabetes*, 60(11), pp. 2701–2709. doi: 10.2337/db11-0489.

Hökfelt, T., Skirboll, L., Everitt, B., Meister, B., Brownstein, M., Jacobs, T., Faden, A., Kuga, S., Goldstein, M. and Markstein, R. (1985) 'Distribution of cholecystokinin-like immunoreactivity in the nervous system. Co-existence with classical neurotransmitters and other neuropeptides.', *Annals of the New York Academy of Sciences*, 448, pp. 255–74.

Horinouchi, Y., Akiyoshi, J., Nagata, A., Matsushita, H., Tsutsumi, T., Isogawa, K., Noda, T. and Nagayama, H. (2004) 'Reduced anxious behavior in mice lacking the CCK2 receptor gene', *European Neuropsychopharmacology*, 14(2), pp. 157–161. doi: 10.1016/S0924-977X(03)00103-2.

Huszar, D., Lynch, C. A., Fairchild-Huntress, V., Dunmore, J. H., Fang, Q., Berkemeier, L. R., Gu, W., Kesterson, R. A., Boston, B. A., Cone, R. D., Smith, F. J., Campfield, L. A., Burn, P. and Lee, F. (1997) 'Targeted Disruption of the Melanocortin-4 Receptor Results in Obesity in Mice', *Cell*, 88(1), pp. 131–141. doi: 10.1016/S0092-8674(00)81865-6.

Ikeda, Y., Luo, X., Abbud, R., Nilson, J. H. and Parker, K. L. (1995) 'The nuclear receptor steroidogenic factor 1 is essential for the formation of the ventromedial hypothalamic nucleus.', *Molecular Endocrinology*, 9(4), pp. 478–486. doi: 10.1210/mend.9.4.7659091.

Ionescu, E., Rohner-Jeanrenaud, F., Berthoud, H.-R. and Jeanrenaud, B. (1983) 'Increases in Plasma Insulin Levels in Response to Electrical Stimulation of the Dorsal Motor Nucleus of the Vagus Nerve*', *Endocrinology*. Oxford University Press, 112(3), pp. 904–910. doi: 10.1210/endo-112-3-904.

Jasnow, A. M., Ressler, K. J., Hammack, S. E., Chhatwal, J. P. and Rainnie, D. G. (2009) 'Distinct subtypes of cholecystokinin (CCK)-containing interneurons of the basolateral amygdala identified using a CCK promoter-specific lentivirus.', *Journal of neurophysiology*. American Physiological Society, 101(3), pp. 1494–506. doi: 10.1152/jn.91149.2008.

Jiang, C., Fogel, R. and Zhang, X. (2003) 'Lateral hypothalamus modulates gut-sensitive neurons in the dorsal vagal complex', *Brain Research*, 980(1), pp. 31–47. doi: 10.1016/S0006-8993(03)02844-0.

De Jonghe, B. C., Hajnal, A. and Covasa, M. (2005) 'Increased oral and decreased intestinal sensitivity to sucrose in obese, prediabetic CCK-A receptor-

deficient OLETF rats', *American Journal of Physiology-Regulatory, Integrative and Comparative Physiology*, 288(1), pp. R292–R300. doi: 10.1152/ajpregu.00481.2004.

Jordan, S. D., Könner, A. C. and Brüning, J. C. (2010) 'Sensing the fuels: glucose and lipid signaling in the CNS controlling energy homeostasis', *Cellular and Molecular Life Sciences*. SP Birkhäuser Verlag Basel, 67(19), pp. 3255–3273. doi: 10.1007/s00018-010-0414-7.

Joseph, S. A., Pilcher, W. H. and Bennett-Clarke, C. (1983) 'Immunocytochemical localization of ACTH perikarya in nucleus tractus solitarius: evidence for a second opiocortin neuronal system.', *Neuroscience letters*, 38(3), pp. 221–5.

Kang, L., Dunn-Meynell, A. A., Routh, V. H., Gaspers, L. D., Nagata, Y., Nishimura, T., Eiki, J., Zhang, B. B. and Levin, B. E. (2006) 'Glucokinase is a critical regulator of ventromedial hypothalamic neuronal glucosensing.', *Diabetes*, 55(2), pp. 412–20.

Kang, L., Routh, V. H., Kuzhikandathil, E. V, Gaspers, L. D. and Levin, B. E. (2004) 'Physiological and molecular characteristics of rat hypothalamic ventromedial nucleus glucosensing neurons.', *Diabetes*, 53(3), pp. 549–59.

Kannan, H., Hayashida, Y. and Yamashita, H. (1989) 'Increase in sympathetic outflow by paraventricular nucleus stimulation in awake rats', *American Journal of Physiology-Regulatory, Integrative and Comparative Physiology*, 256(6), pp. R1325–R1330. doi: 10.1152/ajpregu.1989.256.6.R1325.

Kanoski, S. E., Zhao, S., Guarnieri, D. J., DiLeone, R. J., Yan, J., De Jonghe, B. C., Bence, K. K., Hayes, M. R. and Grill, H. J. (2012) 'Endogenous leptin receptor signaling in the medial nucleus tractus solitarius affects meal size and potentiates intestinal satiation signals', *American Journal of Physiology-Endocrinology and Metabolism*. American Physiological Society Bethesda, MD, 303(4), pp. E496–E503. doi: 10.1152/ajpendo.00205.2012.

Karnani, M. M., Szabó, G., Erdélyi, F. and Burdakov, D. (2013) 'Lateral hypothalamic GAD65 neurons are spontaneously firing and distinct from orexin- and melanin-concentrating hormone neurons', *The Journal of Physiology*, 591(4), pp. 933–953. doi: 10.1113/jphysiol.2012.243493.

Kim, K. W., Donato, J., Berglund, E. D., Choi, Y.-H., Kohno, D., Elias, C. F., DePinho, R. A. and Elmquist, J. K. (2012) 'FOXO1 in the ventromedial hypothalamus regulates energy balance', *Journal of Clinical Investigation*, 122(7), pp. 2578–2589. doi: 10.1172/JCI62848.

Kim, K. W., Sohn, J.-W., Kohno, D., Xu, Y., Williams, K. and Elmquist, J. K. (2011) 'SF-1 in the ventral medial hypothalamic nucleus: A key regulator of homeostasis', *Molecular and Cellular Endocrinology*, 336(1–2), pp. 219–223. doi: 10.1016/j.mce.2010.11.019.

Kim, M. S., Small, C. J., Stanley, S. ., Morgan, D. G. A., Seal, L. J., Kong, W. M., Edwards, C. M. B., Abusnana, S., Sunter, D., Ghatei, M. A. and Bloom, S. R. (2000) 'The central melanocortin system affects the hypothalamo-pituitary thyroid axis and may mediate the effect of leptin', *Journal of Clinical Investigation*, 105(7), pp. 1005–1011. doi: 10.1172/JCI8857.

King, B. M. (2006) 'The rise, fall, and resurrection of the ventromedial hypothalamus in the regulation of feeding behavior and body weight', *Physiology & Behavior*, 87(2), pp. 221–244. doi: 10.1016/j.physbeh.2005.10.007.

Kishi, T., Aschkenasi, C. J., Lee, C. E., Mountjoy, K. G., Saper, C. B. and Elmquist, J. K. (2003) 'Expression of melanocortin 4 receptor mRNA in the central nervous system of the rat', *The Journal of Comparative Neurology*. Wiley Subscription Services, Inc., A Wiley Company, 457(3), pp. 213–235. doi: 10.1002/cne.10454.

Kleinridders, A., Könner, A. C. and Brüning, J. C. (2009) 'CNS-targets in control of energy and glucose homeostasis', *Current Opinion in Pharmacology*, 9(6), pp. 794–804. doi: 10.1016/j.coph.2009.10.006.

Klöckener, T., Hess, S., Belgardt, B. F., Paeger, L., Verhagen, L. A. W., Husch, A., Sohn, J.-W., Hampel, B., Dhillon, H., Zigman, J. M., Lowell, B. B., Williams, K. W., Elmquist, J. K., Horvath, T. L., Kloppenburg, P. and Brüning, J. C. (2011) 'High-fat feeding promotes obesity via insulin receptor/PI3K-dependent inhibition of SF-1 VMH neurons', *Nature Neuroscience*, 14(7), pp. 911–918. doi: 10.1038/nn.2847.

Koch, M., Varela, L., Kim, J. G., Kim, J. D., Hernández-Nuño, F., Simonds, S. E., Castorena, C. M., Vianna, C. R., Elmquist, J. K., Morozov, Y. M., Rakic, P.,

Bechmann, I., Cowley, M. A., Szigeti-Buck, K., Dietrich, M. O., Gao, X.-B., Diano, S. and Horvath, T. L. (2015) 'Hypothalamic POMC neurons promote cannabinoid-induced feeding', *Nature*. Nature Publishing Group, 519(7541), pp. 45–50. doi: 10.1038/nature14260.

Kohno, D., Gao, H.-Z., Muroya, S., Kikuyama, S. and Yada, T. (2003) 'Ghrelin directly interacts with neuropeptide-Y-containing neurons in the rat arcuate nucleus: Ca2+ signaling via protein kinase A and N-type channel-dependent mechanisms and cross-talk with leptin and orexin.', *Diabetes*, 52(4), pp. 948–56.

Koizumi, S., Shigemoto-Mogami, Y., Nasu-Tada, K., Shinozaki, Y., Ohsawa, K., Tsuda, M., Joshi, B. V., Jacobson, K. A., Kohsaka, S. and Inoue, K. (2007) 'UDP acting at P2Y6 receptors is a mediator of microglial phagocytosis', *Nature*. Nature Publishing Group, 446(7139), pp. 1091–1095. doi: 10.1038/nature05704.

Könner, A. C., Janoschek, R., Plum, L., Jordan, S. D., Rother, E., Ma, X., Xu, C., Enriori, P., Hampel, B., Barsh, G. S., Kahn, C. R., Cowley, M. A., Ashcroft, F. M. and Brüning, J. C. (2007) 'Insulin Action in AgRP-Expressing Neurons Is Required for Suppression of Hepatic Glucose Production', *Cell Metabolism*, 5(6), pp. 438–449. doi: 10.1016/j.cmet.2007.05.004.

Könner, A. C., Klöckener, T. and Brüning, J. C. (2009) 'Control of energy homeostasis by insulin and leptin: Targeting the arcuate nucleus and beyond', *Physiology & Behavior*, 97(5), pp. 632–638. doi: 10.1016/j.physbeh.2009.03.027.

Krashes, M. J., Koda, S., Ye, C., Rogan, S. C., Adams, A. C., Cusher, D. S., Maratos-Flier, E., Roth, B. L. and Lowell, B. B. (2011) 'Rapid, reversible activation of AgRP neurons drives feeding behavior in mice', *Journal of Clinical Investigation*, 121(4), pp. 1424–1428. doi: 10.1172/JCI46229.

Krashes, M. J., Shah, B. P., Madara, J. C., Olson, D. P., Strochlic, D. E., Garfield, A. S., Vong, L., Pei, H., Watabe-Uchida, M., Uchida, N., Liberles, S. D. and Lowell, B. B. (2014) 'An excitatory paraventricular nucleus to AgRP neuron circuit that drives hunger', *Nature*, 507(7491), pp. 238–242. doi: 10.1038/nature12956.

Kurrasch, D. M., Cheung, C. C., Lee, F. Y., Tran, P. V, Hata, K. and Ingraham, H. A. (2007) 'The neonatal ventromedial hypothalamus transcriptome reveals novel markers with spatially distinct patterning.', *The Journal of neuroscience : the official journal of the Society for Neuroscience*. Society for

Neuroscience, 27(50), pp. 13624–34. doi: 10.1523/JNEUROSCI.2858-07.2007.

Lam, T. K. T., Pocai, A., Gutierrez-Juarez, R., Obici, S., Bryan, J., Aguilar-Bryan, L., Schwartz, G. J. and Rossetti, L. (2005) 'Hypothalamic sensing of circulating fatty acids is required for glucose homeostasis', *Nature Medicine*, 11(3), pp. 320–327. doi: 10.1038/nm1201.

Langlet, F., Levin, B. E., Luquet, S., Mazzone, M., Messina, A., Dunn-Meynell, A. A., Balland, E., Lacombe, A., Mazur, D., Carmeliet, P., Bouret, S. G., Prevot, V. and Dehouck, B. (2013) 'Tanycytic VEGF-A Boosts Blood-Hypothalamus Barrier Plasticity and Access of Metabolic Signals to the Arcuate Nucleus in Response to Fasting', *Cell Metabolism*, 17(4), pp. 607–617. doi: 10.1016/j.cmet.2013.03.004.

Larsson, L. I. and Rehfeld, J. F. (1979) 'Localization and molecular heterogeneity of cholecystokinin in the central and peripheral nervous system.', *Brain research*, 165(2), pp. 201–18.

Leibowitz, S. F., Hammer, N. J. and Chang, K. (1981) 'Hypothalamic paraventricular nucleus lesions produce overeating and obesity in the rat.', *Physiology & behavior*, 27(6), pp. 1031–40.

Li, Y., Liu, L., Liu, D., Woodward, S., Barger, S. W., Mrak, R. E. and Griffin, W. S. T. (2004) 'Microglial activation by uptake of fDNA via a scavenger receptor.', *Journal of neuroimmunology*. NIH Public Access, 147(1–2), pp. 50–5.

Liao, G.-Y., An, J. J., Gharami, K., Waterhouse, E. G., Vanevski, F., Jones, K. R. and Xu, B. (2012) 'Dendritically targeted Bdnf mRNA is essential for energy balance and response to leptin', *Nature Medicine*, 18(4), pp. 564–571. doi: 10.1038/nm.2687.

Liddle, R. A., Goldfine, I. D., Rosen, M. S., Taplitz, R. A. and Williams, J. A. (1985) 'Cholecystokinin bioactivity in human plasma. Molecular forms, responses to feeding, and relationship to gallbladder contraction.', *Journal of Clinical Investigation*, 75(4), pp. 1144–1152. doi: 10.1172/JCI111809.

Lieverse, R. J., Jansen, J. B., Masclee, A. A. and Lamers, C. B. (1995) 'Satiety effects of a physiological dose of cholecystokinin in humans.', *Gut*, 36(2), pp. 176–9.

Liu, H., Kishi, T., Roseberry, A. G., Cai, X., Lee, C. E., Montez, J. M., Friedman, J. M. and Elmquist, J. K. (2003) 'Transgenic mice expressing green fluorescent protein under the control of the melanocortin-4 receptor promoter', 23(18), pp. 7143–7154.

Liu, H., Kishi, T., Roseberry, A. G., Cai, X., Lee, C. E., Montez, J. M., Friedman, J. M., Elmquist, J. K., Childs, G., Elmquist, J. K., Parker, K. L. and Friedman, J. M. (2003) 'Transgenic mice expressing green fluorescent protein under the control of the melanocortin-4 receptor promoter.', *The Journal of neuroscience : the official journal of the Society for Neuroscience*. Society for Neuroscience, 23(18), pp. 7143–54. doi: 10.1523/jneurosci.0158-05.2005.

Loh, K., Herzog, H. and Shi, Y.-C. (2015) 'Regulation of energy homeostasis by the NPY system', *Trends in Endocrinology & Metabolism*. Elsevier Current Trends, 26(3), pp. 125–135. doi: 10.1016/J.TEM.2015.01.003.

Lu, X.-Y., Barsh, G. S., Akil, H. and Watson, S. J. (2003) 'Interaction between alpha-melanocyte-stimulating hormone and corticotropin-releasing hormone in the regulation of feeding and hypothalamo-pituitary-adrenal responses.', *The Journal of neuroscience : the official journal of the Society for Neuroscience*, 23(21), pp. 7863–72.

MacLaren, D. A. A., Browne, R. W., Shaw, J. K., Krishnan Radhakrishnan, S., Khare, P., España, R. A. and Clark, S. D. (2016) 'Clozapine N-Oxide Administration Produces Behavioral Effects in Long-Evans Rats: Implications for Designing DREADD Experiments.', *eNeuro*. Society for Neuroscience, 3(5). doi: 10.1523/ENEURO.0219-16.2016.

Madisen, L., Zwingman, T. A., Sunkin, S. M., Oh, S. W., Hatim, A., Gu, H., Ng, L. L., Palmiter, R. D., Hawrylycz, M. J., Allan, R., Lein, E. S. and Zeng, H. (2010) 'NIH Public Access', 13(1), pp. 133–140. doi: 10.1038/nn.2467.A.

Maejima, Y., Sedbazar, U., Suyama, S., Kohno, D., Onaka, T., Takano, E., Yoshida, N., Koike, M., Uchiyama, Y., Fujiwara, K., Yashiro, T., Horvath, T. L., Dietrich, M. O., Tanaka, S., Dezaki, K., Hashimoto, K., Shimizu, H., Nakata, M., Mori, M. and Yada, T. (2009) 'Nesfatin-1-Regulated Oxytocinergic Signaling in the Paraventricular Nucleus Causes Anorexia through a Leptin-Independent Melanocortin Pathway', *Cell Metabolism*, 10(5), pp. 355–365. doi:

10.1016/j.cmet.2009.09.002.

Majdic, G., Young, M., Gomez-Sanchez, E., Anderson, P., Szczepaniak, L. S., Dobbins, R. L., McGarry, J. D. and Parker, K. L. (2002) 'Knockout Mice Lacking Steroidogenic Factor 1 Are a Novel Genetic Model of Hypothalamic Obesity', *Endocrinology*. Oxford University Press, 143(2), pp. 607–614. doi: 10.1210/endo.143.2.8652.

Marsollier, N., Kassis, N., Mezghenna, K., Soty, M., Fioramonti, X., Lacombe, A., Joly, A., Pillot, B., Zitoun, C., Vilar, J., Mithieux, G., Gross, R., Lajoix, A.-D., Routh, V., Magnan, C. and Cruciani-Guglielmacci, C. (2009) 'Deregulation of Hepatic Insulin Sensitivity Induced by Central Lipid Infusion in Rats Is Mediated by Nitric Oxide', *PLoS ONE*. Edited by C. Polidori, 4(8), p. e6649. doi: 10.1371/journal.pone.0006649.

Marston, O. J., Hurst, P., Evans, M. L., Burdakov, D. I. and Heisler, L. K. (2011) 'Neuropeptide Y Cells Represent a Distinct Glucose-Sensing Population in the Lateral Hypothalamus', *Endocrinology*, 152(11), pp. 4046–4052. doi: 10.1210/en.2011-1307.

Mascagni, F. and McDonald, A. J. (2003) 'Immunohistochemical characterization of cholecystokinin containing neurons in the rat basolateral amygdala.', *Brain research*, 976(2), pp. 171–84.

Mascagni, F. and McDonald, A. J. (2007) 'A novel subpopulation of 5-HT type 3A receptor subunit immunoreactive interneurons in the rat basolateral amygdala', *Neuroscience*, 144(3), pp. 1015–1024. doi: 10.1016/j.neuroscience.2006.10.044.

Mayer, J. (1953) 'Glucostatic Mechanism of Regulation of Food Intake', *New England Journal of Medicine*. Massachusetts Medical Society , 249(1), pp. 13–16. doi: 10.1056/NEJM195307022490104.

Mazda, T., Yamamoto, H., Fujimura, M. and Fujimiya, M. (2004) 'Gastric distension-induced release of 5-HT stimulates c- *fos* expression in specific brain nuclei via 5-HT3 receptors in conscious rats', *American Journal of Physiology-Gastrointestinal and Liver Physiology*, 287(1), pp. G228–G235. doi: 10.1152/ajpgi.00373.2003.

McClellan, K., Parker, K. and Tobet, S. (2006) 'Development of the

ventromedial nucleus of the hypothalamus', *Frontiers in Neuroendocrinology*, 27(2), pp. 193–209. doi: 10.1016/j.yfrne.2006.02.002.

Melnick, I. V., Price, C. J. and Colmers, W. F. (2011) 'Glucosensing in parvocellular neurons of the rat hypothalamic paraventricular nucleus', *European Journal of Neuroscience*, 34(2), pp. 272–282. doi: 10.1111/j.1460-9568.2011.07742.x.

Mercer, J. G., Hoggard, N., Williams, L. M., Lawrence, C. B., Hannah, L. T. and Trayhurn, P. (1996) 'Localization of leptin receptor mRNA and the long form splice variant (Ob-Rb) in mouse hypothalamus and adjacent brain regions by in situ hybridization.', *FEBS letters*, 387(2–3), pp. 113–6.

Milam, K. M., Stern, J. S., Storlien, L. H. and Keesey, R. E. (1980) 'Effect of lateral hypothalamic lesions on regulation of body weight and adiposity in rats', *American Journal of Physiology-Regulatory, Integrative and Comparative Physiology*, 239(3), pp. R337–R343. doi: 10.1152/ajpregu.1980.239.3.R337.

Moran, T. H., Katz, L. F., Plata-Salaman, C. R. and Schwartz, G. J. (1998) 'Disordered food intake and obesity in rats lacking cholecystokinin A receptors.', *The American journal of physiology*, 274(3 Pt 2), pp. R618-25.

Moran, T. H. and McHugh, P. R. (1982) 'Cholecystokinin suppresses food intake by inhibiting gastric emptying', 11(3).

Morozov, Y. M., Torii, M. and Rakic, P. (2009) 'Origin, early commitment, migratory routes, and destination of cannabinoid type 1 receptor-containing interneurons.', *Cerebral cortex (New York, N.Y. : 1991)*, 19 Suppl 1(suppl_1), pp. i78-89. doi: 10.1093/cercor/bhp028.

Morrison, S. F. (1999) 'RVLM and raphe differentially regulate sympathetic outflows to splanchnic and brown adipose tissue.', *The American journal of physiology*, 276(4 Pt 2), pp. R962-73.

Morton, G. J., Gelling, R. W., Niswender, K. D., Morrison, C. D., Rhodes, C. J. and Schwartz, M. W. (2005) 'Leptin regulates insulin sensitivity via phosphatidylinositol-3-OH kinase signaling in mediobasal hypothalamic neurons', *Cell Metabolism*, 2(6), pp. 411–420. doi: 10.1016/j.cmet.2005.10.009.

Mullier, A., Bouret, S. G., Prevot, V. and Dehouck, B. (2010) 'Differential

distribution of tight junction proteins suggests a role for tanycytes in blood-hypothalamus barrier regulation in the adult mouse brain', *The Journal of Comparative Neurology*, 518(7), pp. 943–962. doi: 10.1002/cne.22273.

Murphy, B. A., Fakira, K. A., Song, Z., Beuve, A. and Routh, V. H. (2009) 'AMP-activated protein kinase and nitric oxide regulate the glucose sensitivity of ventromedial hypothalamic glucose-inhibited neurons', *American Journal of Physiology-Cell Physiology*, 297(3), pp. C750–C758. doi: 10.1152/ajpcell.00127.2009.

Murphy, B. A., Fioramonti, X., Jochnowitz, N., Fakira, K., Gagen, K., Contie, S., Lorsignol, A., Penicaud, L., Martin, W. J. and Routh, V. H. (2009) 'Fasting enhances the response of arcuate neuropeptide Y-glucose-inhibited neurons to decreased extracellular glucose', *American Journal of Physiology-Cell Physiology*, 296(4), pp. C746–C756. doi: 10.1152/ajpcell.00641.2008.

Musatov, S., Chen, W., Pfaff, D. W., Mobbs, C. V., Yang, X.-J., Clegg, D. J., Kaplitt, M. G. and Ogawa, S. (2007) 'Silencing of estrogen receptor in the ventromedial nucleus of hypothalamus leads to metabolic syndrome', *Proceedings of the National Academy of Sciences*, 104(7), pp. 2501–2506. doi: 10.1073/pnas.0610787104.

Mutt, V. and Jorpes, J. E. (1968) 'Structure of porcine cholecystokinin-pancreozymin. 1. Cleavage with thrombin and with trypsin.', *European journal of biochemistry*, 6(1), pp. 156–62.

Myers, M. G. and Olson, D. P. (2012) 'Central nervous system control of metabolism', *Nature*, 491(7424), pp. 357–363. doi: 10.1038/nature11705.

Nakajima, K., Cui, Z., Li, C., Meister, J., Cui, Y., Fu, O., Smith, A. S., Jain, S., Lowell, B. B., Krashes, M. J. and Wess, J. (2016) 'Gs-coupled GPCR signalling in AgRP neurons triggers sustained increase in food intake', *Nature Communications*. Nature Publishing Group, 7, p. 10268. doi: 10.1038/ncomms10268.

Nicholson, J. R., Peter, J.-C., Lecourt, A.-C., Barde, Y.-A. and Hofbauer, K. G. (2007) 'Melanocortin-4 Receptor Activation Stimulates Hypothalamic Brain-Derived Neurotrophic Factor Release to Regulate Food Intake, Body Temperature and Cardiovascular Function', *Journal of Neuroendocrinology*, 19(12), pp. 974–982. doi: 10.1111/j.1365-2826.2007.01610.x.

Norgren, R., Hajnal, A. and Mungarndee, S. S. (2006) 'Gustatory reward and the nucleus accumbens', *Physiology & Behavior*. Elsevier Inc., 89(4), pp. 531–535. doi: 10.1016/j.physbeh.2006.05.024.

Nunzi, M. G., Gorio, A., Milan, F., Freund, T. F., Somogyi, P. and Smith, A. D. (1985) 'Cholecystokinin-immunoreactive cells form symmetrical synaptic contacts with pyramidal and nonpyramidal neurons in the hippocampus.', *The Journal of comparative neurology*, 237(4), pp. 485–505. doi: 10.1002/cne.902370406.

Obici, S., Feng, Z., Morgan, K., Stein, D., Karkanias, G. and Rossetti, L. (2002) 'Central Administration of Oleic Acid Inhibits Glucose Production and Food Intake', *Diabetes*, 51(2), pp. 271–275. doi: 10.2337/diabetes.51.2.271.

Ollmann, M. M., Wilson, B. D., Yang, Y. K., Kerns, J. A., Chen, Y., Gantz, I. and Barsh, G. S. (1997) 'Antagonism of central melanocortin receptors in vitro and in vivo by agouti-related protein.', *Science (New York, N.Y.)*, 278(5335), pp. 135–8.

Overduin, J., Frayo, R. S., Grill, H. J., Kaplan, J. M. and Cummings, D. E. (2005) 'Role of the Duodenum and Macronutrient Type in Ghrelin Regulation', *Endocrinology*. Oxford University Press, 146(2), pp. 845–850. doi: 10.1210/en.2004-0609.

Patterson, C. M., Leshan, R. L., Jones, J. C. and Myers, M. G. (2011) 'Molecular mapping of mouse brain regions innervated by leptin receptor-expressing cells', *Brain Research*, 1378, pp. 18–28. doi: 10.1016/j.brainres.2011.01.010.

Pawelzik, H., Hughes, D. I. and Thomson, A. M. (2002) 'Physiological and morphological diversity of immunocytochemically defined parvalbumin- and cholecystokinin-positive interneurones in CA1 of the adult rat hippocampus.', *The Journal of comparative neurology*, 443(4), pp. 346–67.

Perkins, M. N., Rothwell, N. J., Stock, M. J. and Stone, T. W. (1981) 'Activation of brown adipose tissue thermogenesis by the ventromedial hypothalamus.', *Nature*, 289(5796), pp. 401–2.

Peters, J. H., McDougall, S. J., Kellett, D. O., Jordan, D., Llewellyn-Smith, I. J. and Andresen, M. C. (2008) 'Oxytocin Enhances Cranial Visceral Afferent Synaptic Transmission to the Solitary Tract Nucleus', *Journal of Neuroscience*,

28(45), pp. 11731–11740. doi: 10.1523/JNEUROSCI.3419-08.2008.

Peters, J. H., Ritter, R. C. and Simasko, S. M. (2006) 'Leptin and CCK selectively activate vagal afferent neurons innervating the stomach and duodenum.', *American journal of physiology. Regulatory, integrative and comparative physiology*, 290(6), pp. R1544-9. doi: 10.1152/ajpregu.00811.2005.

Pocai, A., Obici, S., Schwartz, G. J. and Rossetti, L. (2005) 'A brain-liver circuit regulates glucose homeostasis', *Cell Metabolism*, 1(1), pp. 53–61. doi: 10.1016/j.cmet.2004.11.001.

Prentki, M., Matschinsky, F. M. and Madiraju, S. R. M. (2013) 'Metabolic Signaling in Fuel-Induced Insulin Secretion', *Cell Metabolism*, 18(2), pp. 162–185. doi: 10.1016/j.cmet.2013.05.018.

Puskás, N., Papp, R. S., Gallatz, K. and Palkovits, M. (2010) 'Interactions between orexin–immunoreactive fibers and adrenaline or noradrenaline-expressing neurons of the lower brainstem in rats and mice', *Peptides*. Elsevier, 31(8), pp. 1589–1597. doi: 10.1016/J.PEPTIDES.2010.04.020.

Qiu, J., Zhang, C., Borgquist, A., Nestor, C. C., Smith, A. W., Bosch, M. A., Ku, S., Wagner, E. J., Rønnekleiv, O. K. and Kelly, M. J. (2014) 'Insulin Excites Anorexigenic Proopiomelanocortin Neurons via Activation of Canonical Transient Receptor Potential Channels', *Cell Metabolism*, 19(4), pp. 682–693. doi: 10.1016/j.cmet.2014.03.004.

Ramadori, G., Fujikawa, T., Anderson, J., Berglund, E. D., Frazao, R., Michán, S., Vianna, C. R., Sinclair, D. A., Elias, C. F. and Coppari, R. (2011) 'SIRT1 Deacetylase in SF1 Neurons Protects against Metabolic Imbalance', *Cell Metabolism*, 14(3), pp. 301–312. doi: 10.1016/j.cmet.2011.06.014.

Raper, J., Morrison, R. D., Daniels, J. S., Howell, L., Bachevalier, J., Wichmann, T. and Galvan, A. (2017) 'Metabolism and Distribution of Clozapine-N-oxide: Implications for Nonhuman Primate Chemogenetics', *ACS Chemical Neuroscience*. American Chemical Society, 8(7), pp. 1570–1576. doi: 10.1021/acschemneuro.7b00079.

Rehfeld, J. F., Bungaard, J. R., Friis-Hansen, L. and Goetze, J. P. (2003) 'On the tissue-specific processing of procholecystokinin in the brain and gut--a short

review.', *Journal of physiology and pharmacology : an official journal of the Polish Physiological Society*, 54 Suppl 4, pp. 73–9.

Rezai-Zadeh, K., Yu, S., Jiang, Y., Laque, A., Schwartzenburg, C., Morrison, C. D., Derbenev, A. V., Zsombok, A. and Münzberg, H. (2014) 'Leptin receptor neurons in the dorsomedial hypothalamus are key regulators of energy expenditure and body weight, but not food intake', *Molecular Metabolism*, 3(7), pp. 681–693. doi: 10.1016/j.molmet.2014.07.008.

Rinaman, L. (1998) 'Oxytocinergic inputs to the nucleus of the solitary tract and dorsal motor nucleus of the vagus in neonatal rats', *The Journal of Comparative Neurology*, 399(1), pp. 101–109. doi: 10.1002/(SICI)1096-9861(19980914)399:1<101::AID-CNE8>3.0.CO;2-5.

Rinaman, L. (2003) 'Hindbrain Noradrenergic Lesions Attenuate Anorexia and Alter Central cFos Expression in Rats after Gastric Viscerosensory Stimulation', 23(31), pp. 10084–10092.

Rinaman, L., Baker, E. A., Hoffman, G. E., Stricker, E. M. and Verbalis, J. G. (1998) 'Medullary c-Fos activation in rats after ingestion of a satiating meal', 275(1 44-1).

Ritter, R. C. (2004) 'Gastrointestinal mechanisms of satiation for food', *Physiology & Behavior*. Elsevier Inc., 81(2), pp. 249–273. doi: 10.1016/j.physbeh.2004.02.012.

Ritter, S., Dinh, T. T. and Zhang, Y. (2000) 'Localization of hindbrain glucoreceptive sites controlling food intake and blood glucose', *Brain Research*, 856(1–2), pp. 37–47. doi: 10.1016/S0006-8993(99)02327-6.

Ritter, S., Llewellyn-Smith, I. and Dinh, T. T. (1998) 'Subgroups of hindbrain catecholamine neurons are selectively activated by 2-deoxy-d-glucose induced metabolic challenge', *Brain Research*, 805(1–2), pp. 41–54. doi: 10.1016/S0006-8993(98)00655-6.

Rodríguez, E. M., Blázquez, J. L. and Guerra, M. (2010) 'The design of barriers in the hypothalamus allows the median eminence and the arcuate nucleus to enjoy private milieus: The former opens to the portal blood and the latter to the cerebrospinal fluid', *Peptides*, 31(4), pp. 757–776. doi:

10.1016/j.peptides.2010.01.003.

Roepke, T. A. (2009) ‘Oestrogen modulates hypothalamic control of energy homeostasis through multiple mechanisms.’, *Journal of neuroendocrinology*. NIH Public Access, 21(2), pp. 141–50. doi: 10.1111/j.1365-2826.2008.01814.x.

Roh, E., Song, D. K. and Kim, M.-S. (2016) ‘Emerging role of the brain in the homeostatic regulation of energy and glucose metabolism’, *Experimental & Molecular Medicine*, 48(3), p. e216. doi: 10.1038/emm.2016.4.

Rojas, J. M. and Schwartz, M. W. (2014) ‘Control of hepatic glucose metabolism by islet and brain’, *Diabetes, Obesity and Metabolism*, 16(S1), pp. 33–40. doi: 10.1111/dom.12332.

Roland, A. V. and Moenter, S. M. (2011) ‘Glucosensing by GnRH Neurons: Inhibition by Androgens and Involvement of AMP-Activated Protein Kinase’, *Molecular Endocrinology*, 25(5), pp. 847–858. doi: 10.1210/me.2010-0508.

Roscoe B. Jackson Memorial Laboratory. and Green, E. L. (1966) *Biology of the laboratory mouse,*. Blakiston Division, McGraw-Hill.

Roth, B. L., Hill, C. and Carolina, N. (2013) ‘Remote Control of Cellular Signaling Using DREADD Technology’.

Routh, V. H., Donovan, C. M. and Ritter, S. (2012) ‘2. Hypoglycemia Detection.’, *Translational endocrinology & metabolism*, 3(4), pp. 47–87.

Russell, C. D., Ricci, M. R., Brolin, R. E., Magill, E. and Fried, S. K. (2001) ‘Regulation of the leptin content of obese human adipose tissue’, *American Journal of Physiology-Endocrinology and Metabolism*, 280(3), pp. E399–E404. doi: 10.1152/ajpendo.2001.280.3.E399.

Sabatier, N. and Leng, G. (2010) ‘Responses to cholecystokinin in the ventromedial nucleus of the rat hypothalamus in vivo’, *European Journal of Neuroscience*. Blackwell Publishing Ltd, 31(6), pp. 1127–1135. doi: 10.1111/j.1460-9568.2010.07144.x.

Schiffmann, S. N. and Vanderhaeghen, J. J. (1991) ‘Distribution of cells containing mRNA encoding cholecystokinin in the rat central nervous system.’, *The Journal of comparative neurology*, 304(2), pp. 219–33. doi: 10.1002/cne.903040206.

Schwartz, G. J. and Moran, T. H. (1996) ‘Sub-diaphragmatic vagal afferent integration of meal-related gastrointestinal signals’, *Neuroscience & Biobehavioral Reviews*. Elsevier Ltd, 20(1), pp. 47–56. doi: 10.1016/0149-7634(95)00039-H.

Senatorov, V. V, Trudeau, V. L. and Hu, B. (1995) ‘Expression of cholecystokinin mRNA in corticothalamic projecting neurons: a combined fluorescence in situ hybridization and retrograde tracing study in the ventrolateral thalamus of the rat.’, *Brain research. Molecular brain research*, 30(1), pp. 87–96.

Sheng, Z., Santiago, A. M., Thomas, M. P. and Routh, V. H. (2014) ‘Metabolic regulation of lateral hypothalamic glucose-inhibited orexin neurons may influence midbrain reward neurocircuitry’, *Molecular and Cellular Neuroscience*, 62, pp. 30–41. doi: 10.1016/j.mcn.2014.08.001.

Shi, Y.-C., Lau, J., Lin, Z., Zhang, H., Zhai, L., Sperk, G., Heilbronn, R., Mietzsch, M., Weger, S., Huang, X.-F., Enriquez, R. F., Castillo, L., Baldock, P. A., Zhang, L., Sainsbury, A., Herzog, H. and Lin, S. (2013) ‘Arcuate NPY Controls Sympathetic Output and BAT Function via a Relay of Tyrosine Hydroxylase Neurons in the PVN’, *Cell Metabolism*, 17(2), pp. 236–248. doi: 10.1016/j.cmet.2013.01.006.

Shimazu, T. and Minokoshi, Y. (2017) ‘Systemic Glucoregulation by Glucose-Sensing Neurons in the Ventromedial Hypothalamic Nucleus (VMH).’, *Journal of the Endocrine Society*. The Endocrine Society, 1(5), pp. 449–459. doi: 10.1210/js.2016-1104.

Shimizu, N., Oomura, Y., Plata-Salamán, C. R. and Morimoto, M. (1987) ‘Hyperphagia and obesity in rats with bilateral ibotenic acid-induced lesions of the ventromedial hypothalamic nucleus.’, *Brain research*, 416(1), pp. 153–6.

Shin, A. C., Filatova, N., Lindtner, C., Chi, T., Degann, S., Oberlin, D. and Buettner, C. (2017) ‘Insulin Receptor Signaling in POMC, but Not AgRP, Neurons Controls Adipose Tissue Insulin Action’, *Diabetes*, 66(6), pp. 1560–1571. doi: 10.2337/db16-1238.

Skibicka, K. P. and Grill, H. J. (2009) ‘Hypothalamic and Hindbrain Melanocortin Receptors Contribute to the Feeding, Thermogenic, and Cardiovascular Action of Melanocortins’, *Endocrinology*, 150(12), pp. 5351–5361. doi: 10.1210/en.2009-0804.

Sloviter, R. S. and Nilaver, G. (1987) 'Immunocytochemical localization of GABA-, cholecystokinin-, vasoactive intestinal polypeptide-, and somatostatin-like immunoreactivity in the area dentata and hippocampus of the rat.', *The Journal of comparative neurology*, 256(1), pp. 42–60. doi: 10.1002/cne.902560105.

Smith, G. P. (1996) 'The direct and indirect controls of meal size', *Neuroscience & Biobehavioral Reviews*. Elsevier Ltd, 20(1), pp. 41–46. doi: 10.1016/0149-7634(95)00038-G.

Sohn, J.-W., Oh, Y., Kim, K. W., Lee, S., Williams, K. W. and Elmquist, J. K. (2016) 'Leptin and insulin engage specific PI3K subunits in hypothalamic SF1 neurons.', *Molecular metabolism*. Elsevier, 5(8), pp. 669–79. doi: 10.1016/j.molmet.2016.06.004.

Somogyi, P. and Klausberger, T. (2005) 'Defined types of cortical interneurone structure space and spike timing in the hippocampus.', *The Journal of physiology*. Wiley-Blackwell, 562(Pt 1), pp. 9–26. doi: 10.1113/jphysiol.2004.078915.

Song, Z., Levin, B. E., McArdle, J. J., Bakhos, N. and Routh, V. H. (2001) 'Convergence of pre- and postsynaptic influences on glucosensing neurons in the ventromedial hypothalamic nucleus.', *Diabetes*, 50(12), pp. 2673–81.

Song, Z. and Routh, V. H. (2006) 'Recurrent hypoglycemia reduces the glucose sensitivity of glucose-inhibited neurons in the ventromedial hypothalamus nucleus', *American Journal of Physiology-Regulatory, Integrative and Comparative Physiology*, 291(5), pp. R1283–R1287. doi: 10.1152/ajpregu.00148.2006.

Spanswick, D., Smith, M. A., Mirshamsi, S., Routh, V. H. and Ashford, M. L. J. (2000) 'Insulin activates ATP-sensitive K+ channels in hypothalamicneurons of lean, but not obese rats', *Nature Neuroscience*, 3(8), pp. 757–758. doi: 10.1038/77660.

Stanley, B. G. and Leibowitz, S. F. (1984) 'Neuropeptide Y: stimulation of feeding and drinking by injection into the paraventricular nucleus.', *Life sciences*, 35(26), pp. 2635–42.

Stanley, S., Domingos, A. I., Kelly, L., Garfield, A., Damanpour, S., Heisler, L. and Friedman, J. (2013) 'Profiling of Glucose-Sensing Neurons Reveals that

GHRH Neurons Are Activated by Hypoglycemia', *Cell Metabolism*, 18(4), pp. 596–607. doi: 10.1016/j.cmet.2013.09.002.

Steculorum, S. M., Ruud, J., Karakasilioti, I., Backes, H., Engström Ruud, L., Timper, K., Hess, M. E., Tsaousidou, E., Mauer, J., Vogt, M. C., Paeger, L., Bremser, S., Klein, A. C., Morgan, D. A., Frommolt, P., Brinkkötter, P. T., Hammerschmidt, P., Benzing, T., Rahmouni, K., Wunderlich, F. T., Kloppenburg, P. and Brüning, J. C. (2016) 'AgRP Neurons Control Systemic Insulin Sensitivity via Myostatin Expression in Brown Adipose Tissue', *Cell*, 165(1), pp. 125–138. doi: 10.1016/j.cell.2016.02.044.

Sternson, S. M., Shepherd, G. M. G. and Friedman, J. M. (2005) 'Topographic mapping of VMH → arcuate nucleus microcircuits and their reorganization by fasting', *Nature Neuroscience*, 8(10), pp. 1356–1363. doi: 10.1038/nn1550.

Straub, R. H., Cutolo, M., Buttgereit, F. and Pongratz, G. (2010) 'Review: Energy regulation and neuroendocrine-immune control in chronic inflammatory diseases', *Journal of Internal Medicine*, 267(6), pp. 543–560. doi: 10.1111/j.1365-2796.2010.02218.x.

Sutton, G. M., Duos, B., Patterson, L. M. and Berthoud, H.-R. (2005) 'Melanocortinergic Modulation of Cholecystokinin-Induced Suppression of Feeding through Extracellular Signal-Regulated Kinase Signaling in Rat Solitary Nucleus', *Endocrinology*, 146(9), pp. 3739–3747. doi: 10.1210/en.2005-0562.

Szepietowska, B., Zhu, W., Chan, O., Horblitt, A., Dziura, J. and Sherwin, R. S. (2011) 'Modulation of -Adrenergic Receptors in the Ventromedial Hypothalamus Influences Counterregulatory Responses to Hypoglycemia', *Diabetes*, 60(12), pp. 3154–3158. doi: 10.2337/db11-0432.

Thaler, J. P., Guyenet, S. J., Dorfman, M. D., Wisse, B. E. and Schwartz, M. W. (2013) 'Hypothalamic Inflammation: Marker or Mechanism of Obesity Pathogenesis?', *Diabetes*, 62(8), pp. 2629–2634. doi: 10.2337/db12-1605.

Thorens, B. (2010) 'Central control of glucose homeostasis: the brain – endocrine pancreas axis', *Diabetes & Metabolism*, 36, pp. S45–S49. doi: 10.1016/S1262-3636(10)70466-3.

Tolhurst, G., Reimann, F. and Gribble, F. M. (2012) 'Intestinal Sensing of Nutrients', in, pp. 309–335. doi: 10.1007/978-3-642-24716-3_14.

Tong, Q., Ye, C., McCrimmon, R. J., Dhillon, H., Choi, B., Kramer, M. D., Yu, J., Yang, Z., Christiansen, L. M., Lee, C. E., Choi, C. S., Zigman, J. M., Shulman, G. I., Sherwin, R. S., Elmquist, J. K. and Lowell, B. B. (2007) 'Synaptic Glutamate Release by Ventromedial Hypothalamic Neurons Is Part of the Neurocircuitry that Prevents Hypoglycemia', *Cell Metabolism*, 5(5), pp. 383–393. doi: 10.1016/j.cmet.2007.04.001.

Travagli, R. A., Hermann, G. E., Browning, K. N. and Rogers, R. C. (2003) 'III. Activity-dependent plasticity in vago-vagal reflexes controlling the stomach', *American Journal of Physiology-Gastrointestinal and Liver Physiology*, 284(2), pp. G180–G187. doi: 10.1152/ajpgi.00413.2002.

Tricoire, L., Pelkey, K. A., Erkkila, B. E., Jeffries, B. W., Yuan, X. and McBain, C. J. (2011) 'A blueprint for the spatiotemporal origins of mouse hippocampal interneuron diversity.', *The Journal of neuroscience : the official journal of the Society for Neuroscience*, 31(30), pp. 10948–70. doi: 10.1523/JNEUROSCI.0323-11.2011.

Vanderhaeghen, J. J., Lotstra, F., De Mey, J. and Gilles, C. (1980) 'Immunohistochemical localization of cholecystokinin- and gastrin-like peptides in the brain and hypophysis of the rat.', *Proceedings of the National Academy of Sciences of the United States of America*, 77(2), pp. 1190–4.

Verberne, A. J. M., Sabetghadam, A. and Korim, W. S. (2014) 'Neural pathways that control the glucose counterregulatory response.', *Frontiers in neuroscience*. Frontiers Media SA, 8, p. 38. doi: 10.3389/fnins.2014.00038.

Vizi, S. E., Bertaccini, G., Impicciatore, M. and Knoll, J. (1973) 'Evidence that Acetylcholine Released by Gastrin and Related Polypeptides Contributes to their Effect on Gastrointestinal Motility', *Gastroenterology*. Elsevier, 64(2), pp. 268–277. doi: 10.1016/S0016-5085(73)80038-1.

Vogt, M. C. and Brüning, J. C. (2013) 'CNS insulin signaling in the control of energy homeostasis and glucose metabolism – from embryo to old age', *Trends in Endocrinology & Metabolism*, 24(2), pp. 76–84. doi: 10.1016/j.tem.2012.11.004.

Voss-Andreae, A., Murphy, J. G., Ellacott, K. L. J., Stuart, R. C., Nillni, E. A., Cone, R. D. and Fan, W. (2007) 'Role of the Central Melanocortin Circuitry in Adaptive Thermogenesis of Brown Adipose Tissue', *Endocrinology*, 148(4), pp. 1550–1560. doi: 10.1210/en.2006-1389.

Wang, L., Martínez, V., Barrachina, M. D. and Taché, Y. (1998) 'Fos expression in the brain induced by peripheral injection of CCK or leptin plus CCK in fasted lean mice.', *Brain research*, 791(1–2), pp. 157–66.

Warne, J. P., Varonin, J. M., Nielsen, S. S., Olofsson, L. E., Kaelin, C. B., Chua, S., Barsh, G. S., Koliwad, S. K. and Xu, A. W. (2013) 'Coordinated Regulation of Hepatic Energy Stores by Leptin and Hypothalamic Agouti-Related Protein', *Journal of Neuroscience*, 33(29), pp. 11972–11985. doi: 10.1523/JNEUROSCI.0830-13.2013.

Waterson, M. J. and Horvath, T. L. (2015) 'Neuronal Regulation of Energy Homeostasis: Beyond the Hypothalamus and Feeding', *Cell Metabolism*, 22(6), pp. 962–970. doi: 10.1016/j.cmet.2015.09.026.

Weatherford, S. C., Laughton, W. B., Salabarria, J., Danho, W., Tilley, J. W., Netterville, L. A., Schwartz, G. J. and Moran, T. H. (1993) 'CCK satiety is differentially mediated by high- and low-affinity CCK receptors in mice and rats', *American Journal of Physiology-Regulatory, Integrative and Comparative Physiology*, 264(2), pp. R244–R249. doi: 10.1152/ajpregu.1993.264.2.R244.

West, D. B., Fey, D. and Woods, S. C. (1984) 'Cholecystokinin persistently suppresses meal size but not food intake in free-feeding rats', *American Journal of Physiology-Regulatory, Integrative and Comparative Physiology*, 246(5), pp. R776–R787. doi: 10.1152/ajpregu.1984.246.5.R776.

Williams, K. W., Margatho, L. O., Lee, C. E., Choi, M., Lee, S., Scott, M. M., Elias, C. F. and Elmquist, J. K. (2010) 'Segregation of Acute Leptin and Insulin Effects in Distinct Populations of Arcuate Proopiomelanocortin Neurons', *Journal of Neuroscience*, 30(7), pp. 2472–2479. doi: 10.1523/JNEUROSCI.3118-09.2010.

Williams, R. H., Alexopoulos, H., Jensen, L. T., Fugger, L. and Burdakov, D. (2008) 'Adaptive sugar sensors in hypothalamic feeding circuits', *Proceedings of the National Academy of Sciences*, 105(33), pp. 11975–11980. doi: 10.1073/pnas.0802687105.

Woltman, T., Castellanos, D. and Reidelberger, R. (1995) 'Role of cholecystokinin in the anorexia produced by duodenal delivery of oleic acid in rats', *American Journal of Physiology-Regulatory, Integrative and Comparative Physiology*, 269(6), pp. R1420–R1433. doi: 10.1152/ajpregu.1995.269.6.R1420.

Xu, B., Goulding, E. H., Zang, K., Cepoi, D., Cone, R. D., Jones, K. R., Tecott, L. H. and Reichardt, L. F. (2003) 'Brain-derived neurotrophic factor regulates energy balance downstream of melanocortin-4 receptor', *Nature Neuroscience*, 6(7), pp. 736–742. doi: 10.1038/nn1073.

Xu, Y., Hill, J. W., Fukuda, M., Gautron, L., Sohn, J.-W., Kim, K.-W., Lee, C. E., Choi, M. J., Lauzon, D. A., Dhillon, H., Lowell, B. B., Zigman, J. M., Zhao, J. J. and Elmquist, J. K. (2010a) 'PI3K Signaling in the Ventromedial Hypothalamic Nucleus Is Required for Normal Energy Homeostasis', *Cell Metabolism*, 12(1), pp. 88–95. doi: 10.1016/j.cmet.2010.05.002.

Xu, Y., Hill, J. W., Fukuda, M., Gautron, L., Sohn, J.-W., Kim, K.-W., Lee, C. E., Choi, M. J., Lauzon, D. A., Dhillon, H., Lowell, B. B., Zigman, J. M., Zhao, J. J. and Elmquist, J. K. (2010b) 'PI3K Signaling in the Ventromedial Hypothalamic Nucleus Is Required for Normal Energy Homeostasis', *Cell Metabolism*, 12(1), pp. 88–95. doi: 10.1016/j.cmet.2010.05.002.

Xu, Y., Nedungadi, T. P., Zhu, L., Sobhani, N., Irani, B. G., Davis, K. E., Zhang, X., Zou, F., Gent, L. M., Hahner, L. D., Khan, S. A., Elias, C. F., Elmquist, J. K. and Clegg, D. J. (2011) 'Distinct Hypothalamic Neurons Mediate Estrogenic Effects on Energy Homeostasis and Reproduction', *Cell Metabolism*, 14(4), pp. 453–465. doi: 10.1016/j.cmet.2011.08.009.

Yamaizumi, M., Mekada, E., Uchida, T. and Okada, Y. (1978) 'One molecule of diphtheria toxin fragment A introduced into a cell can kill the cell.', *Cell*, 15(1), pp. 245–50.

Yang, Y., Atasoy, D., Su, H. H. and Sternson, S. M. (2011) 'Hunger States Switch a Flip-Flop Memory Circuit via a Synaptic AMPK-Dependent Positive Feedback Loop', *Cell*, 146(6), pp. 992–1003. doi: 10.1016/j.cell.2011.07.039.

Yokosuka, M., Kalra, P. S. and Kalra, S. P. (1999) 'Inhibition of Neuropeptide Y (NPY)-Induced Feeding and c-Fos Response in Magnocellular Paraventricular Nucleus by a NPY Receptor Antagonist: A Site of NPY Action [1]', *Endocrinology*,

140(10), pp. 4494–4500. doi: 10.1210/endo.140.10.7058.

Zhan, C., Zhou, J., Feng, Q., Zhang, J.-E., Lin, S., Bao, J., Wu, P. and Luo, M. (2013) 'Acute and long-term suppression of feeding behavior by POMC neurons in the brainstem and hypothalamus, respectively.', *The Journal of neuroscience : the official journal of the Society for Neuroscience*. Society for Neuroscience, 33(8), pp. 3624–32. doi: 10.1523/JNEUROSCI.2742-12.2013.

Zhang, R., Dhillon, H., Yin, H., Yoshimura, A., Lowell, B. B., Maratos-Flier, E. and Flier, J. S. (2008) 'Selective Inactivation of *Socs3* in SF1 Neurons Improves Glucose Homeostasis without Affecting Body Weight', *Endocrinology*, 149(11), pp. 5654–5661. doi: 10.1210/en.2008-0805.

Zhao, S., Kanoski, S. E., Yan, J., Grill, H. J. and Hayes, M. R. (2012) 'Hindbrain leptin and glucagon-like-peptide-1 receptor signaling interact to suppress food intake in an additive manner', *International Journal of Obesity*. Nature Publishing Group, 36(12), pp. 1522–1528. doi: 10.1038/ijo.2011.265.

Zheng, H., Patterson, L. M. and Berthoud, H.-R. (2005) 'Orexin-A projections to the caudal medulla and orexin-induced c-Fos expression, food intake, and autonomic function', *The Journal of Comparative Neurology*, 485(2), pp. 127–142. doi: 10.1002/cne.20515.

Zheng, H., Patterson, L. M., Rhodes, C. J., Louis, G. W., Skibicka, K. P., Grill, H. J., Myers, M. G. and Berthoud, H.-R. (2010) 'A potential role for hypothalamomedullary POMC projections in leptin-induced suppression of food intake', *American Journal of Physiology-Regulatory, Integrative and Comparative Physiology*. American Physiological Society Bethesda, MD, 298(3), pp. R720–R728. doi: 10.1152/ajpregu.00619.2009.

Zhu, G., Yan, J., Smith, W. W., Moran, T. H. and Bi, S. (2012) 'Roles of dorsomedial hypothalamic cholecystokinin signaling in the controls of meal patterns and glucose homeostasis.', *Physiology & behavior*, 105(2), pp. 234–41. doi: 10.1016/j.physbeh.2011.08.007.

Zigman, J. M., Jones, J. E., Lee, C. E., Saper, C. B. and Elmquist, J. K. (2006a) 'Expression of ghrelin receptor mRNA in the rat and the mouse brain', *The Journal of Comparative Neurology*. Wiley Subscription Services, Inc., A Wiley Company, 494(3), pp. 528–548. doi: 10.1002/cne.20823.

Zigman, J. M., Jones, J. E., Lee, C. E., Saper, C. B. and Elmquist, J. K. (2006b) ‘Expression of ghrelin receptor mRNA in the rat and the mouse brain’, *The Journal of Comparative Neurology*, 494(3), pp. 528–548. doi: 10.1002/cne.20823.

Zorrilla, E. P., Inoue, K., Fekete, É. M., Tabarin, A., Valdez, G. R. and Koob, G. F. (2005) ‘Measuring meals: structure of prandial food and water intake of rats’, *American Journal of Physiology-Regulatory, Integrative and Comparative Physiology*. American Physiological Society, 288(6), pp. R1450–R1467. doi: 10.1152/ajpregu.00175.2004.

Zséli, G., Vida, B., Szilvásy-Szabó, A., Tóth, M., Lechan, R. M. and Fekete, C. (2017) ‘Neuronal connections of the central amygdalar nucleus with refeeding-activated brain areas in rats’, *Brain Structure and Function*. Springer Berlin Heidelberg, pp. 1–24. doi: 10.1007/s00429-017-1501-4.

Zwanzger, P., Domschke, K. and Bradwejn, J. (2012) ‘NEURONAL NETWORK OF PANIC DISORDER: THE ROLE OF THE NEUROPEPTIDE CHOLECYSTOKININ’, *Depression and Anxiety*, 29(9), pp. 762–774. doi: 10.1002/da.21919.